Engineering Geologic Investigation of an Irrigation-Induced Debris Flow Near Cordova, Rio Arriba County, New Mexico

by

WILLIAM C. HANEBERG

Engineering Geologist

New Mexico Bureau of Mines and Mineral Resources

New Mexico Institute of Mining and Technology

Socorro, New Mexico 87801

and

GERALD TRIPP

Research Assistant

Department of Mining, Environmental and Geological Engineering

New Mexico Institute of Mining and Technology

Socorro, New Mexico 87801

New Mexico Bureau of Mines and Mineral Resources

Open-File Report 371

December 6, 1990

CONTENTS

ABSTRACT

Analysis of field and laboratory data suggests that an unexpected June 8, 1990 debris flow– mobilized from Holocene stream terrace deposits along the Rio Quemado near Cordova, New Mexico– occurred due to accumulation of perched irrigation water along the top of the Miocene Tesuque Formation.

The Cordova flow involved approximately 10,000 m^3 (12,000 cubic yards) of poorly-sorted low plasticity debris composed primarily of sand, gravel, and cobbles. Dry bulk density of 16 undisturbed samples falling into Unified Soil Classifiation System categories SW and SP, ranged from 1430 to 1780 kg/m^3 (89 to 111 pounds per cubic foot *or* pcf). Shear strength of the flowing debris was estimated to be about 2.8 kPa (0.4 pounds per square inch *or* psi) under a maximum of 41 kPa (5.9 psi) confining pressure, and results of direct shear tests on remolded debris suggest that the strength of the debris at rest was about an order of magnitude greater for the same confining pressure. There is evidence for large amounts of water in the debris prior to failure, but Stage I calcic soil horizons throughout undisturbed portions of the terrace suggest that the deposit has been well-drained throughout its existence. The approximate mobility index (AMI) of the undisturbed terrace material is in the range of $2 < AMI < 3$, meaning that the slope was susceptible to mobilization after the initial failure occurred.

Slope stability analyses using original terrace geometry also require a phreatic surface coincident, or very nearly so, with the ground surface in order to calculate factors of safety against sliding < 1 for reasonable angles of internal friction. Therefore, we conclude that the failure was almost certainly due to the unprecedented development of a perched water table above a clayey paleosol at the top of the Tesuque Formation. The two most likely sources of water were seepage from an irrigation ditch above the failed slope and/or over-irrigation of the terrace, which was being used a pasture. Stability analyses also suggest that the post-failure debris mass is stable in its present configuration.

Failure of well-drained stream terrace deposits in an area with no evidence of past instability shows that potential geologic hazards cannot always be delineated solely on the basis of historical occurrences or the geologic record. Thus, the potential impacts of events unprecedented in geologic history– for example road building or extensive irrigation– should be evaluated using rational analyses as well as empirical observations.

INTRODUCTION

The use of *acequias*, or community ditches, is a traditional irrigation practice in mountain valleys throughout northern New Mexico and southern Colorado. Because *acequias* are maintained and used by irrigators with little or no engineering expertise, virtually no consideration is given to the effects of irrigation water on slope stability. Although irrigation-induced slope failures have historically not presented problems in northern New Mexico, a recent incident has shown that such failures are possible. In this paper we describe field and laboratory investigations of a 10,000 m^3 (about 12,000 cubic yards) debris flow near the town of Cordova, in north-central New Mexico, that occurred on the morning of June 8, 1990. Based upon our analysis of the conditions likely to have triggered the failure, we also suggest ways in which the potential for similar debris flows in irrigated valleys might be assessed and reduced.

Geologic Setting

The failure described in this paper, hereafter referred to as the Cordova debris flow, occurred on private land along the southeastern bank of the Rio Quemado, approximately 1 km (1.6 miles) northeast of the village of Cordova, in southernmost Rio Arriba County. This area, which lies in the Nuesta Senora del Rosario San Fernando y Santiago grant, is covered by the far southwestern corner of the USGS Truchas 7.5' quadrangle (Figure 1). The Rio Quemado is a small stream, several meters (about 6-12 ft) wide and a meter (about 3 ft) or less in depth at the time of failure. A 1 m (about 3 ft) wide *acequia*, diverted approximately 0.8 km (0.5 miles) northeast of the debris flow, runs along the valley wall some 25 m (82 ft) above the river. Vegetation along the lower, irrigated slopes consists of grasses and deciduous trees, whereas the upper slopes are dominated by a sparse pinon-juniper forest.

The valley of the Rio Quemado has been cut into flay-lying beds of the Miocene Tesuque Formation, a clastic unit derived from the Sangre de Cristo mountains to the south and east. Miller *et al.* (1963) and Baltz (1978) describe the Tesuque Formation as a series of slightly consolidated sands, silts, gravels, and clays ranging from 150 m (500 ft) to perhaps as much as 1000 m (3300 ft) in thickness. Volcanic ash layers, containing latite and andesite clasts, are locally abundant and olivine basalt flows have been described, but neither are evident in the immediate vicinity of the Cordova debris flow. Bedding in the Tesuque Formation can be locally well-developed, but abrupt vertical and horizontal textural changes are common. Miller *et al.* (1963) map terraces along the Rio Quemado as Quaternary alluvium consisting of post-glacial Holocene floodplain deposits and stream terraces, and suggest that post-Pleistocene downcutting has been on the order of 100 m (330 ft). In a previous study, Miller and Wendorf (1958) described two sets of Holocene stream terraces along lower reaches of several valleys along the Sangre de Cristo front. The upper terraces,

is typically several hundred meters in width and developed on silt and fine sands, whereas the lower terraces are typically much narrower and developed on slightly coarser materials. Radiocarbon and pottery dates (Miller and Wendorf, 1958) suggest that alluvium underlying the upper terrace was deposited between 267 B.C. and 1250 A.D., and that alluvium underlying the lower terrace was deposited between 1250 and 1880. The regime of the Rio Quemado has been erosional since 1880.

Regional 1:500,000 landslide inventory maps compiled from aerial photographs show no landslides or debris flows along the Rio Quemado drainage, although many other places along the Sangre de Cristo front are mapped as sediment source areas, with closely-spaced rills and headscarps (Guzetti and Brabb, 1987). Limited reconnaissance during visits to Cordova did not reveal any additional evidence to suggest that slope instability has been a persistent problem along the Rio Quemado, and the landowner was not able to recall any other landslides or debris flows in the valley during the past 50 years (C. Trujillo, personal communication, 1990). The *mayordomo*, or ditch foreman, however, informed the New Mexico State Engineer Office that the terrace was under irrigation at the time of failure, and that a slight reversal of gradient had impeded flow through the ditch immediately above the failure area for some time (J. Garcia, personal communication, 1990).

Terminology

Throughout this paper we will use the term "soil" in the pedologic sense. In order to emphasize this distinction, we will generally refer to pedologic soils as "organic soils", "buried soils", or "horizons". Geotechnical or engineering soils, consisting of various unconsolidated sedimentary materials, will generally be referred to as "deposits".

DESCRIPTION

During the week after the failure we mapped the Cordova debris flow at a scale of 1:300 and collected representative samples for laboratory analysis. The stratigraphy, geometry, and basic engineering properties of the original slope, the debris flow, and associated deposits are described below.

Stratigraphic Units

We identified five major lithologic units in the field and classified them according to the genesis-lithology-qualifier system (Keaton, 1984). The units are, from youngest to oldest:

Slump deposits, Soc-k(sl).– Produced by sloughing of nearly-vertical head scarp. Sand to large cobbles 0.25 to 0.30 m (10 to 12 in) with grassy blocks of organic soil, small trees, shrubs, and fence posts.

Small alluvial fan deposits, As-k(f).– Produced by water flowing from the head scarp and distal edges of the main debris deposit (Figure 2). Fine sand to gravel with some cobbles, locally

segregated into sandy braided channel deposits and gravel to cobble lag deposits on a scale of centimeters.

Main debris flow deposits, Soc-k(fl).– Poorly-sorted sand to 0.30 m (12 in) cobbles with subsidiary blocks of organic soil, trees, and shrubs (Figure 3). Weak segregation of finer-grained material, organic soil, and vegetation into transverse troughs and coarser-grained material into transverse ridges.

Flood plain deposits, As-k(fp).– Flat-lying, sand to 0.25 or 0.30 (10 to 12 in) cobbles along the pre-failure course of the Rio Quemado.

Alluvial terrace deposits, Al/Roc-k(te).– Series of flat-lying Quaternary (?) stream terrace sands, gravels, and cobbles up to 0.30 m (12 in), truncated by steeply-dipping buried soil horizons (Figure 4). Stage I calcic horizons (*e.g.*, Gile *et al.*, 1966) are locally developed in gravelly to cobbley B horizon material, but absent in clayey B horizon material.

Geometry

The failure consists of two parts: a nearly circular, steep-walled amphitheater bounded by a head scarp, and an elongate tongue of predominantly coarse-grained debris (Figure 5). The former is primarily an erosional feature, whereas the latter is primarily a depositional feature.

The amphitheater has a maximum height of approximately 6 to 8 m (20 to 25 ft), and is surrounded by terraced pasture land. A buried organic soil horizon, dipping approximately 25° to the northwest, is present directly beneath the head scarp. The eastern portion of this horizon is covered with a veneer of coarse-grained debris a meter or more in thickness; however, the western portion has been largely stripped clean of debris except for localized erosional remnants. We did not observe any seepage from the head scarp during our field work; however, coalescing braided sand and gravel channels forming a small alluvial fan deposit in the amphitheater imply that a large amount of water was released after the amphitheater had been formed. Seeps almost to the top of the scarp were observed shortly after the failure was discovered (G. Towles, personal communication, 1990), and representatives of the New Mexico State Engineer Office reported seeps near the base of the scarp during a visit on the afternoon of June 8 (J. Garcia, personal communication, 1990).

The debris tongue consists of poorly-sorted sand, gravel, cobbles, and small boulders of very low plasticity mixed with small deciduous trees and intact blocks of topsoil and grass of 1 m^3 (1 cu yd) or less. In contrast to the grassy blocks of topsoil, we did not observe any intact blocks of terrace sand and gravel within the debris. However, we did observe a series of curvilinear transverse waves, the troughs filled with blocks of grass-covered topsoil and the crests composed primarily of coarse gravel and cobbles. Wavelengths are on the order of 1 to 10 m (3 to 32 ft.), and amplitudes on the order of about 1 m (3 ft.) or

less. Many small puddles are scattered over the surface of the debris and, although there was a light rain on Saturday, June 9, the puddles had apparently existed before the rain. In addition, much of the debris remained soft and wet at the time of our visit. Longitudinal levees were not apparent on the hummocky debris surface. Excavation of several small holes in the debris showed water within 0.30 m (12 in) of the ground surface, and one hole near the head of the debris filled to within 0.02 m (1 in) of the surface within several minutes. The flow temporarily blocked both the only access road to two mobile homes and the course of the Rio Quemado, which flows through a pasture along the toe of the debris. Small, elongate lobes of dark, fine to medium sand occur along the toe of the debris mass. Estimated volume of the debris, calculated both from the approximate volume of the amphitheater and the size of the debris tongue, is on the order of 10^4 m^3 (12,000 cubic yards).

Organic Soil Profiles

We were particularly interested in the lowermost exposed organic soil profile, which appears as a sloping surface at the base of the head scarp, and to this end excavated two small pits in order to describe the soil in more detail.

In the northeastern corner of the amphitheater, where the soil is covered with approximately 0.6 to 0.8 m (24 to 32 in) of sand and gravel debris, the A horizon is 0.1 to 0.2 m (4 to 8 in) thick and is composed of slightly plastic gritty black clay. This A horizon clay becomes less gritty with depth, and contains small streaks of charcoal and well-preserved roots. Reaction with HCl ranges from moderately strong at the top to none at the bottom of the A horizon. The underlying B horizon, about 0.2 m (8 in) thick, is composed of sandy to gravelly, slightly less plastic orange-brown clay near the top of the horizon, becoming progressively finer with depth. Reaction with HCl is mild to weak, and the B horizon clay does not break into well-defined peds. A stage I calcic horizon (Gile *et al.*, 1966) composed of well-rounded igneous and metamorphic coarse gravel and cobbles with partial $CaC0_3$ coatings lies near the base of the pit. This soil profile is shown in Figure 6.

The soil profile in the southeastern corner of the amphitheater, which has been stripped clean of debris, appears to be much less well-developed than that described above. The 0.1 to 0.2 m (4 to 8 in) thick A horizon is composed of brown-gray clay with no roots or charcoal. Reaction with HCl is extremely weak to nonexistent. A orange B horizon composed of gritty orange clay, which reacts weakly with HCl, extends to a depth of at least 1 m (39 in) with no evidence of a calcic horizon. The moist, slightly plastic upper portion of the B horizon breaks into chunks more easily than does the lower portion of the B horizon, but, as above, there is no well-defined ped structure. In general, both the A and B horizon material in the second pit was noticably drier and less plastic than that in the first pit, and excavation of the orange clay with a pick-axe

was difficult even though no cobble-rich horizon was encountered.

Soil Mechanics Laboratory Testing

In addition to describing the lithologic attributes of each map unit in the field, we collected 26 representative samples for laboratory testing. Where possible, we tried to collect undisturbed samples in order to estimate soil bulk density. This was accomplished by pushing sample tins of known volume into the soil and then excavating around the tins; although the procedure is not foolproof, we were able to collect 16 relatively undisturbed and 10 disturbed samples. Grain size distribution of the coarse fraction (greater than 50 μm or 0.002 in), ambient moisture content, bulk density, plastic limit, and liquid limit were measured. Each sample was also classified according to the Unified Soil Classification System (USCS). Clay mineralogy of the fraction passing a #200 sieve (< 70 μm or 0.003 in) of 25 of the samples was also determined by X-ray diffraction analysis.

Results of our laboratory testing are summarized in Table 1. With the exception of those from the buried soil horizon, all of the samples tested were well-graded or poorly-graded sands of low plasticity (USCS SW or SP) with, in two cases, minor amounts of silt (USCS SW-M). Ambient moisture content was low, generally below 10% by weight, and dry bulk density of the 16 relatively undisturbed samples ranged from 1430 to 1780 kg/m^3 (89 to 111 pcf). Plasticity indices for the two sand samples for which both Atterburg limits could be obtained were 1.3 and 1.9. With only one exception, all of the buried soil horizon samples consisted of at least 50% fines and had moisture contents ranging from 11.5 to 21.3% by weight. Plasticity indices, which were obtained for all of the buried soil horizon samples, ranged from 3.3 to 19.9, with most values 10.0 or more. Of the 7 buried soil horizon samples, 6 fell into USCS class CL and one, with only 35.4% fines, into class ML. Dry bulk density of the undisturbed buried soil horizon samples, ranging from 1180 to 1380 kg/m^3 (74 to 86 pcf), was also slightly less than that of the sandy samples.

Sorting of the coarse fraction of each sample is reflected by the uniformity and gradation coefficients (Table 1), which are are used for USCS classification of coarse-grained samples (*e.g.*, Das, 1983, pp. 38-39). Graphically, coarse-fraction grain size distributions for stream terrace (A/Roc-k(te)), debris (Soc-k(fl)), and alluvial fan (As-k(f)) samples show a striking increase in variability from terrace to debris to alluvial samples (Figure 7). This pattern agrees with our field observations of grain-size segregation in both the debris and especially the alluvial deposits. While examining the laboratory test results, we also noted that the mean weight percentage of fines decreased from 3.7% in terrace samples to 3.0% in debris samples and 1.7% in alluvial samples. We initially believed that these figures might reflect progressive winnowing of fines during debris mobilization, flow, and dewatering. However, an anaysis of variance (Appendix B) showed that these small differences are not statistically significant. At the same time, we emphasize that our

samples were not collected with statistical analysis in mind, so the possibility of statistically-significant loss of fine-grained material during the debris flow process cannot be ruled out.

Peak and residual shear strengths of remolded material from sample #10, the only stream terrace sample for which both Atterburg limits could be measured, were estimated from direct shear tests on both dry and saturated drained samples. Shear box size was 5.7 × 5.7 × 1.27 cm (2.25 × 2.25 × 0.5 in), and deformation rate was 2% per minute. We also conducted one test at a deformation rate of 0.5% per minute, and found no noticable difference in shear strength. Peak angle of internal friction results for both dry and saturated samples (Table 2 and Appendix C), are 4° to 6° higher than typical values for cohesionless gravelly sands (USCS SW or SP) of comparable density (*e.g.*. Hunt, 1986, p. 80). Two of the three samples contracted during shearing, whereas the third dilated (Appendix A).

Clay Mineralogy

Clay fraction (< 2 μm or 0.0001 in) mineralogy for 25 of the 26 soil samples was determined by x-ray diffraction analysis. The fine fraction of the twenty-sixth sample was dropped onto the floor during sieving, as was not tested. For samples with greater than trace amounts, smectite content ranged from 1% to 10%, with a mean of 6.2% and a standard deviation of 2.2%; illite content ranged from 1% to 3% with a mean of 1.8% and a standard deviation of 0.8%; mixed illite-smectite ranged from 1% to 3% with a mean of 1.8% and a standard deviation of 0.8%; and kaolinite content ranged from 1% to 3% with a mean of 1.8% and a standard deviation of 0.7. Chlorite was absent from all of the samples tested; however, quartz, calcite, and feldspar were present in a number of samples. Clay mineralogy analysis results are tabulated in Appendix D.

STABILITY ANALYSES

Pre-Failure

Rigorous evaluation of slope stability requires complete knowledge of slope geometry, soil properties, and pore water pressures along potential failure surfaces, which we do not possess. We were, nonetheless, able to use the method of Janbu (1973) to evaluate some geologically-reasonable possibilities by assuming that the debris flow mobilized by remolding of landslide material (*e.g.*, Johnson, 1984). Results are presented in terms of the conventional factor of safety against sliding, which is the ratio of resisting forces to driving forces along a potential failure surface. Factors of safety less than unity indicate an unstable slope, whereas factors of safety greater than unity indicate a stable slope.

Original topography and four possible slip surfaces (Figure 8) were inferred on the basis of field observations and mapping, and our laboratory analyses suggested that a moist soil density of 1700 kg/m^3 (106 pounds per cubic foot *or* pcf) is a good first estimate. Because we have no information about pore

water pressures along any of the four failure surfaces, we examined two limiting cases: zero pore pressure (which we refer to as "dry") and a phreatic surface coincident with the ground surface (which we refer to as "wet"). The very coarse-grained nature of the debris, which ranged from sand to 0.25 m (10 in) cobbles, made it impossible to collect representative undisturbed samples and ruled out laboratory estimates of shear strength. Therefore, one of the goals of our stability analyses was to back-calculate maximum possible angles of internal friction for different failure masses. In order to eliminate one degree of freedom in the Terzaghi-Coulomb failure equation, we also assumed zero cohesive strength along the failure surface although, as emphasized by Fleming *et al.* (1990), a small amount of cohesive strength can be the difference between stability and instability of coarse-grained deposits.

We back-calculated maximum possible angles of internal friction, ϕ, for slopes 1 through 3 by trial and error, adjusting values until we obtained factors of safety close to 1 for wet conditions. Final values were $\phi = 30°$ for slope 1, $\phi = 27°$ for slope 2, and $\phi = 26°$ for slope 3, which are noticably lower than residual values estimated from direct shear testing (previous section). Therefore, for a given angle of internal friction slope 1 is the least stable and slope 3 is the most stable. We also analyzed slope 4 in order to determine whether mobilization of the entire stream terrace could have been triggered by a small slide loading the head of the slope, but a wet factor of safety of approximately 2.7 for $\phi = 30°$ suggests that such a scenario is unlikely.

Plots of local factor of safety (Figure 9), found by dividing the driving force into the resisting force for each slice, show that slopes 1 through 3 are supported by the toe of the stream terrace, beneath which the slopes of the potential failure surfaces decrease. Slope 4 is supported by slice 4, beneath which the potential failure surface is horizontal. Conversely, the lowest factors of safety, particularly for wet slopes, were calculated for slices beneath which the slopes of the potential failure surfaces are the greatest. Complete computer listings of these results are given in Appendix E. Slices with factors of safety greater than 1 are analogous to the "self-supporting ground" of Baum *et al.* (in press), in which shearing resistance of the soil is greater than the driving force due to its own weight.

Debris Strength

Johnson (1970, 1984) presents three techniques for estimating the maximum Bingham shear strength of debris. Two of the techniques, which require knowledge of channel geometry and size of the largest boulders transported by the flowing debris, could not be applied to the Cordova flow because channelization was weak to nonexistent and boulder size was limited by the nature of the source materials, which contained clasts only as large as cobbles. We can, however, estimate the maximum Bingham shear strength of the flowing debris from snout thickness using (Johnson, 1970, p. 503):

$$k = T_k \rho_d g \sin \delta \qquad \text{Eq. 1}$$

where k is shear strength, T_k is the thickness below which viscous flow cannot occur, ρ_d is the density of the debris, g is gravitational acceleration, and δ is the slope of the surface of the debris just above the snout[1]. In Eq. 1 it is implicit that debris movement ceased when total debris thickness decreased to the critical plug thickness T_k, and that the snout thickness represents the critical thickness of the rigid debris plug at the top of the flow. We estimate density of the flowing debris, however, somewhat differently than does Johnson (1984). Our laboratory data suggest an average dry bulk density on the order of ρ_{dry} = 1700 kg/m^3 (106 pcf); therefore, if we assume a grain density of ρ_g = 2700 kg/m^3 (168 pcf) to reflect the quartzo-feldspathic mineralogy, we can estimate porosity as:

$$n = 1 - (\rho_{dry}/\rho_g) \qquad \text{Eq. 2}$$

Using the densities cited above, we estimate that $n = 0.37$. Further assuming that the debris was completely saturated as it came to rest, bulk density can be estimated as:

$$\rho_d = (1 - n)\,\rho_g + n\,\rho_{water} \qquad \text{Eq. 3}$$

which gives a value of ρ_d = 2071 kg/m^3 (129 pcf) for the Cordova debris flow. Slope of the debris surface just behind the snout of the Cordova debris is about 4° and snout thickness is about 2 m (6.4 ft), giving a shear strength of k = 2.8 kPa (0.4 pounds per square inch *or* psi) for the saturated debris under a maximum of 41 kPa (5.9 psi) lithostatic stress. For comparison, Johnson (1984) estimates k = 2.0 kPa (0.3 psi) for a debris flow on the Surprise Canyon alluvial fan in Panamint Valley, California, and an average of k = 0.2 kPa (0.02 psi) for more fluid debris flows in the San Joaquin Valley, California. Our saturated direct shear tests, described above, yielded values of k = 40 kPa (5.8 psi) and k = 67 kPa (9.7 psi) peak shear strength for normal stresses of 51 kPa (7.4 psi) and 101 kPa (14.6 psi), so the strength of the flowing debris must have been about an order of magnitude less than the strength of the original stream terrace sands. As above, we note that the recompacted material used for the direct shear tests was denser than the undisturbed sample from which it was taken, which may have introduced some error into our results.

Post-Failure

We envision two possibilities for remobilization of the existing debris mass. First, the flow could be initiated by sliding, the likelihood of which can be determined using a limit-equilibrium stability analysis. The factor of safety against sliding for a fully-saturated, infinitely long and wide soil mass with slope parallel seepage is approximated by the well-known equation:

$$F = (1/2)\tan\phi/\tan\beta \qquad \text{Eq. 4}$$

If we assume that ϕ = 30°, the value back-calculated for the source material in the previous section, then we

[1] Note that English equivalents of density are given in terms of unit weight. Therefore, if English units are used, the g term should be eliminated from Eq. 1.

would expect the debris mass to be stable on slopes of $\beta < 15°$. Potential failure surface and debris surface slopes in the field are very low, generally only a few degrees, so the debris mass would appear to be stable even if completely saturated. The factor of safety for a dry infinite slope is approximately twice that given by Eq. 4. However, because our back-calculated value is a maximum possible value, it is likely that in reality $\phi < 30°$. In order to consider the possible consequences of under-estimating ϕ, we calculated factors of safety for $20° < \phi < 30°$ and $0° < \phi < 10°$ (Figure 10) and found that $F > 1$ for slopes as steep as $\beta = 10°$ and angles of internal friction as low as $\phi = 20°$. Second, the flow could be initiated by the so-called "firehose effect" (Johnson, 1984), in which debris is mobilized when struck by fast-moving water. This mechanism is apparently rare, and is most often associated with loose talus at the mouths of steep, narrow channels. Barring a catastrophic flood, in which mobilization of the debris mass would be of comparatively minor concern, the second possibility can be discounted.

DISCUSSION

Our investigations lead us to conclude that the Cordova debris flow mobilized from a landslide– which was in turn caused by the accumulation of perched water along a sloping buried soil horizon– in Holocene stream terrace deposits along the Rio Quemado. Three lines of evidence lead us to conclude that the terrace must have been almost completely saturated before failure. These are:

- Remolding of debris and increased water content is necessary in order to transform landslides into debris flows (Johnson, 1984; Fleming *et al.*, 1989). The lack of large, intact blocks of terrace material within the debris, even at elevations well above stream level, shows that the debris must have been completely mobilized before it reached the Rio Quemado.

- Eyewitnesses reported considerable seepage from the head scarp for a short time after failure, which is supported by our observations of braided channel and small alluvial fan deposits running downslope from the head scarp.

- Limit equilibrium stability analyses of completely saturated slopes yield reasonable back-estimates for the angle of internal friction. Had the slope not been fully saturated, the terrace sands and gravels would have had to have been unrealistically weak in order for failure to have occurred. Moreover, if the somewhat higher laboratory shear strength values are correct, then artesian pore pressures must have existed in order for failure to have occurred.

Given the lack of antecedent rainfall, the only likely sources of water were irrigation and *acequia* leakage. Historical problems with the *acequia* gradient directly above the head scarp suggest that the failure was progressive, and not the direct result of any single irrigation. However, the fact that the stream terrace was being irrigated immediately before failure suggests that excessive irrigation exacerbated a pre-existing condition.

Geologic evidence also implies that terraces along the Rio Quemado have been well-drained,

unsaturated, and stable throughout throughout the Holocene. Neither our field reconnaissance nor the air photo inventories of Guzetti and Brabb (1987) yield any evidence of prior slope stability problems along the Rio Quemado or nearby valleys. In addition, Gile *et al.* (1966, p. 348) state that soils with calcic horizons, which are weakly developed throughout the terrace sequence, were probably never affected by capillary rise from shallow water tables. Therefore, complete saturation must have been an event unprecedented in the geologic history of the stream terrace. This finding suggests that potential for debris flows cannot be be evaluated solely by examining the geologic record for evidence of past occurrences. The impact of fuman activity-- for example, roadbuilding, irrigation, or logging-- on debris flow susceptibility must therefore be evaluated using rational as well as empirical methods.

Ellen and Fleming (1987) and Fleming *et al.* (1989) analyzed in detail the mobilization of debris flows from landslides in the San Francisco Bay region during a heavy storm. Landslides in contractive soils tended to mobilize suddenly and completely, whereas landslides in dilative soils tended to mobilize slowly and partially. Fleming *et al.* (1989) were also able to measure 2% to 5% volume increases near the failure surface of dilative landslide blocks. We do not know how long it took to moblize the Cordova debris flow from the original landslide, but it was certainly less than 8 or 10 hours. Complete moblization of the debris well above the elevation of the Rio Quemado means that flow must have been possible without the addition of excess water. Comparison of limit equilibrium stability analysis results from four trial slopes shows that the entire terrace probably failed simultaneously as one large landslide, rather than sequentially as a series of smaller slides. In addition to inferring contractive behavior from field observations, we also observed contraction during two of three direct shear tests. Ellen and Fleming (1987) also introduce the approximate mobility index (AMI), which is the ratio of saturated water content to liquid limit. Based upon their field observations, Ellen and Fleming conclude that soils with AMI > 1.00 can flow without the addition of any water, whereas soils with 1.00 > AMI > 0.45 can flow only if water is added. They did not observe any flows mobilized from soils with AMI < 0.45. Moreover, rapidly-moving flows were composed of primarily sand and gravel, whereas slowly-moving flows were composed of primarily silt with less sand and gravel. Calculation of porosity using the dry densities in Table 1 and an assumed grain density of 2700 kg/m^3 yields values between 36% and 50% for our undisturbed sand and gravel samples, and comparison with whole-sample liquid limits in the range of 13% to 16% suggests that 2 < AMI < 3 for terrace deposits near Cordova.

Although well-drained terrace deposits such as those near Cordova are naturally unsaturated and stable, AMI values in the range of 2 to 3 suggest to us that prolonged and frequent irrigation or undetected *acequia* leakage increases the danger of debris flow similar to the event of June 8. Comparison of our field and laboratory results with those of Ellen and Fleming (1987) and Fleming *et al.* (1989) leads us to believe that

mobilization of contractive stream terrace deposits will occur suddenly and with little or no sensible warning. The flowing debris can be expected to move rapidly, posing a threat to humans, livestock, and structures directly down gradient.

It is unrealistic to suggest that irrigation of stream terraces be prohibited in order to reduce debris flow hazards, particularly since terraces may provide the only pasture land available in narrow valleys. Our experience with the Cordova debris flow, however, does lead us to recommend that:

- Irrigation of stream terraces, particularly those above or directly upstream from homes, be discouraged or limited to a bare minimum.

- *Acequias* be inspected regularly for signs of leakage or progressive failure. In areas where failure may be imminent, we suggest that irrigation be curtailed and a detailed site investigation be conducted in order to mitigate the hazard. Piezometers and tiltmeters might also be installed to monitor pore water pressure and slope deformation in areas where sudden failure would be life-threatening. Leakage can be significantly reduced by lining *acequias* with clay, plastic sheeting, or culverts.

- Approximate mobility indices (AMIs) be routinely calculated in order to estimate the susceptiblity of slopes to mobilization in the event of landsliding. Reconnaissance studies combining engineering geologic mapping with AMI estimates can provide a useful first estimate of debris flow susceptibility in irrigated mountain valleys.

Acknowledgements.– This project was funded by the New Mexico Bureau of Mines and Mineral Resources and the New Mexico Tech Department of Mining, Environmental and Geological Engineering. David Love, Garret Ross, and Susan Schima assisted with field and laboratory work. Frank Kottlowski reviewed a draft of this report, and made several suggestions that helped to clarify several points. Rex Baum of the U.S. Geological Survey kindly provided a preprint on longitudinal forces in landslides. John Hall performed the x-ray diffraction tests, and George Austin interpreted the results. John Hawley provided information on the buried soils and local stratigraphy, and Chris Trujillo of Cordova allowed access to his land.

REFERENCES

Baltz, E.H., 1978, Resume of the Rio Grande depression in north-central New Mexico, *in* J.W. Hawley, compiler, Guidebook to the Rio Grande rift in New Mexico and Colorado: New Mexico Bureau of Mines & Mineral Resources Circular 163, p. 210-228.

Baum, R.L., Fleming, R.W., and Ellen, S.D., *in press*, Longitudinal forces in landslides– A comparison between field observations and a one-dimensional model: Geological Society of America Bulletin.

Das, B.M., 1983, Advanced Soil Mechanics: Washington, DC, Hemisphere Publishing, 511 p.

Ellen, S.D., and Fleming, R.W., 1987, Mobilization of debris flows from soil slips, San Francisco Bay region, California, *in* J.E. Costa and Wieczorek, G.F., Debris Flows/Avalanches: Geological Society of America, Reviews in Engineering Geology, Vol. VII, p. 31-40.

Fleming, R.W., Ellen, S.D., and Algus, M.A., 1989, Transformation of dilative and contractive landslide debris into debris flows– an example from Marin County, California, *in* A.M. Johnson, C.W. Burnham, C.R. Allen, and W. Muehlberger, editors, Richard H. Jahns Memorial Volume: Engineering Geology, v. 27, p. 201-233.

Gile, L.H., Peterson, F.F., and Grossman, R.B., 1966, Morphological and genetic sequences of carbonate accumulation in desert soils: Soil Science, v. 101, p. 347-360.

Guzetti, F. and Brabb, E.E., 1987, Map showing landslide deposits in northwestern New Mexico (1:500,000): U.S. Geological Survey Open File Report 87-70, 2 sheets.

Hunt, R.E., 1986, Geotechnical Engineering Analysis and Evaluation: New York, McGraw-Hill, 729 p.

Janbu, N., 1973, Slope stability computations, *in* R.C. Hirschfield and S.J. Poulos, editors, Embankment Dam Engineering (Casagrande Volume) : New York, Wiley-Interscience, p. 47-86.

Johnson, A.M., 1970, Physical Processes in Geology: San Francisco, Freeman-Cooper, 576 p.

Johnson, A.M., with contributions by Rodine, J.R., 1984, Debris flow, *in* D. Brunsden and D.B. Prior, editors, Slope Instability: London, Wiley, p. 257-361.

Keaton, J.R., 1984, Genesis-lithology-qualifier (GLQ) system of engineering geology mapping symbols: Bulletin of the Association of Engineering Geologists, v. XXI, p. 355-364.

Miller, J.P., Montgomery, A., and Sutherland, P.K., 1963, Geology of part of the southern Sangre de Cristo Mountains, New Mexico: New Mexico Bureau of Mines and Mineral Resources Memoir 11, 106 p.

Miller, J.P. and Wendorf, F., 1958, Alluvial chronology of the Tesuque Valley, New Mexico: Journal of Geology, v. 66, p. 117-194.

FIGURE CAPTIONS

Figure 1.– Index map of the study area showing towns, drainages, and topography. Approximate location of the Cordova debris flow is marked by a circle NE of the town.

Figure 2.– Small alluvial deposit, As-k(f), in center and foreground of photo. These water-laid deposits eminate from the base of the scarp. Poorly-sorted slump material, Soc-k(sl), containing woody debris and grassy blocks of A-horizon soil, covers As-k(f) alluvial deposits in center left and center right of photo. Geologist for scale.

Figure 3.– Poorly sorted, clayey to cobbley main debris flow deposit, Soc-k(fl), with scarp in background. Note transverse ridges or waves.

Figure 4.– Exposure of undisturbed Holocene terrace deposits, A/Roc-k(te) truncated by buried soil horizons. Original terrace stratification is horizontal, but is largely obscured by steeply-dipping soil profiles typically consisting of a dark A horizon, a tan B horizon, and a light-colored B_k horizon. Pick-axe for scale.

Figure 5.– Engineering geologic map and interpretive cross-sections of the Cordova debris flow. Topography and major geologic boundaries mapped with a plane table and alidade at a scale of 1:300. Large figure in pocket.

Figure 6.– Lowermost exposed buried soil horizon, illustrating dark gray to black A horizon, orange B horizon, and cobble-rich calcic B_k horizon.

Figure 7.– Coarse fraction grain size distribution curves for undisturbed terrace (top), debris flow (middle), and alluvial (bottom) samples from the Cordova debris flow. Sieve sizes used for analyses were nos. 4, 10, 20, 40, 60, 100, and 200.

Figure 8.– Geometry of the four pre-flow stream terrace slopes analyzed using Janbu's method. Angles of internal friction, ϕ, were adjusted by trial and error until an average factor of safety of $F = 1$ was found for fully-saturated conditions.

Figure 9.– Local factors of safety, calculated by dividing the driving force into the resisting force for each slice in the Janbu analysis, for the pre-flow stream terrace. Angle of internal friction, ϕ, is the value back-calculated by assuming that $F = 1$. Slice numbers for each of the four slopes correspond to those shown in Figure 8.

Figure 10.– Factor of safety against sliding for a fully-saturated infinite slope, used to estimate the stability of the post-flow debris mass.

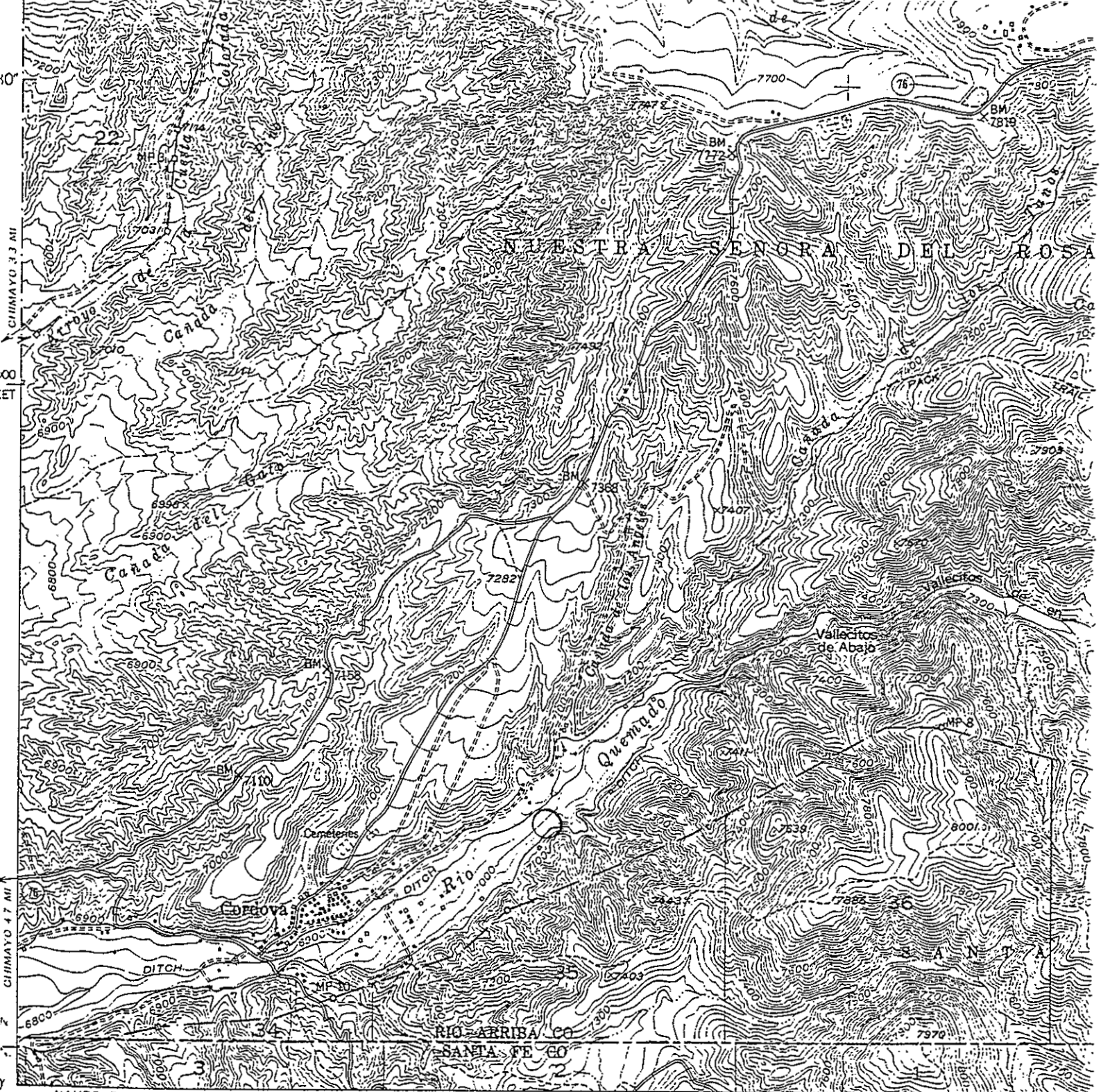

SCALE 1:24000

1 MILE

1000 0 1000 2000 3000 4000 5000 6000 7000 FEET

1 KILOMETER

CONTOUR INTERVAL 20 FEET

DATUM IS MEAN SEA LEVEL

NEW MEXICO

QUADRANGLE LOCATION

○ LOCATION OF FLOW

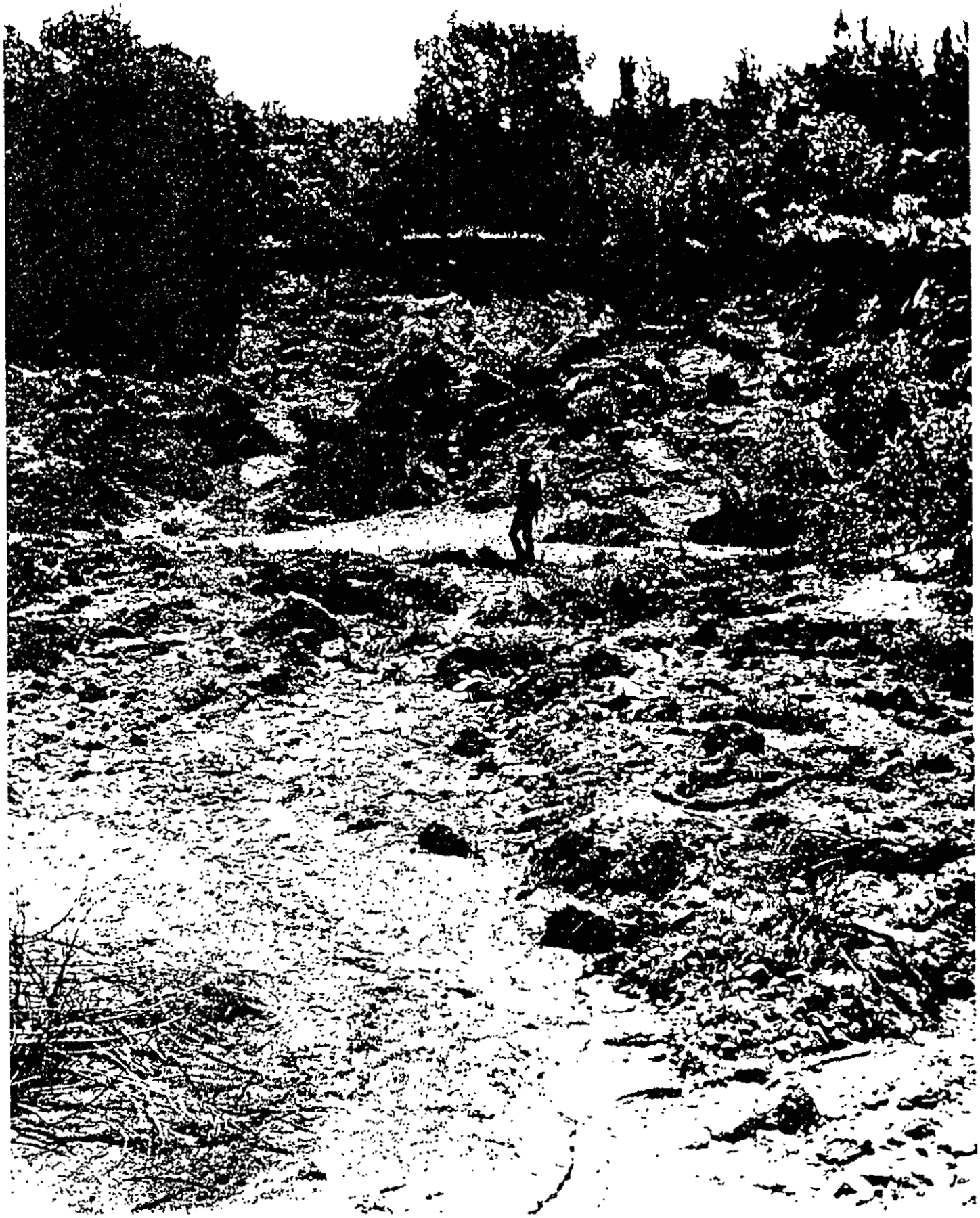

Fig. 2.

Fig. 2

FIG. 4

ENGINEERING GEOLOGIC MAP OF THE CORDOVA DEBRIS FLOW OF JUNE 8, 1990

Mapped by W. Haneberg, G. Tripp, & G. Ross

June 14–15, 1990

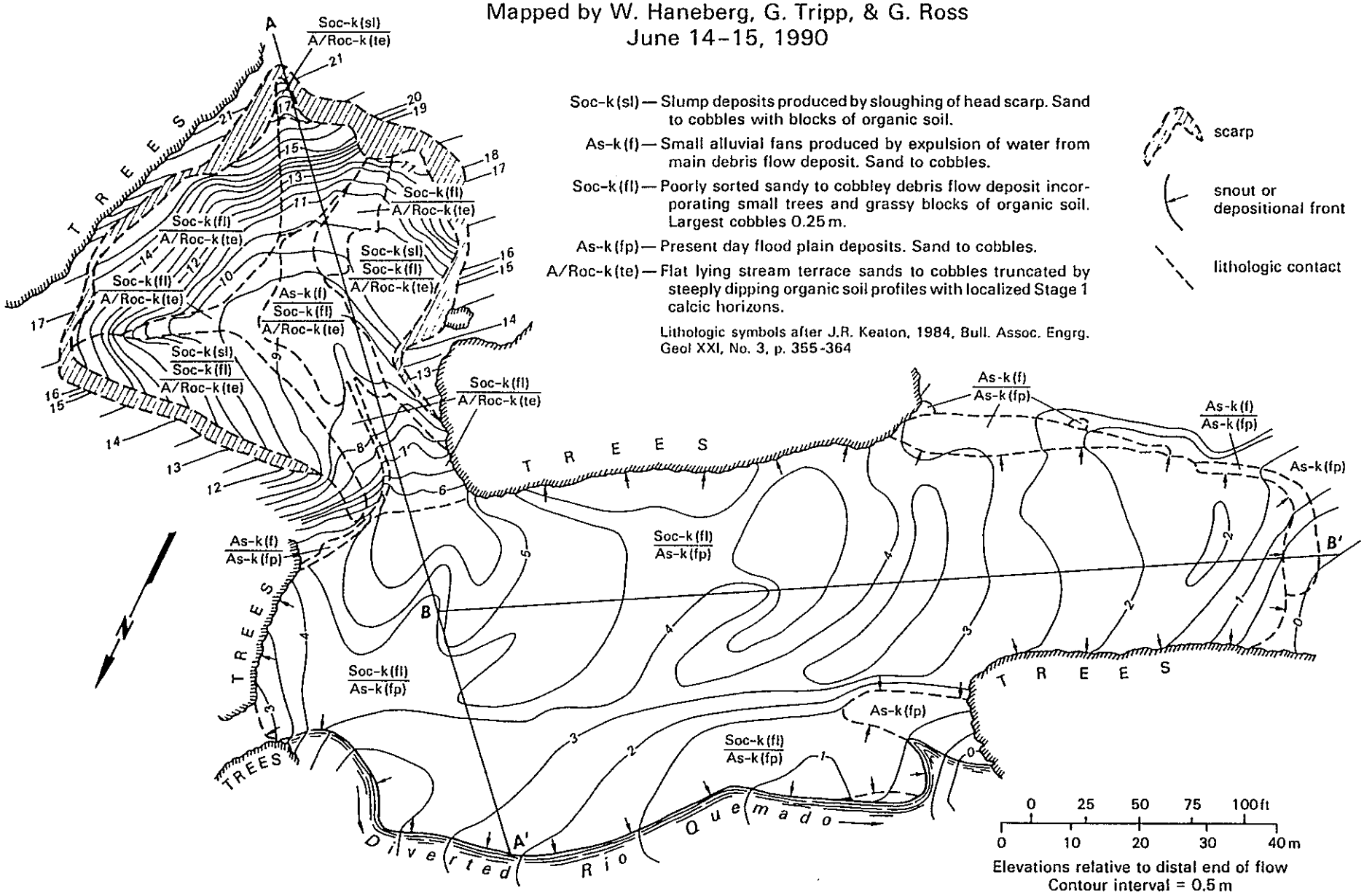

Soc-k(sl) — Slump deposits produced by sloughing of head scarp. Sand to cobbles with blocks of organic soil.

As-k(f) — Small alluvial fans produced by expulsion of water from main debris flow deposit. Sand to cobbles.

Soc-k(fl) — Poorly sorted sandy to cobbley debris flow deposit incorporating small trees and grassy blocks of organic soil. Largest cobbles 0.25 m.

As-k(fp) — Present day flood plain deposits. Sand to cobbles.

A/Roc-k(te) — Flat lying stream terrace sands to cobbles truncated by steeply dipping organic soil profiles with localized Stage 1 calcic horizons.

Lithologic symbols after J.R. Keaton, 1984, Bull. Assoc. Engrg. Geol XXI, No. 3, p. 355-364

scarp

snout or depositional front

lithologic contact

0 25 50 75 100 ft

0 10 20 30 40 m

Elevations relative to distal end of flow

Contour interval = 0.5 m

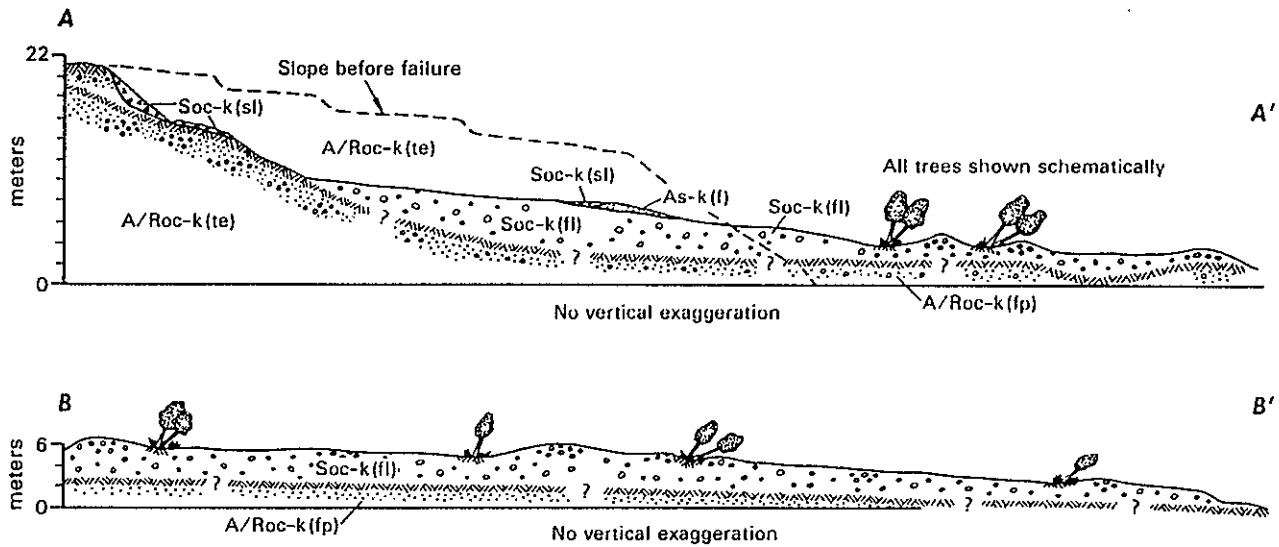
A
A'
22
0
meters
Slope before failure
Soc-k(sl)
A/Roc-k(te)
Soc-k(sl)
As-k(f)
Soc-k(fl)
All trees shown schematically
A/Roc-k(te)
Soc-k(fl)
A/Roc-k(fp)
No vertical exaggeration
B
B'
6
0
meters
Soc-k(fl)
A/Roc-k(fp)
No vertical exaggeration

Fig 56

FIG. 6

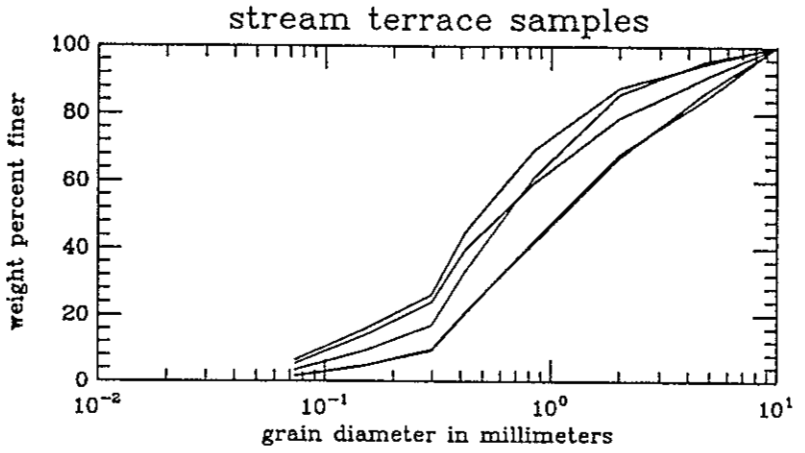
stream terrace samples
weight percent finer
100
80
60
40
20
0
10^{-2}
10^{-1}
10^{0}
10^{1}
grain diameter in millimeters

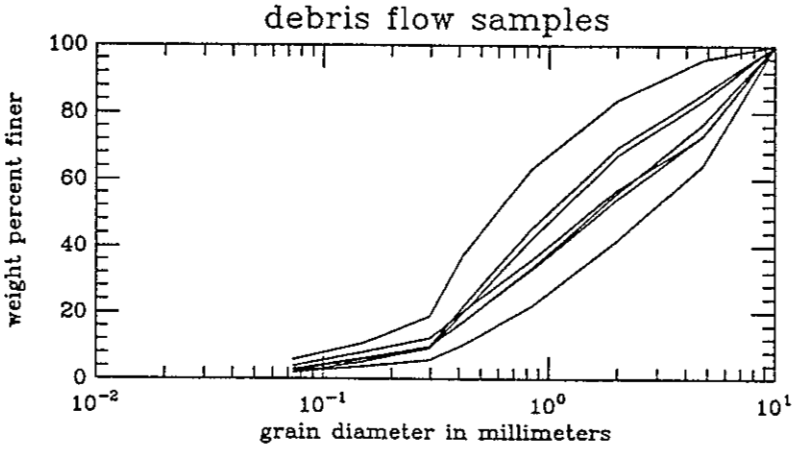
debris flow samples
weight percent finer
100
80
60
40
20
0
10^{-2}
10^{-1}
10^{0}
10^{1}
grain diameter in millimeters

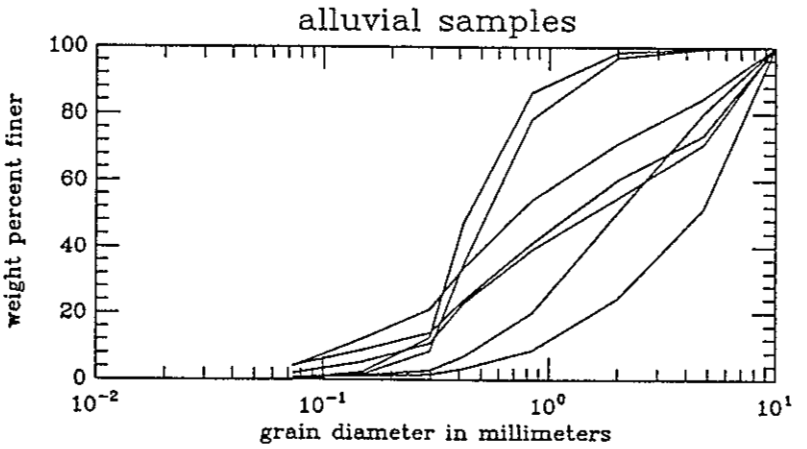
alluvial samples
weight percent finer
100
80
60
40
20
0
10^{-2}
10^{-1}
10^{0}
10^{1}
grain diameter in millimeters

Fig. 7

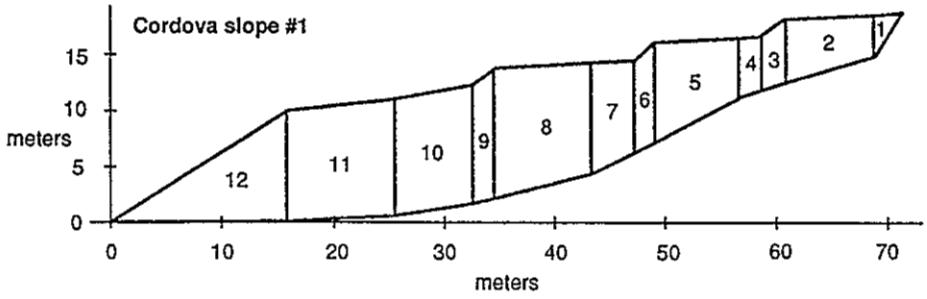
Cordova slope #1
meters
0
5
10
15
0
10
20
30
40
50
60
70
meters
12
11
10
9
8
7
6
5
4
3
2
1

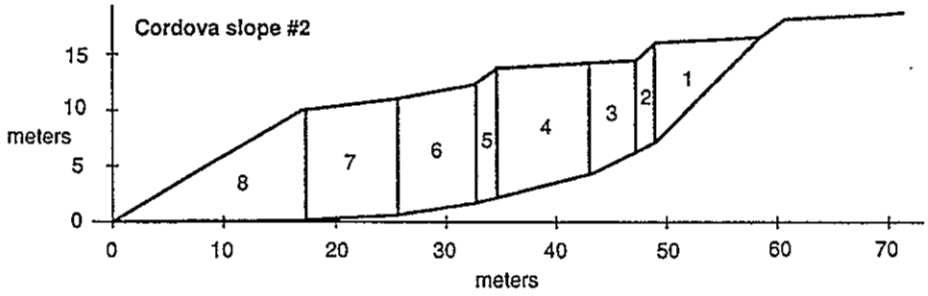
Cordova slope #2
meters
0
5
10
15
0
10
20
30
40
50
60
70
meters
8
7
6
5
4
3
2
1

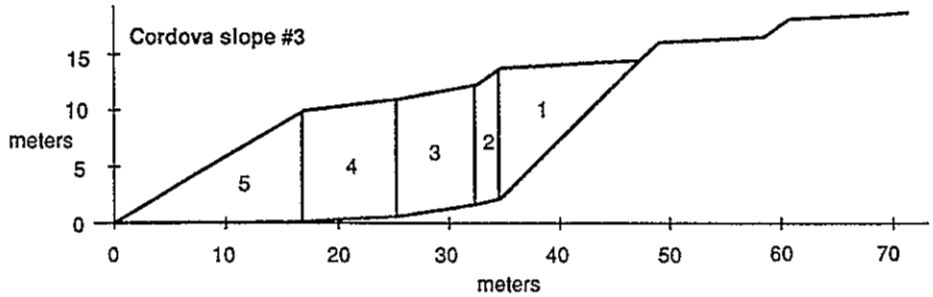
Cordova slope #3
meters
0
5
10
15
0
10
20
30
40
50
60
70
meters
5
4
3
2
1

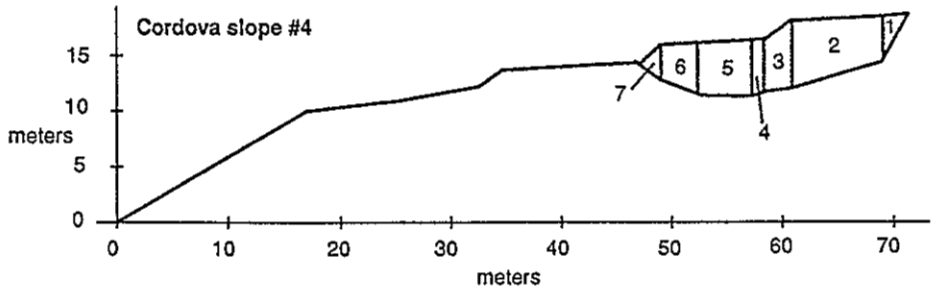
Cordova slope #4
meters
0
5
10
15
0
10
20
30
40
50
60
70
meters
7
6
5
4
3
2
1

FIG. 8

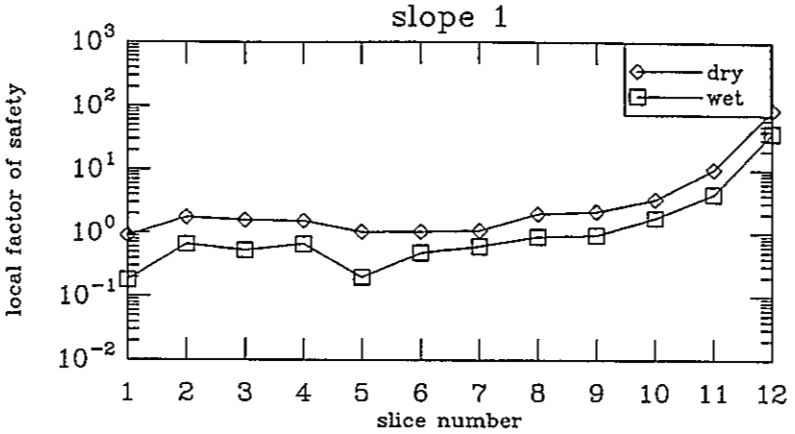
slope 1
local factor of safety
10^3
10^2
10^1
10^0
10^{-1}
10^{-2}
dry
wet
1 2 3 4 5 6 7 8 9 10 11 12
slice number

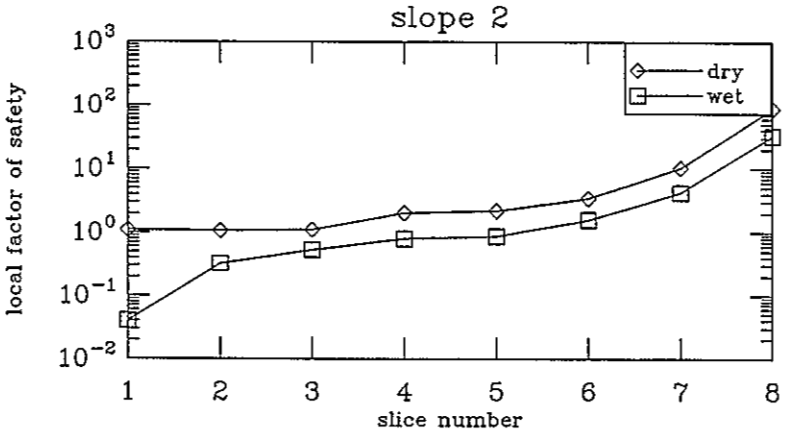
slope 2
local factor of safety
10^3
10^2
10^1
10^0
10^{-1}
10^{-2}
dry
wet
1 2 3 4 5 6 7 8
slice number

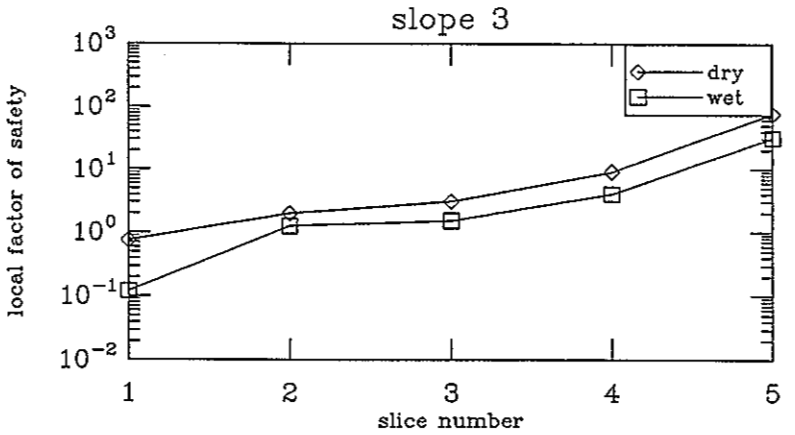
slope 3
local factor of safety
10^3
10^2
10^1
10^0
10^{-1}
10^{-2}
dry
wet
1 2 3 4 5
slice number

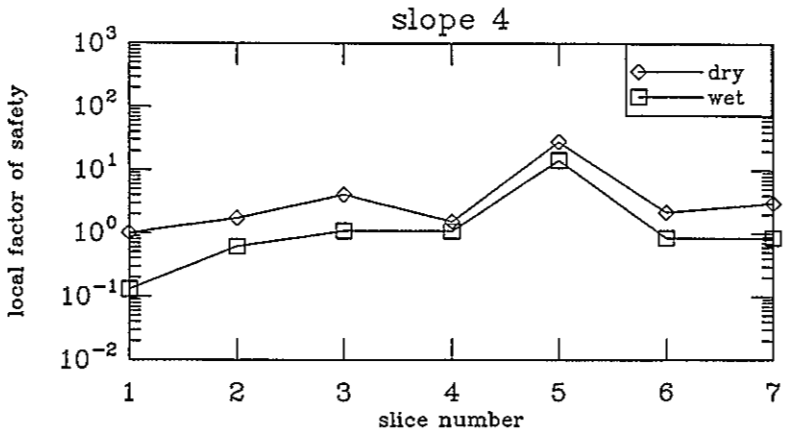
slope 4
local factor of safety
10^3
10^2
10^1
10^0
10^{-1}
10^{-2}
dry
wet
1 2 3 4 5 6 7
slice number

FIG. 9

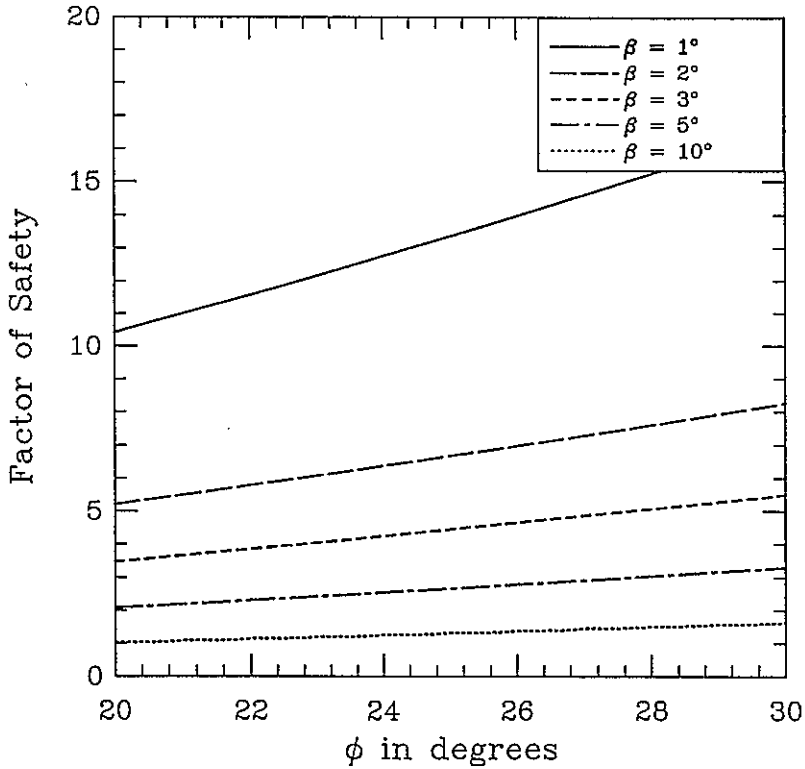
Factor of Safety
20
15
10
5
0
20
22
24
26
28
30
ϕ in degrees
β = 1°
β = 2°
β = 3°
β = 5°
β = 10°

FIG. 10

TABLE 1- Summary of geotechnical properties of samples from the Cordova debris flow of June 8, 1990. Sample locations shown in Figure 5.

sample location	state (D/U)[1]	description	uniformity coefficient[2]	gradation coefficient[3]	fines (weight %)[4]	moisture content (weight %)	dry density (kg/m^3)	Atterburg limits plastic	liquid	plasticity index	USCS class
1	D	buried A horizon	-.-	-.-	52.4	21.3	1380	12.1	32.0	19.9	CL
2	U	unfailed terrace	5.8	0.9	1.6	3.9	1560	---.-	---.-	---.-	SW
3	U	"	5.3	1.2	3.5	7.6	1570	---.-	---.-	---.-	SP
4	U	debris mass	9.6	0.9	3.1	8.0	1430	12.9	---.-	---.-	SW
5	U	"	12.0	0.8	3.9	7.8	1660	11.4	---.-	---.-	SW
6	U	unfailed terrace	6.2	1.4	6.5	16.2	1490	---.-	---.-	---.-	SW-ML
7	U	"	6.0	1.0	1.7	4.0	1600	---.-	---.-	---.-	SW
8	U	alluvial deposit	11.1	0.8	4.2	10.4	1780	---.-	---.-	---.-	SP
9	D	"	5.1	1.3	0.8	0.4	1620	---.-	---.-	---.-	SP
10	U	unfailed terrace	8.1	1.0	5.4	11.2	1460	14.7	16.6	1.9	SW-ML
11	D	alluvial deposit	2.0	1.3	0.2	0.6	1500	---.-	---.-	---.-	SP
12	D	"	2.0	1.1	0.2	1.1	1510	---.-	---.-	---.-	SP
13	D	"	11.3	0.5	1.9	2.6	1620	---.-	---.-	---.-	SP
14	U	debris mass	1.0	1.0	1.9	5.0	1720	---.-	---.-	---.-	SW
15	D	"	5.7	1.2	5.8	7.2	1440	---.-	---.-	---.-	SW
16	D	alluvial deposit	7.2	1.1	0.6	0.3	1660	---.-	---.-	---.-	SP
17	D	buried A horizon	-.-	-.-	52.5	11.5	920	10.4	20.6	10.2	CL
18	U	debris mass	5.9	0.8	2.0	5.1	1520	---.-	---.-	---.-	SW
19	U	"	6.0	0.8	1.9	5.1	1530	---.-	---.-	---.-	SP
20	D	alluvial deposit	7.9	0.9	4.1	5.4	1350	---.-	---.-	---.-	SP
21	U	buried A horizon	-.-	-.-	35.4	16.2	1570	10.6	13.9	3.3	ML
22	U	debris mass	10.4	0.9	2.6	9.5	1520	12.3	13.6	1.3	SW
23	D	buried B horizon	-.-	-.-	52.2	14.1	980	11.5	23.5	12.0	CL
24	U	buried B horizon	-.-	-.-	52.3	18.1	1380	11.5	27.8	16.3	CL
25	U	buried A horizon	-.-	-.-	55.7	20.3	1380	10.5	20.5	10.0	CL
26	U	buried B horizon	-.-	-.-	56.4	21.2	1180	14.1	24.1	10.0	CL

[1] U = undisturbed, D = disturbed

[2] D_{60}/D_{10}

[3] $(D_{30})^2/(D_{60}\,D_{10})$

[4] grain diameter < 70 μm

Table 2– Results of direct shear testing, sample #10.

	density		$\tau = \sigma \tan \phi$		$\tau = c + \sigma \tan \phi$			
	undisturbed	recompacted	peak	residual	peak		residual	
			ϕ	ϕ	c	ϕ	c	ϕ
dry	1460 kg/m^3	1830 kg/m^3	41°	29°	21 kPa	32°	20 kPa	18°
saturated	1460 kg/m^3	1665 kg/m^3	36°	34°	10 kPa	32°	12 kPa	28°

APPENDIX A

Soil Mechanics Laboratory Test Results

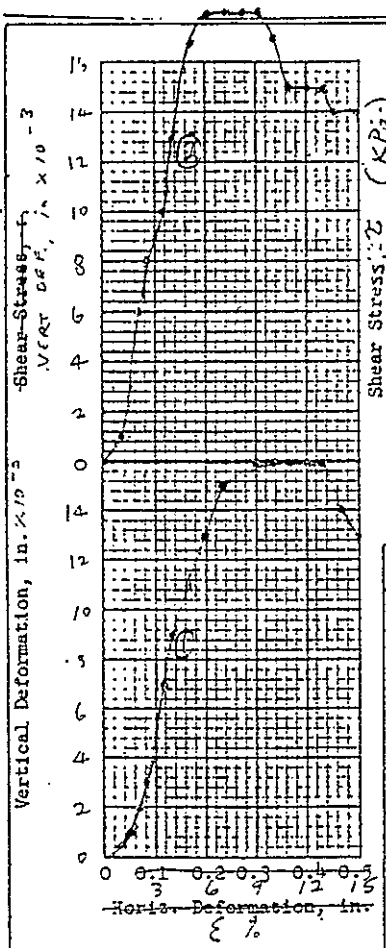

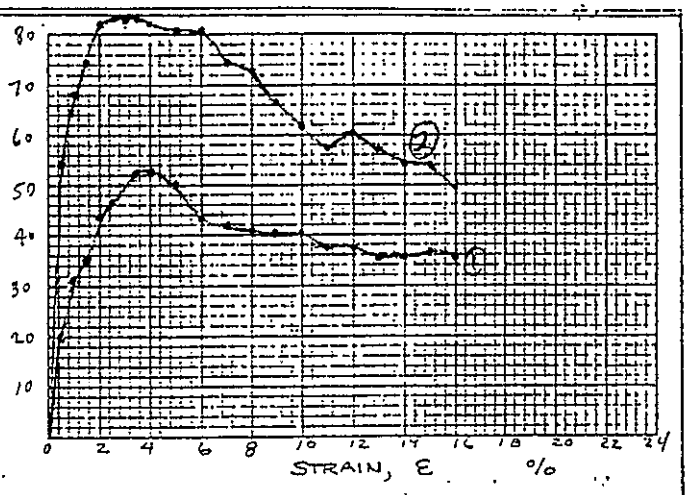

Test No.			1	2		
Initial	Water content	w_o	0 %	0 %	%	%
	Void ratio	e_o	0.45	0.45		
	Saturation	S_o	0 %	0 %	%	%
	Dry density, Mg/m^3	γ_d	1.83	1.83		
Void ratio after consolidation		e_c				
Time for 50 percent consolidation, min		t_{50}				
Final	Water content	w_f	%	%	%	%
	Void ratio	e_f				
	Saturation	S_f	%	%	%	%
Normal stress, KPa		σ	51.1	101.4		
Maximum shear stress, KPa		τ_{max}	52.7	83.6		
Actual time to failure, min		t_f				
Rate of strain,			2% /min	2% /min		
Ultimate shear stress, KPa		τ_{ult}				

Shear Strength Parameters

ϕ' = 44 °

tan ϕ' = 0.966

c' = 0

☐ Controlled stress

☒ Controlled strain

Type of specimen DEBRIS FLOW (SAND) 31.67 cm. square 1.27 cm. thick

Classification SW-ML

LL 16.6 PL 14.7 PI 1.9 G_s 2.65

Remarks LT BRN WELL GRADED SIL/FINE SAND TO GRAVEL SL. SILTY

Project CORDOVA DEBRIS FLOW

Area

Boring No. Sample No. 10

Depth FT ~ 2 m Date 24/7/90

DIRECT SHEAR TEST REPORT

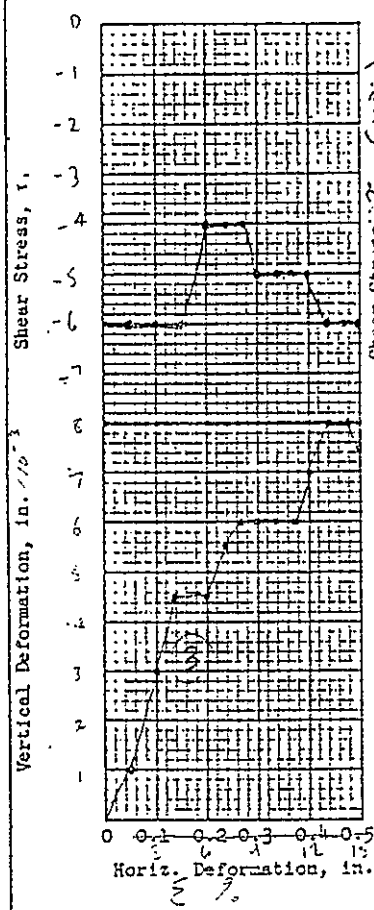

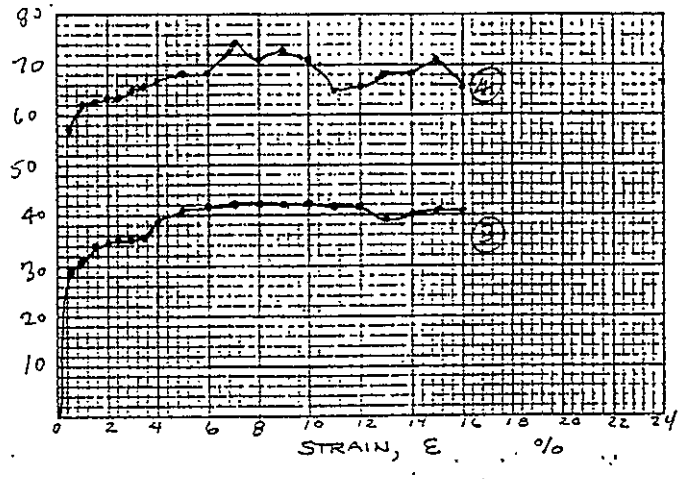

Test No.			3	4		
Initial	Water content	w_o	23 %	22 %	%	%
	Void ratio	e_o	0.61	0.58		
	Saturation	S_o	100 %	100 %	%	%
	Dry density, Mg/m^3	γ_d	1.65	1.68		
Void ratio after consolidation		e_c				
Time for 50 percent consolidation, min		t_{50}				
Final	Water content	w_f	%	%	%	%
	Void ratio	e_f				
	Saturation	S_f	%	%	%	%
Normal stress, KPa		σ	51.1	101.4		
Maximum shear stress, KPa		τ_{max}	41.8	74.4		
Actual time to failure, min		t_f				
Rate of strain,			29./min	27./min		
Ultimate shear stress, KPa		τ_{ult}				

Shear Strength Parameters

ϕ' = _____ °

tan ϕ' = _____

c' = _____

☐ Controlled stress

☒ Controlled strain

Type of specimen DISP. S (SAND) 31.67 cm. square 1.27 cm. thick

Classification SW - ML

LL 16.6 PL 14.7 PI 1.9 G_s 2.65

Remarks LT BPN WELL
BORDER TIL/FELD
SAND TO SAND
SL [illegible]

Project [illegible] : FLOW

Area

Boring No. Sample No. 10

Depth ft Date 10/17/9[illegible]

DIRECT SHEAR TEST REPORT

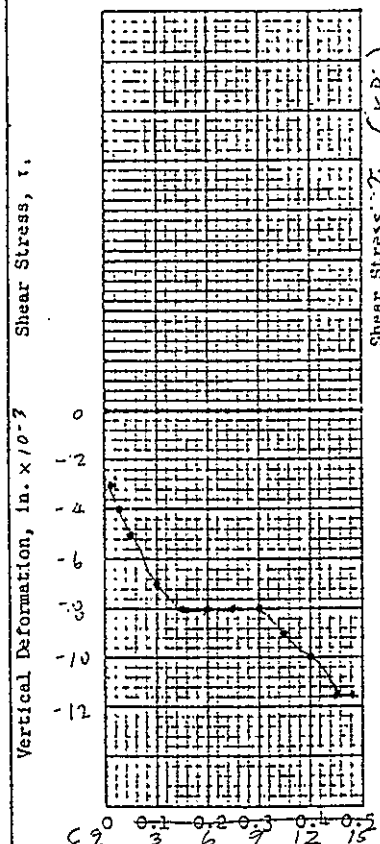

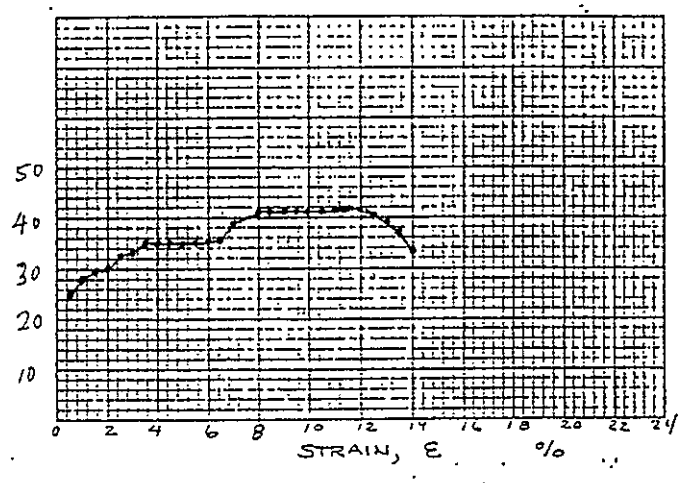

Test No.			5			
Initial	Water content	w_o	28 %	%	%	%
	Void ratio	e_o	0.75			
	Saturation	S_o	100 %	%	%	%
	Dry density, Mg/m³	γ_d	1.51			
Void ratio after consolidation		e_c				
Time for 50 percent consolidation, min		t_{50}				
Final	Water content	w_f	%	%	%	%
	Void ratio	e_f				
	Saturation	S_f	%	%	%	%
Normal stress, KPa		σ	51.1			
Maximum shear stress, KPa		τ_{max}	41.5			
Actual time to failure, min		t_f				
Rate of strain,			0.51/min			
Ultimate shear stress, KPa		τ_{ult}				

Shear Strength Parameters

$\phi' =$ _____ °

$\tan \phi' =$ _____

$c' =$ _____

☐ Controlled stress

☒ Controlled strain

Type of specimen SHELBY : SAND — 31.67 cm. square — 1.27 cm. thick

Classification SW-ML

LL 16.6 — PL 14.7 — PI 1.9 — G_s 2.65

Remarks AT APII WELL GRADED, SIL/FELD SAND W GRAVEL SL SILTY [illegible] SATURATED

Project CORDOVA DEBRIS FLOW

Area

Boring No. — Sample No. 10

Depth 31 ~ 2m — Date 7/29/90

DIRECT SHEAR TEST REPORT

LIQUID AND PLASTIC LIMIT TESTS

Project CORDOVA DEBRIS FLOW Date JUNE 27/90

Boring No. _____ Sample No. 10

LIQUID LIMIT

Run No.		1	2	3	4	5	6
Tare No.		30	31	32	33		
Weight in grams: Tare plus wet soil		18.51	16.49	16.70	16.06		
Tare plus dry soil		17.15	15.14	15.60	15.32		
Water	W_w	1.36	1.35	1.10	0.74		
Tare		8.45	7.69	8.51	10.56		
Dry soil	W_s	8.70	7.45	7.09	4.66		
Water content	w	15.6	18.1	15.5	15.9		
Number of blows		40	13	25	35		

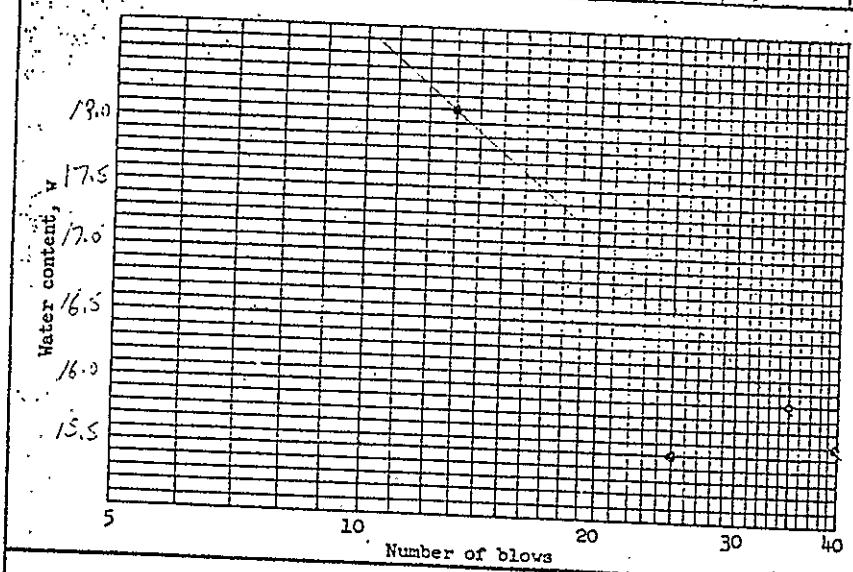

LL 16.6

PL 14.7

PI 1.9

Symbol from plasticity chart

ML

PLASTIC LIMIT

Run No.		1	2	3	4	5	Natural Water Content
Tare No.		22	23				11.2
Weight in grams: Tare plus wet soil		9.86	9.94				
Tare plus dry soil		9.44	9.49				
Water	W_w	0.42	0.45				
Tare		6.44	6.54				
Dry soil	W_s	3.00	2.95				
Water content	w						
Plastic limit		14.0	15.3				

Remarks WALL SAMPLE

Technician _____ Computed by JDT Checked by _____

LIQUID AND PLASTIC LIMIT TESTS

Project CORDOVA DEBRIS FLOW Date JUNE 30/90

Boring No. _____ Sample No. 22

LIQUID LIMIT

Run No.		1	2	3	4	5	6
Tare No.		17	14	16	5		
Weight in grams: Tare plus wet soil		8.08	9.40	7.06	7.81		
Tare plus dry soil		7.27	8.37	6.30	7.06		
Water	W_w	0.81	1.03	0.74	0.75		
Tare		1.08	1.06	1.09	1.08		
Dry soil	W_s	6.19	7.31	5.21	5.98		
Water content	w	13.1	14.1	14.2	12.5		
Number of blows		31	18	22	40		

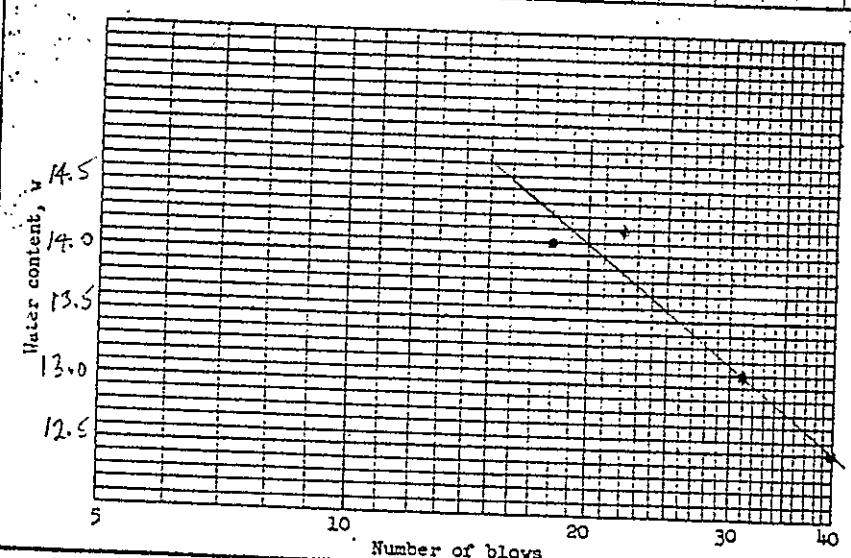

LL 13.6

PL 12.3

PI 1.3

Symbol from plasticity chart

ML

PLASTIC LIMIT

Run No.		1	2	3	4	5	Natural Water Content
Tare No.		1	2				9.5
Weight in grams: Tare plus wet soil		3.66	2.59				
Tare plus dry soil		3.37	2.43				
Water	W_w	0.29	0.16				
Tare		1.08	1.07				
Dry soil	W_s	2.29	1.36				
Water content	w						
Plastic limit		12.7	11.8				

Remarks DEBRIS

Technician _____ Computed by _____ Checked by _____

LIQUID AND PLASTIC LIMIT TESTS

Date June 26/95

Project CORDOVA DEBRIS FLOW

Boring No. _____ Sample No. 21

LIQUID LIMIT

		Run No.	1	2	3	4	5	6
		Tare No.	16	17	18	19		
Weight in grams		Tare plus wet soil	6.88	6.40	5.65	7.10		
		Tare plus dry soil	6.15	5.76	5.11	6.37		
	W_w	Water	0.73	0.64	0.55	0.73		
		Tare	1.09	1.08	1.08	1.09		
	W_s	Dry soil	5.06	4.68	4.03	5.28		
	w	Water content	14.4	13.7	13.6	13.8		
		Number of blows	22	35	30	22		

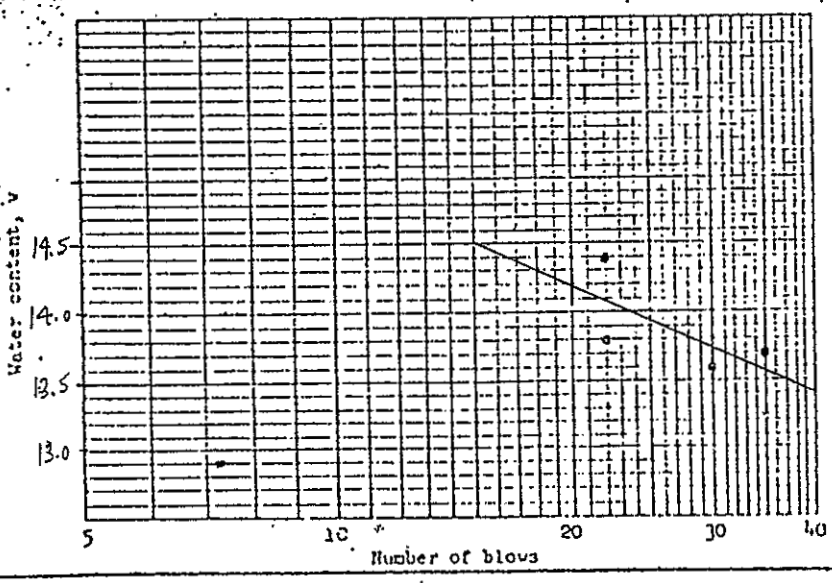

LL 13.9

PL 10.6

PI 3.3

Symbol from plasticity chart

ML

SOFT - DIFFICULT TO ROLL

PLASTIC LIMIT

		Run No.	1	2	3	4	5	Natural Water Content
		Tare No.	13	14	15			
Weight in grams		Tare plus wet soil	3.50	3.02	3.15			
		Tare plus dry soil	3.25	2.85	2.95			
	W_w	Water	0.25	0.17	0.20			
		Tare	1.09	1.06	1.08			
	W_s	Dry soil	2.16	1.79	1.87			
	w	Water content						
		Plastic limit	11.6	9.5	10.7			

Remarks LT GRY TOP 'A' HORIZON

Technician _____ Computed by _____ Checked by _____

LIQUID AND PLASTIC LIMIT TESTS

Date JUNE 26/90

Project CORDOVA DEBRIS FLOW

Boring No. _____ Sample No. 24

LIQUID LIMIT

	Run No.		1	2	3	4	5	6
	Tare No.		8	9	10	11		
Weight in grams	Tare plus wet soil		8.90	8.64	7.16	7.31		
	Tare plus dry soil		7.42	7.09	5.80	5.85		
	Water	W_w	1.50	1.54	1.36	1.51		
	Tare		1.08	1.08	1.08	1.08		
	Dry soil	W_s	6.33	6.00	4.72	4.77		
	Water content	w	23.7	26.0	28.8	31.7		
	Number of blows		34	27	24	20		

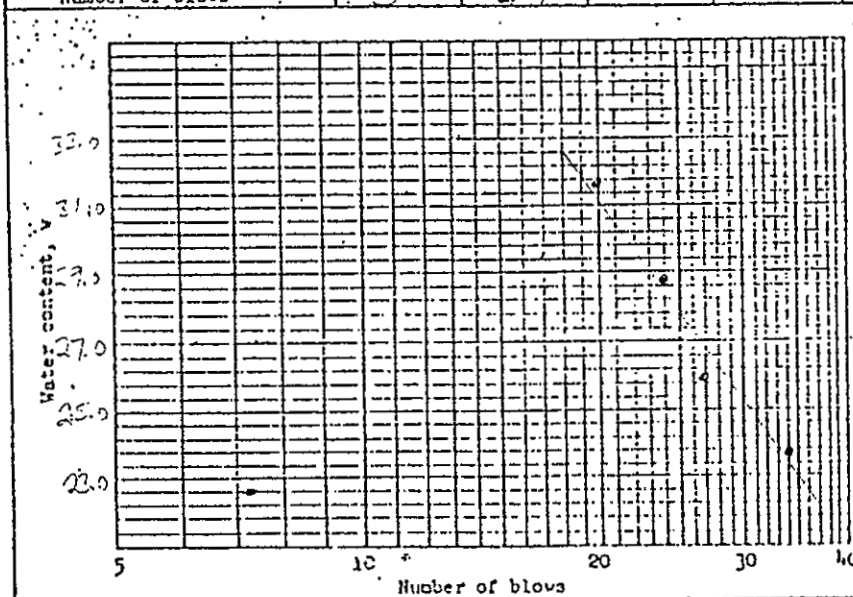

LL 27.8

PL 11.5

PI 16.3

Symbol from plasticity chart

CL

PLASTIC LIMIT

	Run No.		1	2	3	4	5	Natural Water Content
	Tare No.		7	8	9			
Weight in grams	Tare plus wet soil		3.81	4.45	3.78			
	Tare plus dry soil		3.52	4.09	3.51			
	Water	W_w	0.28	0.36	0.27			
	Tare		1.09	1.08	1.08			
	Dry soil	W_s	2.44	3.01	2.43			
	Water content	w						
	Plastic limit		11.5	12.0	11.1			

Remarks TOP 6 INCHES - ROOTS

Technician _____ Computed by JT Checked by _____

LIQUID AND PLASTIC LIMIT TESTS

Date JUNE 26/90

Project CORDOVA DEBRIS FLOW

Boring No. _____ Sample No. 23

LIQUID LIMIT

	Run No.	1	2	3	4	5	6
	Tare No.	25	26	27	28		
Weight in grams	Tare plus wet soil	13.95	15.45	14.68	14.09		
	Tare plus dry soil	12.89	14.12	13.40	13.02		
	Water W_w	1.06	1.32	1.28	1.07		
	Tare	8.40	8.48	7.96	8.41		
	Dry soil W_s	4.49	5.64	5.44	4.61		
	Water content w	23.6	23.4	23.5	23.2		
	Number of blows	40	38	27	23		

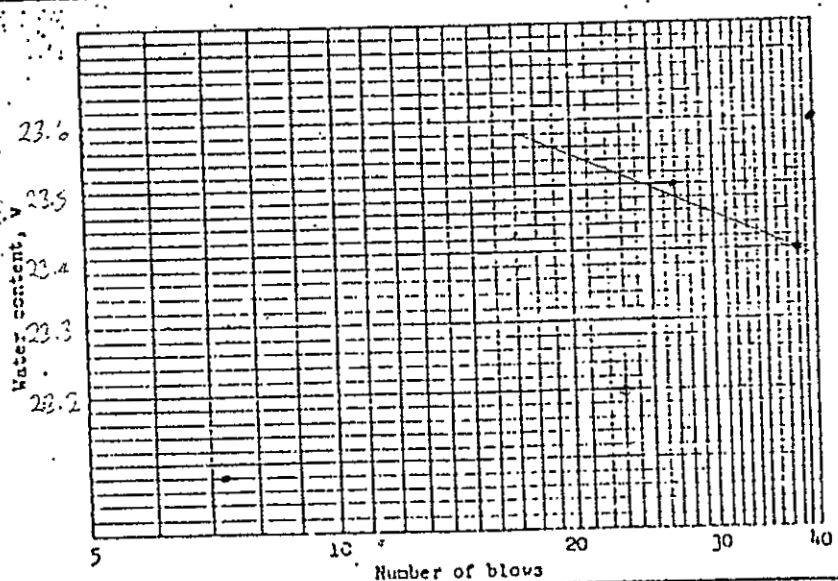

LL 23.5

PL 11.5

PI 12.0

Symbol from plasticity chart

CL

PLASTIC LIMIT

	Pan No.	1	2	3	4	5	Natural Water Content
	Tare No.	1	2	3			
Weight in grams	Tare plus wet soil	3.39	2.80	4.74			
	Tare plus dry soil	3.13	2.62	4.39			
	Water W_w	0.25	0.19	0.35			
	Tare	1.08	1.07	1.09			
	Dry soil W_s	2.05	1.55	3.31			
	Water content w						
	Plastic limit	12.2	11.6	10.6			

Remarks _____

Technician _____ Computed by _____ Checked by _____

LIQUID AND PLASTIC LIMIT TESTS

Date JUNE 26/90

Project CORDOVA DEBRIS FLOW

Boring No. _____ Sample No. 17

LIQUID LIMIT

	Run No.		1	2	3	4	5	6
	Tare No.		21	22	23	24		
Weight in grams	Tare plus wet soil		12.23	13.77	13.60	14.75		
	Tare plus dry soil		11.19	12.54	12.33	13.58		
	Water	W_w	1.02	1.23	1.27	1.17		
	Tare		6.09	6.44	6.54	8.30		
	Dry soil	W_s	5.09	6.10	5.79	5.28		
	Water content	w	20.0	20.2	21.9	22.2		
	Number of blows		30	25	20	18		

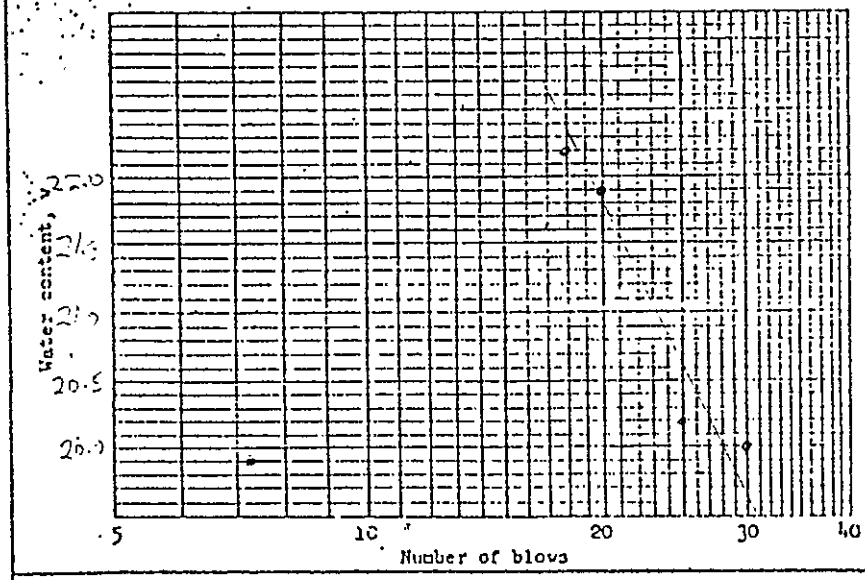

LL 20.6

PL 10.4

PI 10.2

Symbol from plasticity chart

CL

PLASTIC LIMIT

	Run No.		1	2	3	4	5	Natural Water Content
	Tare No.		4	5	6			
Weight in grams	Tare plus wet soil		4.12	3.87	4.15			
	Tare plus dry soil		3.83	3.60	3.87			
	Water	W_w	0.29	0.27	0.28			
	Tare		1.08	1.09	1.08			
	Dry soil	W_s	2.75	2.52	2.79			
	Water content	w						
	Plastic limit		10.5	10.7	10.0			

Remarks _____

Technician _____ Computed by DK Checked by _____

LIQUID AND PLASTIC LIMIT TESTS

Date JUNE 27/90

Project CORDOVA DEBRIS FLOW

Boring No. _____ Sample No. 26

LIQUID LIMIT

Run No.		1	2	3	4	5	6
Tare No.		12	13	14	15		
Weight in grams: Tare plus wet soil		9.49	10.68	9.59	6.64		
Tare plus dry soil		7.74	8.99	7.93	5.51		
Water	W_w	1.75	1.79	1.66	1.13		
Tare		1.08	1.09	1.06	1.08		
Dry soil	W_s	6.86	7.80	6.87	4.43		
Water content	w	25.6	22.9	24.2	25.5		
Number of blows		12	36	24	22		

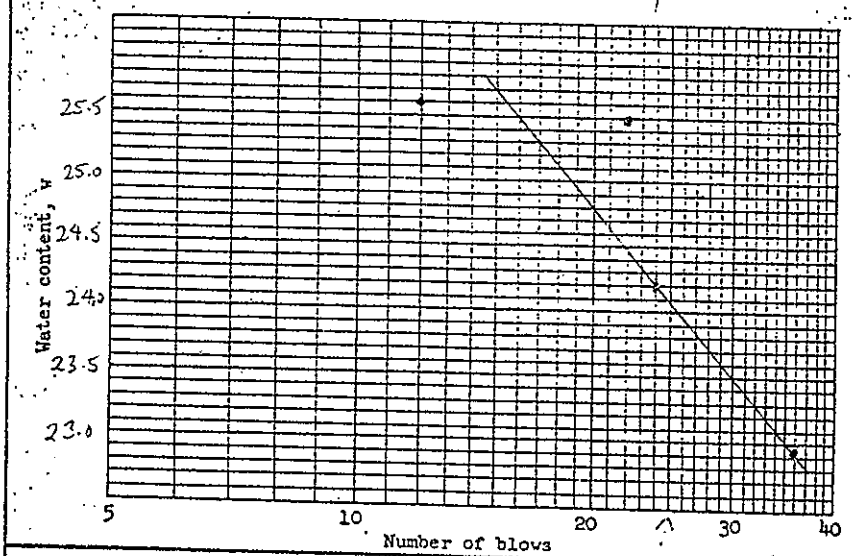

LL 24.1

PL 14.1

PI 10.0

Symbol from plasticity chart

CL

PLASTIC LIMIT

Run No.		1	2	3	4	5	Natural Water Content
Tare No.		16	17	18			
Weight in grams: Tare plus wet soil		4.35	3.41	3.37			
Tare plus dry soil		2.92	3.13	3.10			
Water	W_w	0.43	0.28	0.27			
Tare		1.09	1.09	1.09			
Dry soil	W_s	2.93	2.05	2.02			
Water content	w						
Plastic limit		15.2	13.7	13.4			

Remarks LT BRN LOOSE '3' HOR [illegible]

Technician _____ Computed by _____ Checked by _____

LIQUID AND PLASTIC LIMIT TESTS

Date JUNE 26/90

Project CORDOVA DEBRIS FLOW

Boring No. _____ Sample No. 25

LIQUID LIMIT

	Run No.		1	2	3	4	5	6
	Tare No.		20	5	6	7		
Weight in grams	Tare plus wet soil		6.59	7.48	10.11	7.53		
	Tare plus dry soil		5.72	6.41	8.69	6.39		
	Water	W_w	0.87	1.07	1.42	1.14		
	Tare		1.09	1.08	1.08	1.09		
	Dry soil	W_s	4.83	5.33	7.61	5.30		
Water content		w	18.0	20.1	18.7	21.5		
Number of blows			40	30	27	22		

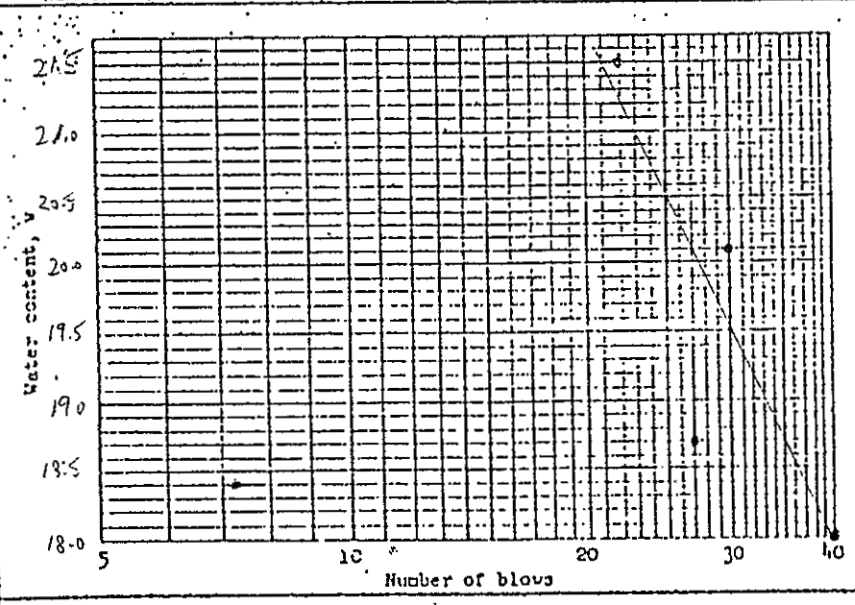

LL 20.5

PL 10.5

PI 10.0

Symbol from plasticity chart

CL

PLASTIC LIMIT

	Run No.		1	2	3	4	5	Natural Water Content
	Tare No.		10	11	12			
Weight in grams	Tare plus wet soil		3.32	2.49	3.62			
	Tare plus dry soil		3.11	2.36	3.37			
	Water	W_w	0.21	0.13	0.25			
	Tare		1.08	1.08	1.08			
	Dry soil	W_s	2.03	1.28	2.29			
Water content		w						
Plastic limit			10.3	10.2	10.9			

Remarks MEO SOIL BELOW 'A' HORIZON

Technician _____ Computed by DT Checked by _____

15 - 25

25 - 35

LIQUID AND PLASTIC LIMIT TESTS

Project: CORDOVA DEBRIS FLOW Date: JUNE 27/90.

Boring No. ______ Sample No. 1

LIQUID LIMIT

			1	2	3	4	5	6
Run No.			1	2	3	4		
Tare No.			1	2	3	4		
Weight in grams	Tare plus wet soil		9.71	7.90	8.19	5.61		
	Tare plus dry soil		7.82	6.08	6.46	4.51		
	Water	W_w	1.89	1.82	1.73	1.10		
	Tare		1.08	1.07	1.08	1.08		
	Dry soil	W_s	6.74	5.01	5.38	3.43		
Water content		w	28.0	36.3	32.2	32.1		
Number of blows			40	28	16	24		

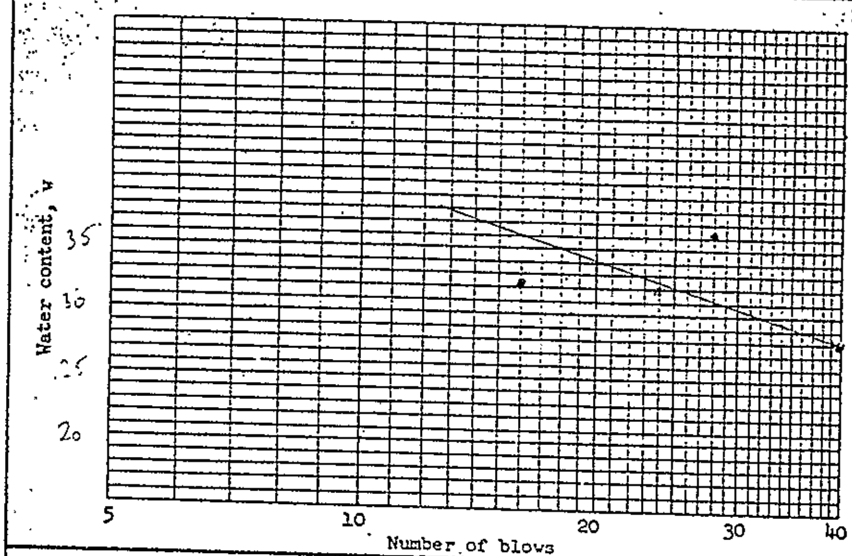

LL 32.0

PL 12.1

PI 19.9

Symbol from plasticity chart: CL

PLASTIC LIMIT

			1	2	3	4	5	Natural Water Content
Run No.			1	2	3	4	5	
Tare No.			19	20	21			
Weight in grams	Tare plus wet soil		4.46	3.25	8.76			
	Tare plus dry soil		4.06	3.01	8.51			
	Water	W_w	0.40	0.24	0.25			
	Tare		1.09	1.09	6.09			
	Dry soil	W_s	2.97	1.92	2.42			
Water content		w						
Plastic limit			13.5	12.5	10.3			

Remarks: LT BRN [illegible] 'B' [illegible]

Technician ______ Computed by [illegible] Checked by ______

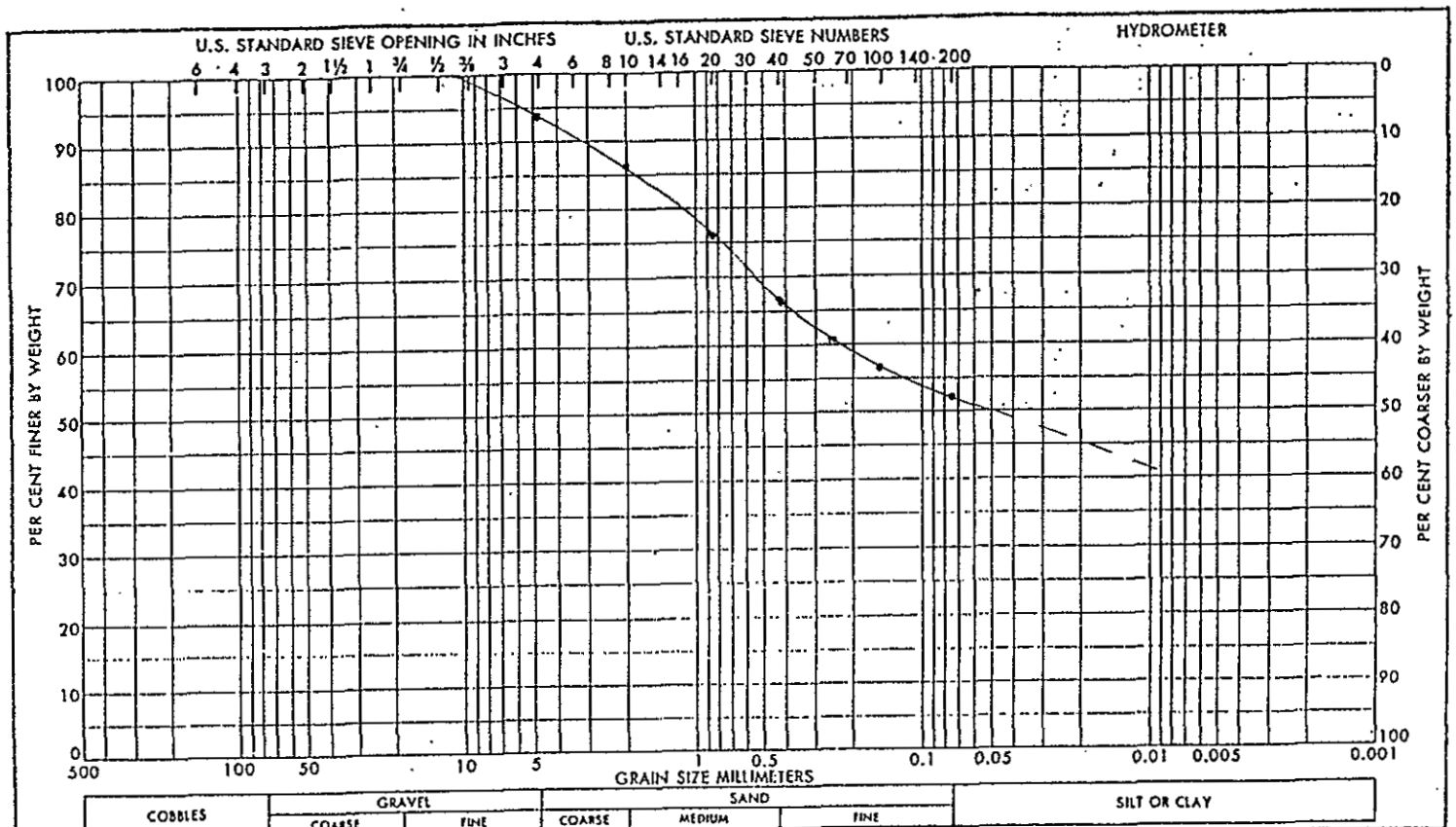

SAMPLE NO.	ELEV OR DEPTH	CLASSIFICATION	NAT W%	LL	PL	PI
1			21.3			

GRADATION CURVES

PROJECT CORDOVA DEBRIS FLOW
(UPPER 'B') LT BRN
AREA
BORING NO.
DATE July 2/90

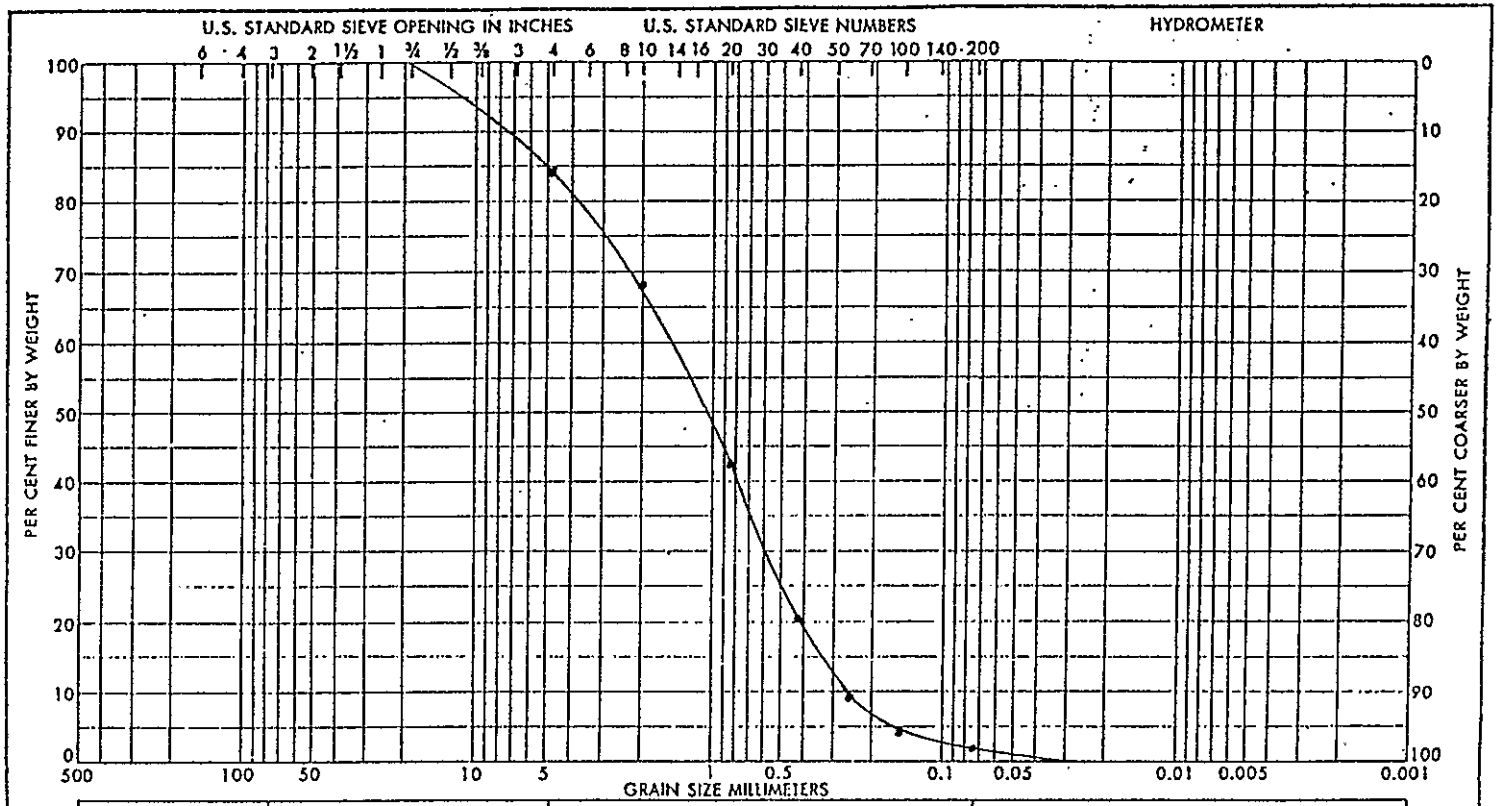

SAMPLE NO.	ELEV OR DEPTH	CLASSIFICATION	NAT W%	LL	PL	PI
2		SW	3.9			

GRADATION CURVES

PROJECT CORDOVA DEBRIS FLOW

AREA SOUTHERN WALL

BORING NO.

DATE JUNE 25/90

$C_U = \frac{\quad}{.26}$

40

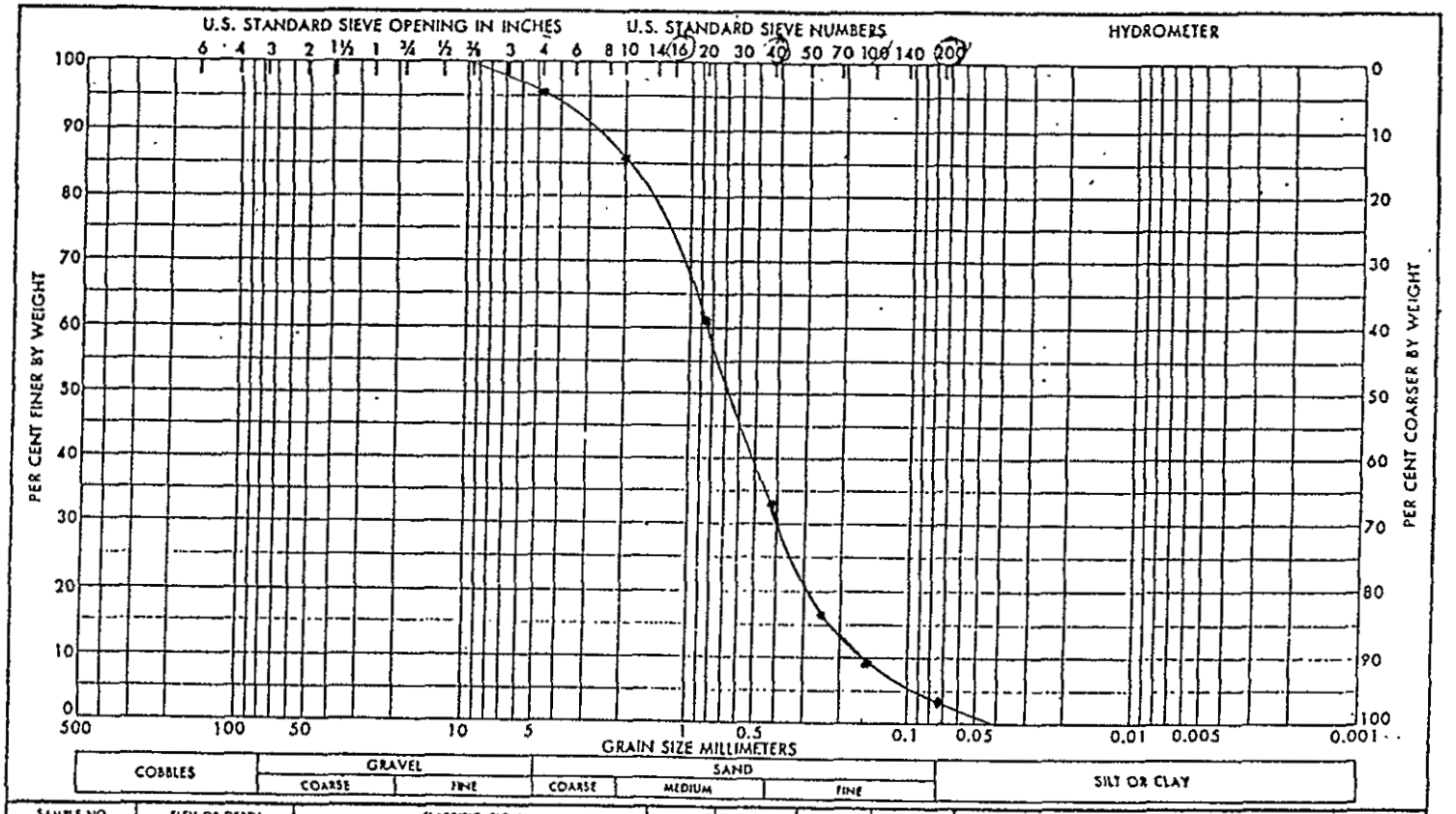

SAMPLE NO.	ELEV OR DEPTH	CLASSIFICATION	NAT W%	LL	PL	PI
3		SP	7.6			

GRADATION CURVES

PROJECT CORDOVA DEBRIS FLOW

AREA SOUTHERN WALL

BORING NO.

DATE

$C_u = \frac{D_{60}}{D_{10}} = \frac{0.85}{0.16} = 5.3$ $C_c = \frac{D_{30}^2}{D_{60} \times D_{10}} =$

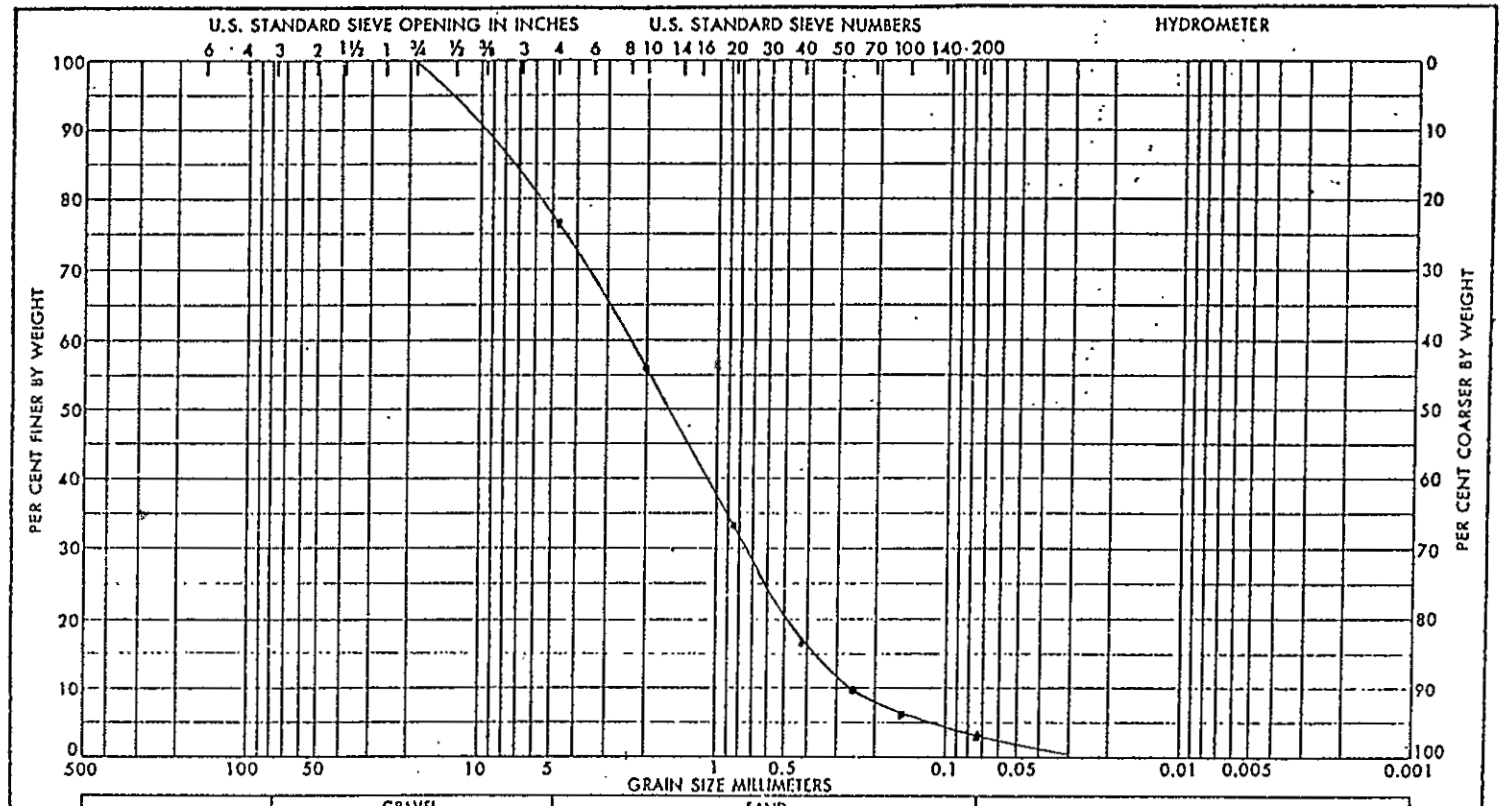

SAMPLE NO.	ELEV OR DEPTH	CLASSIFICATION	NAT W%	LL	PL	PI
4		SW	8.0			

GRADATION CURVES

PROJECT CORDOVA

AREA DEBRIS

BORING NO.

DATE JUNE 25/90

A.) 2" - 4.6.

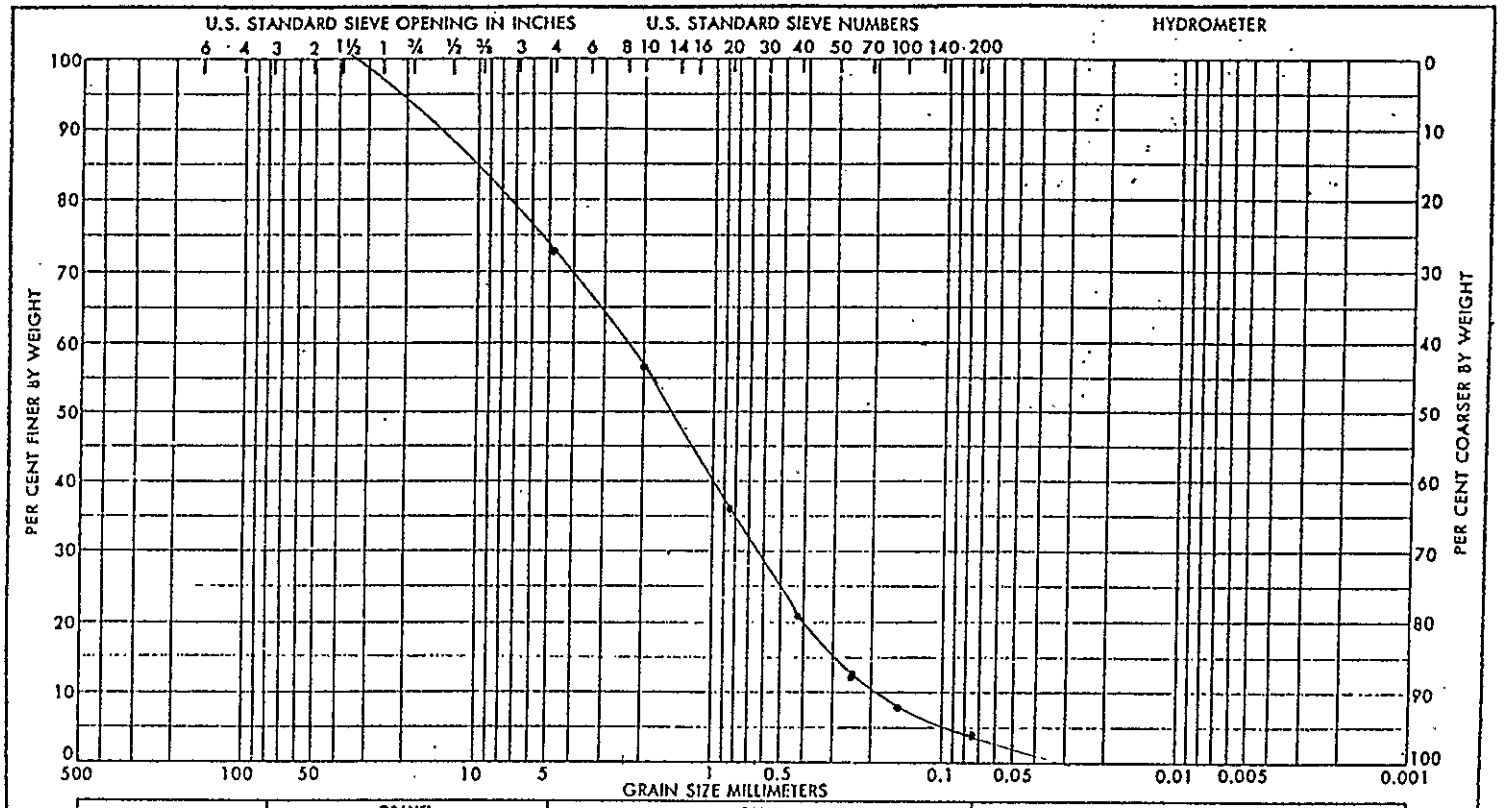

SAMPLE NO.	ELEV OR DEPTH	CLASSIFICATION	NAT W%	LL	PL	PI
S		SW	9.8			

GRADATION CURVES

PROJECT CORDOVA

AREA DEBRIS

BORING NO.

DATE JUNE 25, 1990.

$C_U = \frac{2.4}{\quad} = 10.0$

$\frac{1.64^2}{\quad}$

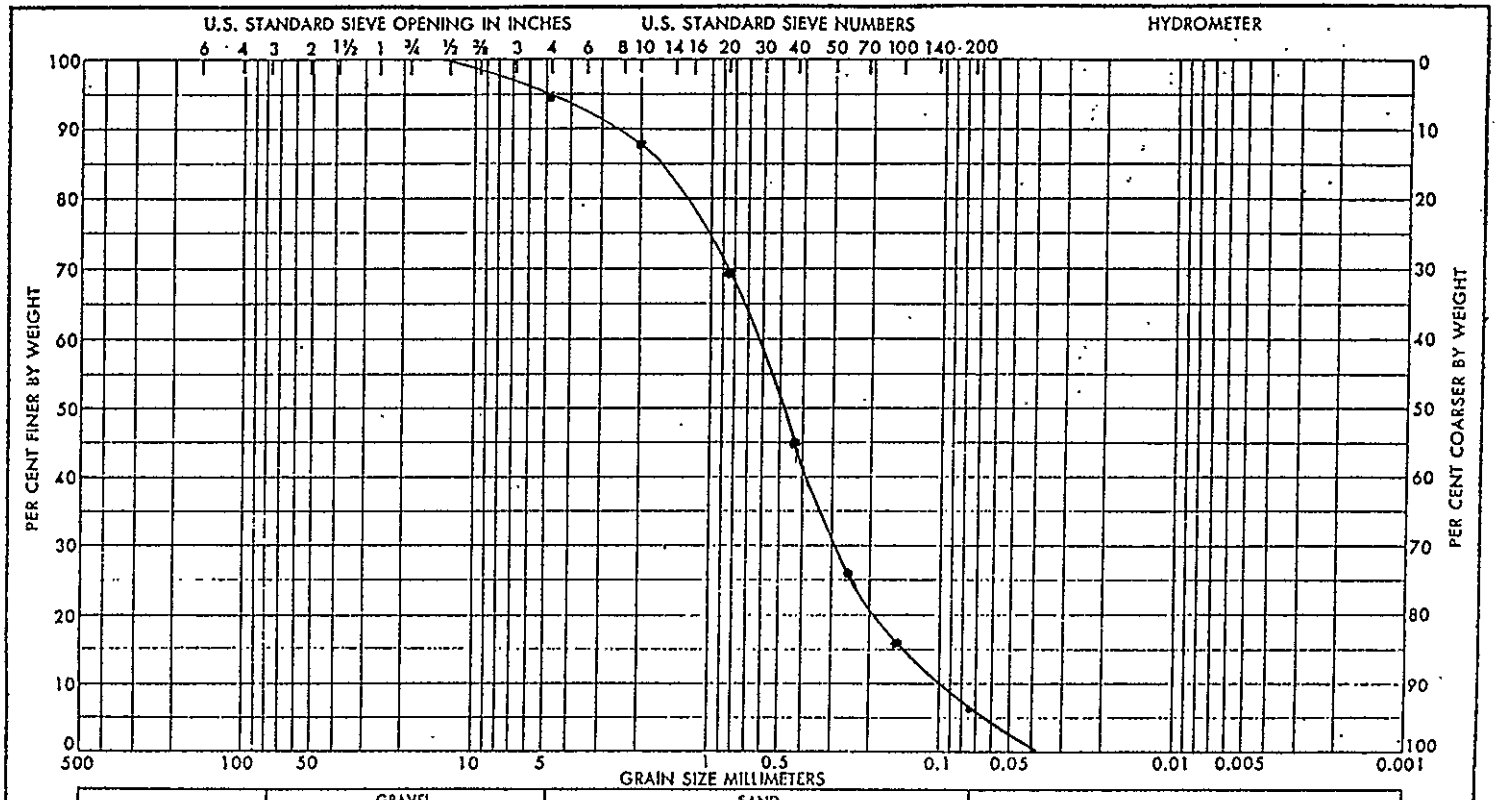

SAMPLE NO.	ELEV OR DEPTH	CLASSIFICATION	NAT W%	LL	PL	PI
6		SW - M1	16.2			

GRADATION CURVES

PROJECT CORDOVA DEBRIS FLOW

AREA SOUTHERN WALL

BORING NO.

DATE

$C_u = 6.2$ $\quad C_u = \frac{.42}{.07} = 6.2$

$C_c = 1.4$ $\quad C_c = \frac{.294^2}{.42 \times .07} = 1.4$

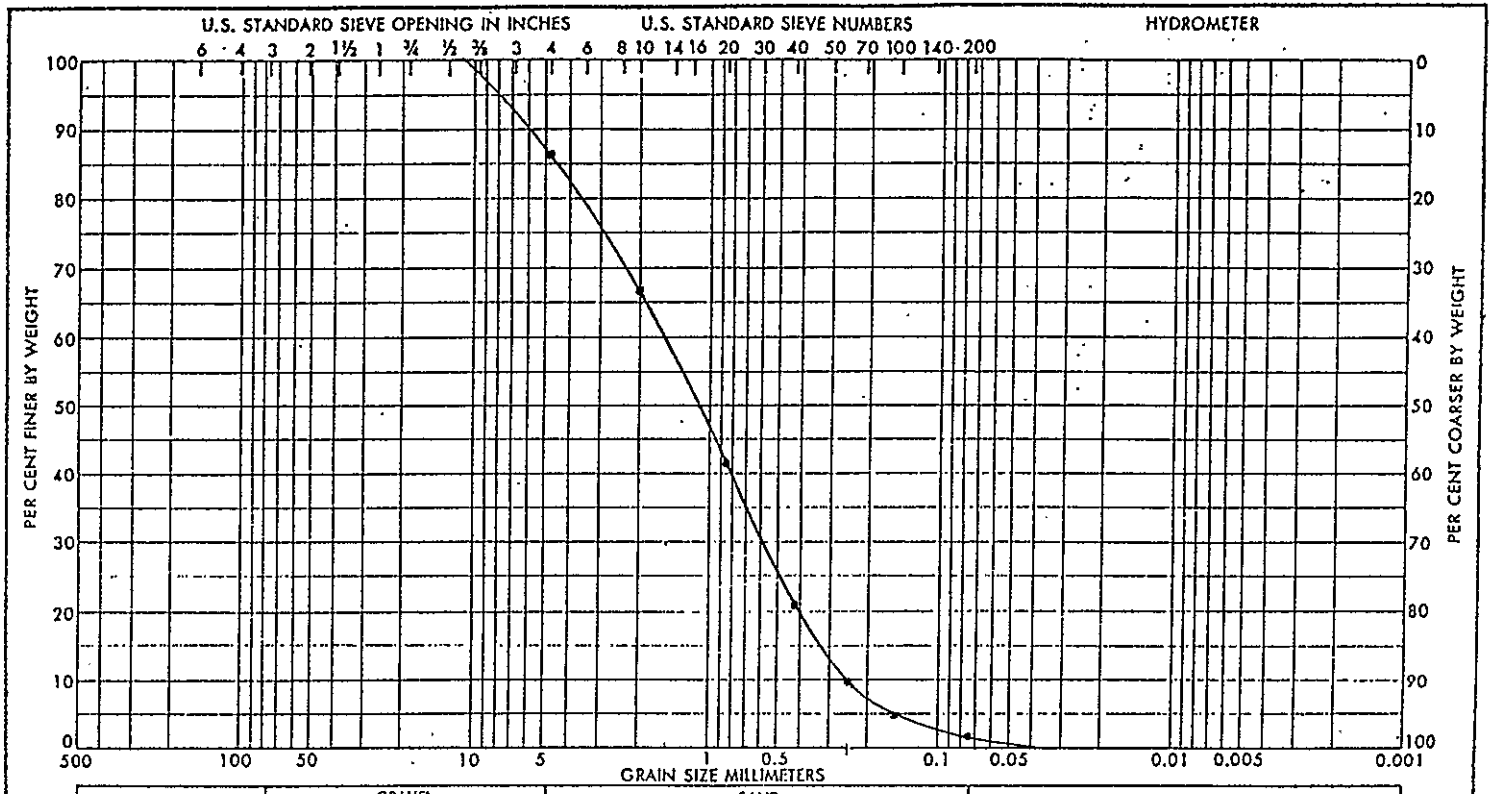

SAMPLE NO.	ELEV OR DEPTH	CLASSIFICATION	NAT W%	LL	PL	PI
7		SW	4.0			

GRADATION CURVES

PROJECT CORDOVA DEBRIS FLOW

AREA SOUTHERN WALL

BORING NO.

DATE JUNE 25, 1990

$C_U = \frac{1.5}{.25} = 6.0$

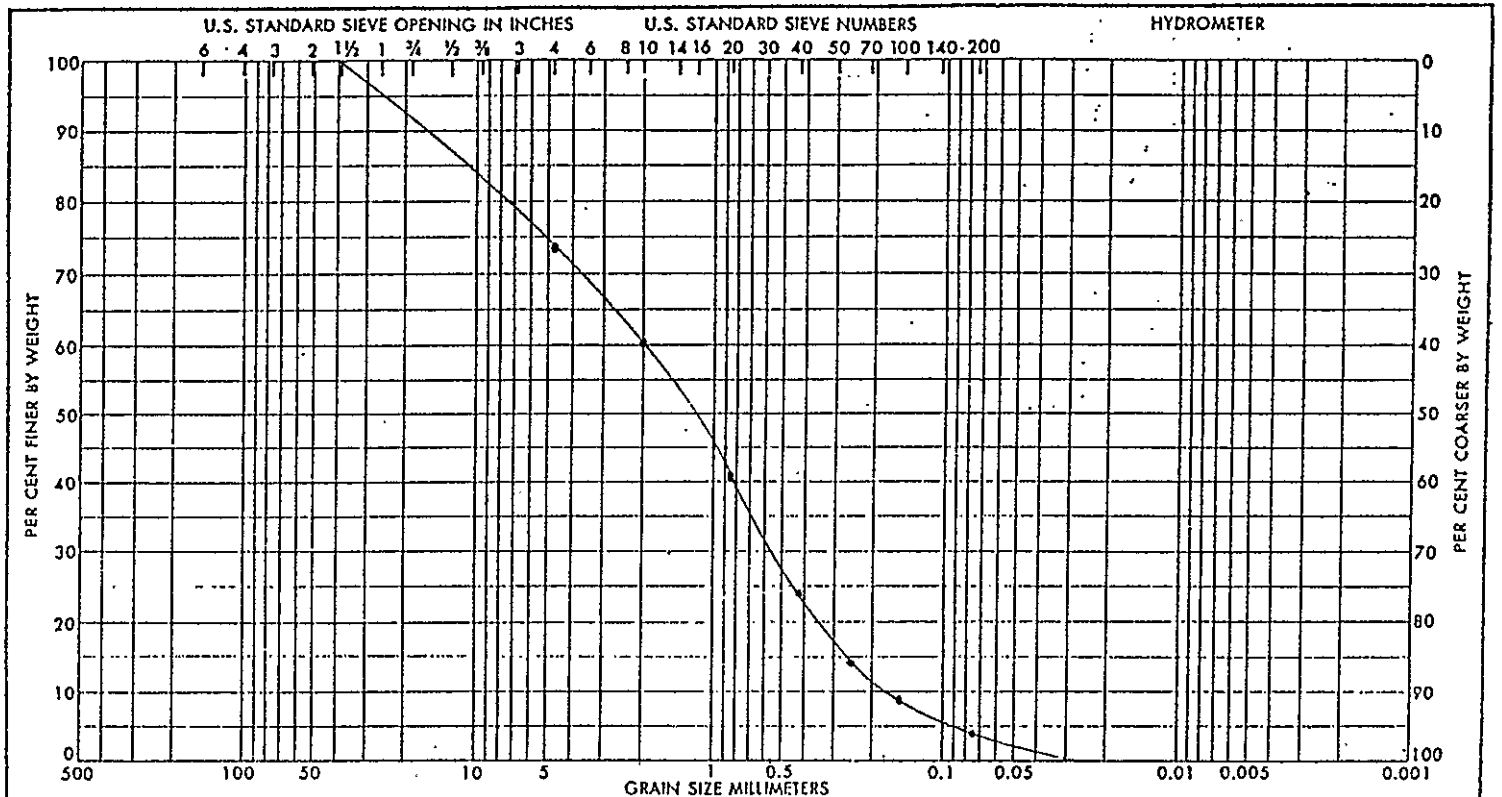

SAMPLE NO.	ELEV OR DEPTH	CLASSIFICATION	NAT W%	LL	PL	PI
6		SP	10.4			

GRADATION CURVES

PROJECT CORDOVA

AREA CLAYEY SAND (SOUTHERN SIDE OF FLOW)

BORING NO.

DATE JUNE 25/90

$C_U = \frac{2.0}{.18} = 11.11$

$C_C = \frac{(.5)}{2.0 \times .18}$

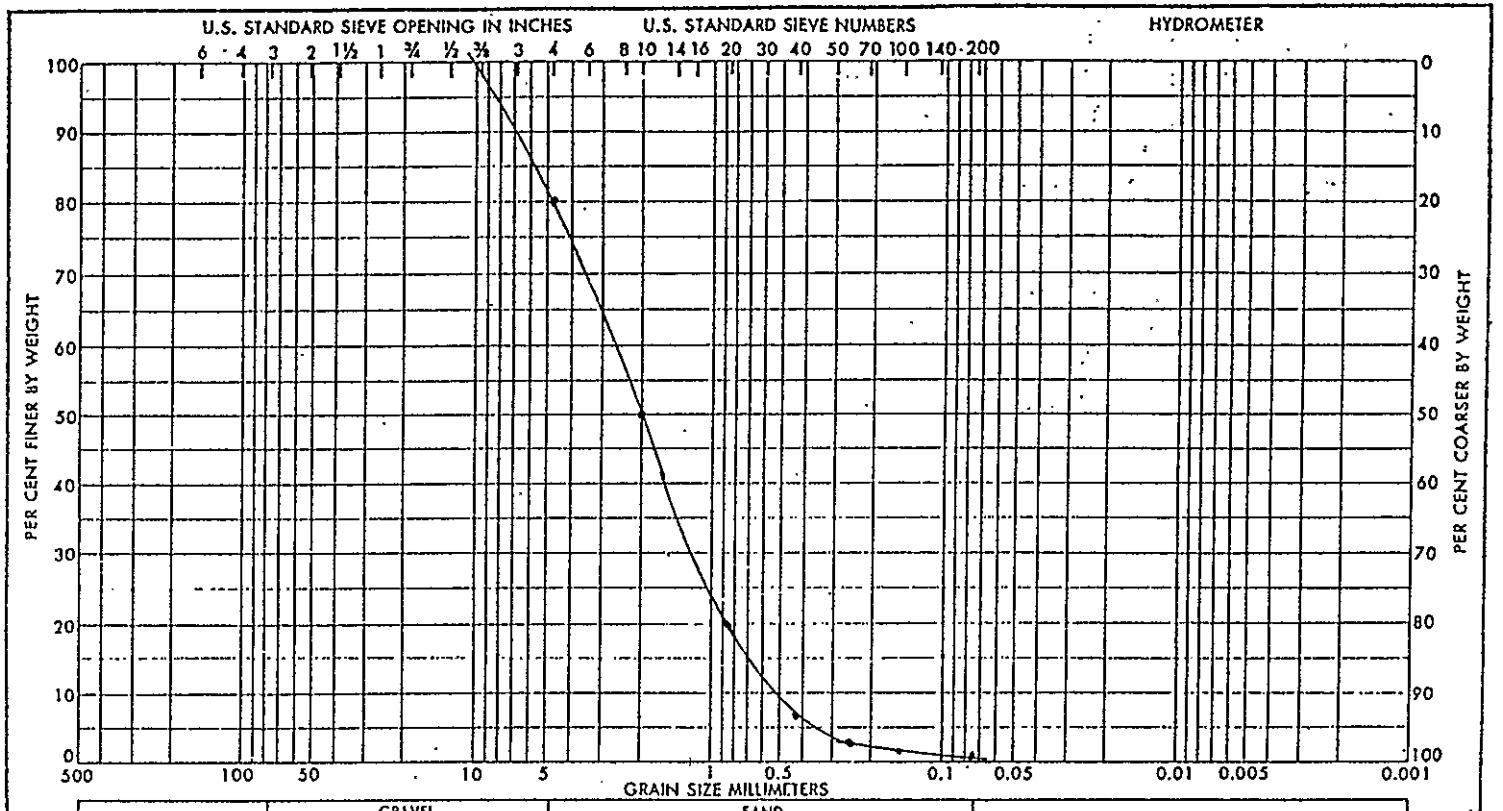

SAMPLE NO.	ELEV OR DEPTH	CLASSIFICATION	NAT W%	LL	PL	PI
9		SP	0.4			

GRADATION CURVES

PROJECT CORDOVA

AREA DISTAL END

BORING NO.

DATE JUNE 25/90

$C_U = \frac{2.6}{.51} = 5.10$

$C_c = \frac{1.2^2}{2.6} = 1.01$

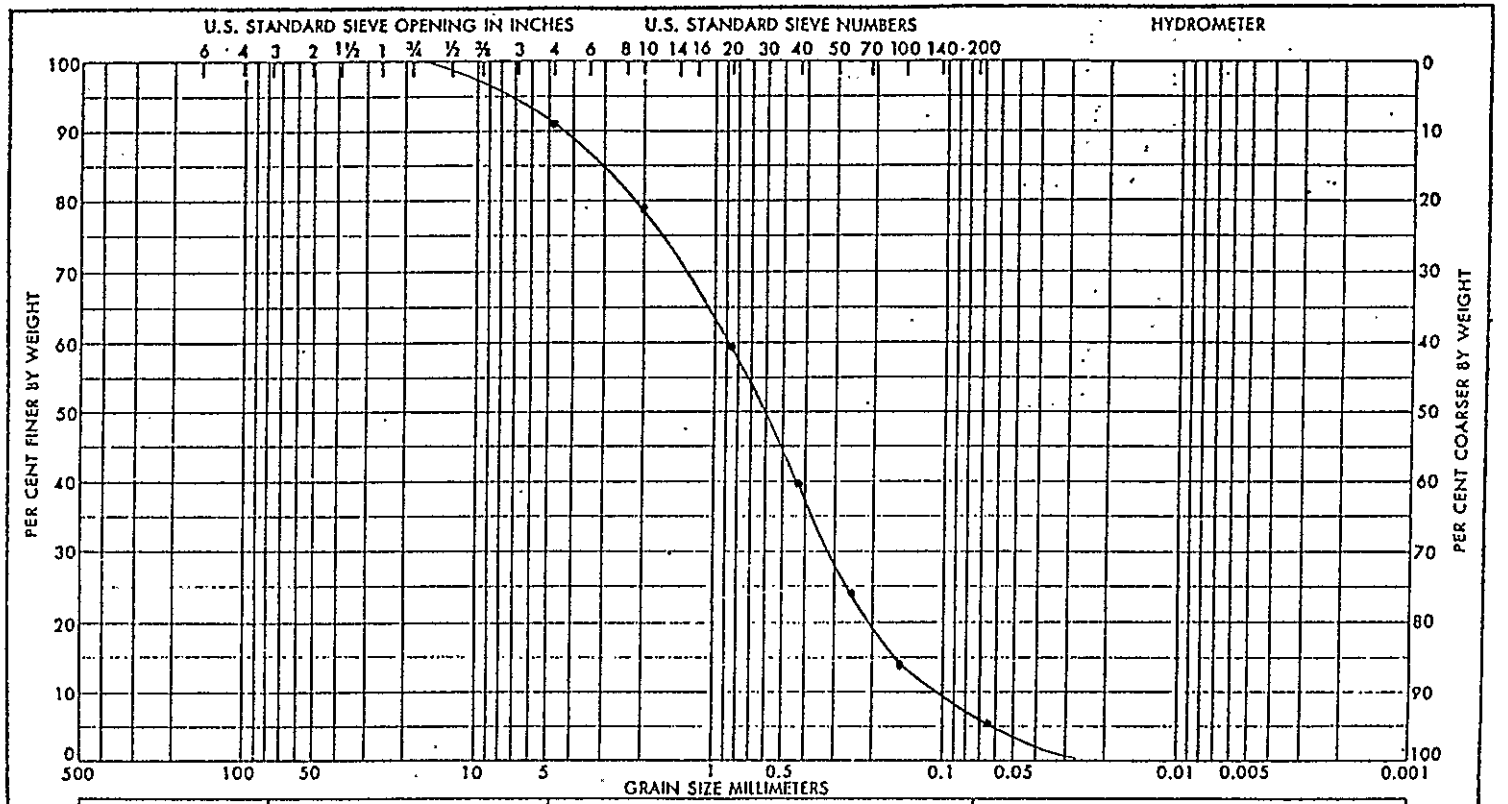

SAMPLE NO.	ELEV OR DEPTH	CLASSIFICATION	NAT W%	LL	PI	PI
10		SW - III	11.2			

GRADATION CURVES

PROJECT CORDOVA DEBRIS FLOW

AREA NORTHERN WALL

BORING NO.

DATE JUNE 25/90

$C_U = \frac{.84}{.11} =$

$= \frac{.32^2}{\quad} =$

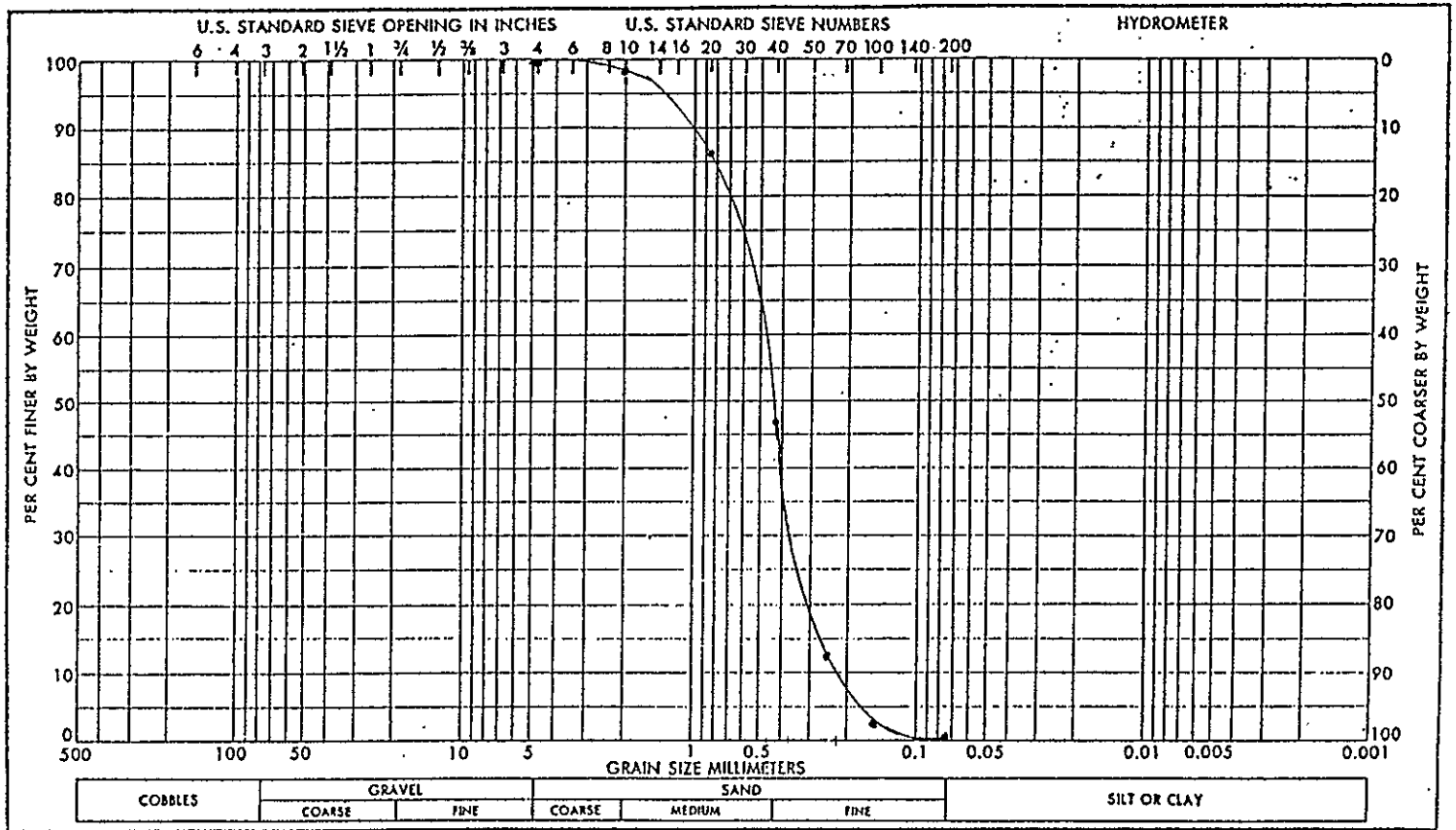

SAMPLE NO.	ELEV OR DEPTH	CLASSIFICATION	NAT W%	LL	PL	PI
11		SP	0.6			

GRADATION CURVES

PROJECT CORDOVA

AREA DISTAL END OF FLOW

BORING NO.

DATE JUNE 25 1990

$C_U = \frac{.46}{.02} = (23)$

$C_C = \frac{(.1)^2}{(.46)(.02)} = .11$

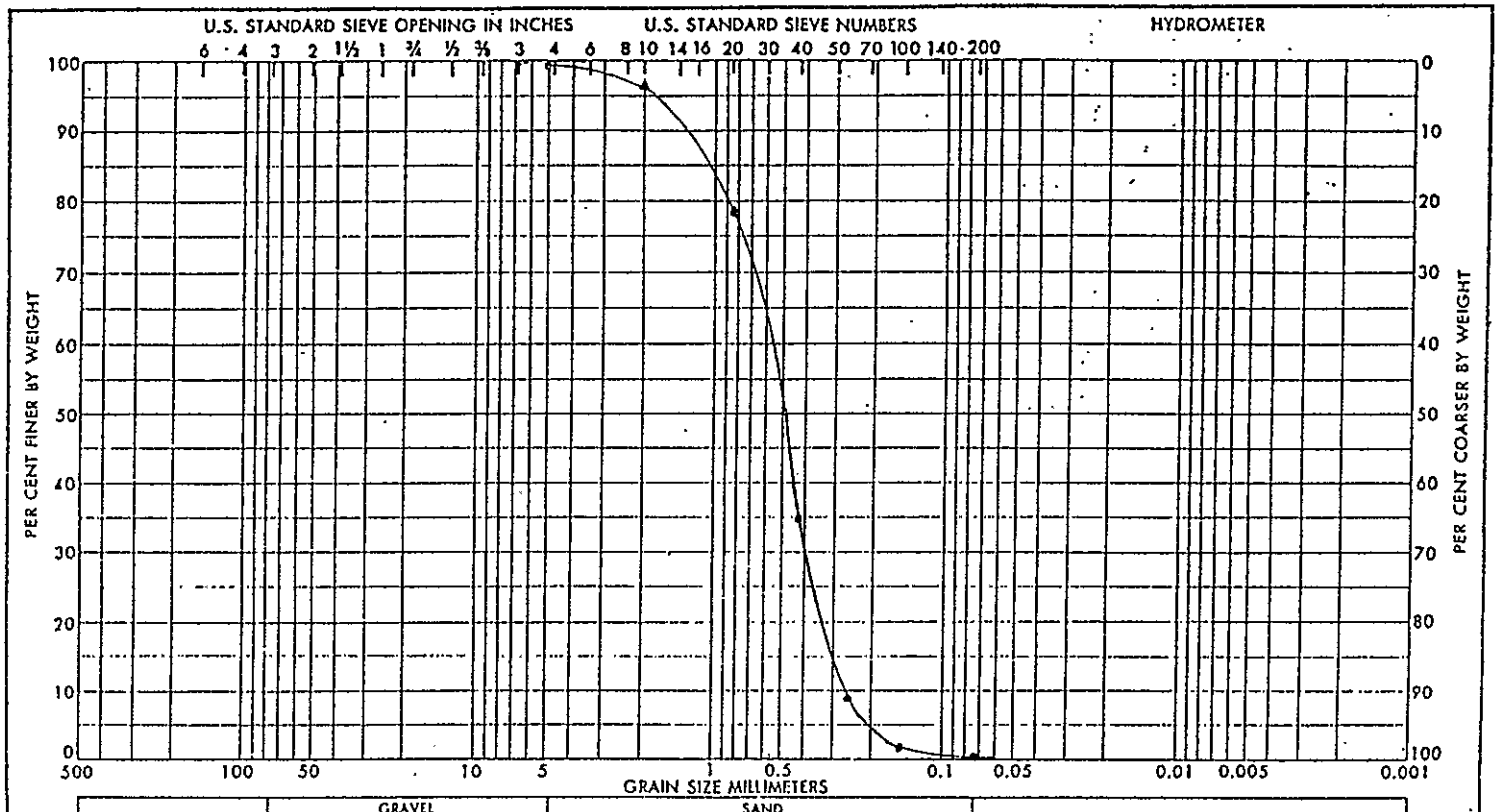

SAMPLE NO.	ELEV OR DEPTH	CLASSIFICATION	NAT W%	LL	PL	PI
12		SP	1.1			

GRADATION CURVES

PROJECT CORDOVA DEBRIS FLOW

AREA DISTAL END.

BORING NO.

DATE JUNE 25, 1990

$C_U = \frac{.55}{.1} = 2.5$

$C_C = \frac{.14^2}{.55 \times .1} = .36$

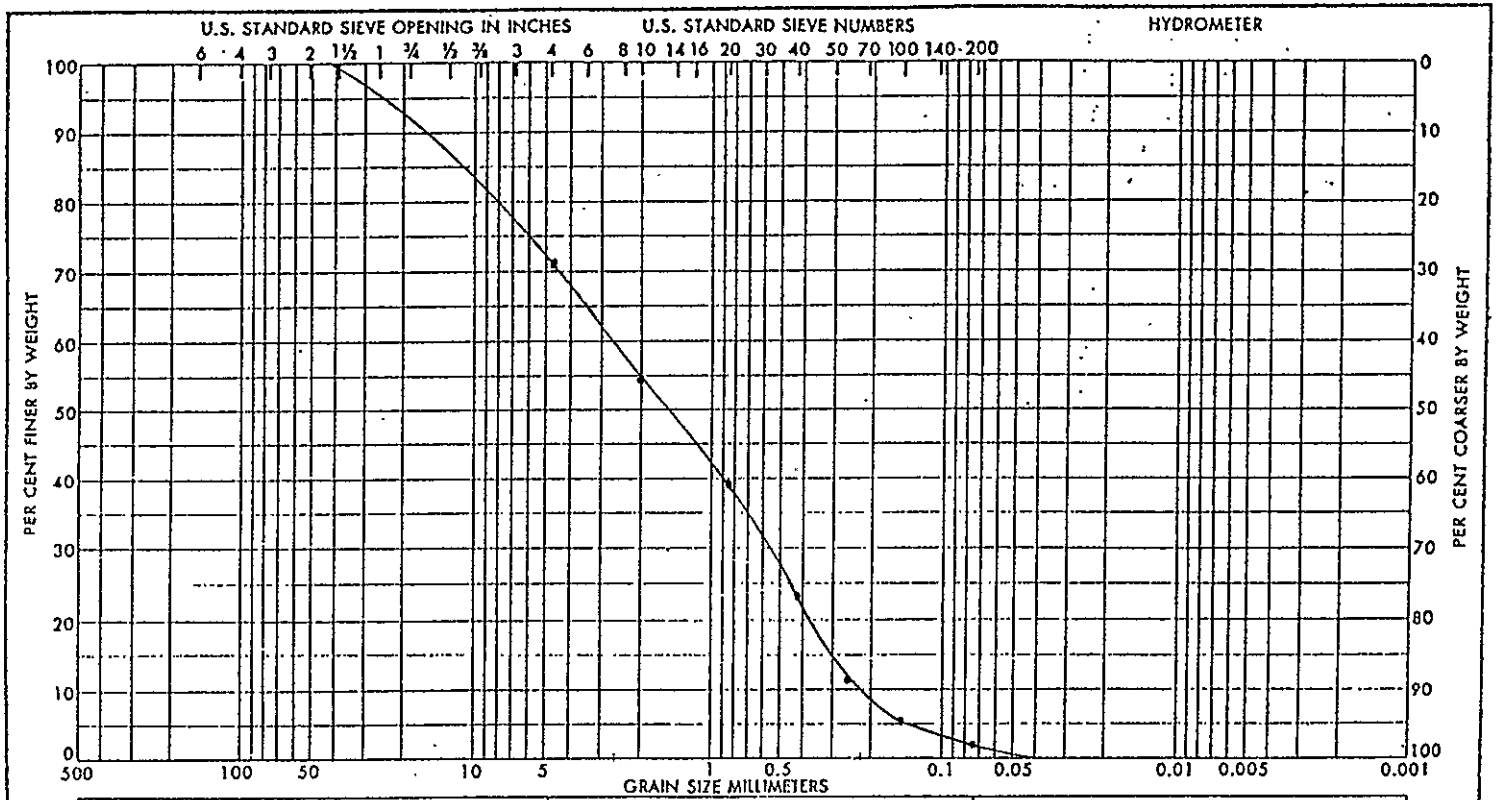

SAMPLE NO.	ELEV OR DEPTH	CLASSIFICATION	NAT W%	LL	PL	PI
13		SP	2.6			

GRADATION CURVES

PROJECT CORDOVA DEBRIS FLOW

AREA GRAVELLY OUTWASH

BORING NO.

DATE JUNE 25/90

$C_U = \frac{2.6}{.23} = 11.30$

$C_c = \frac{(1.55)^2}{2.6} = .51$

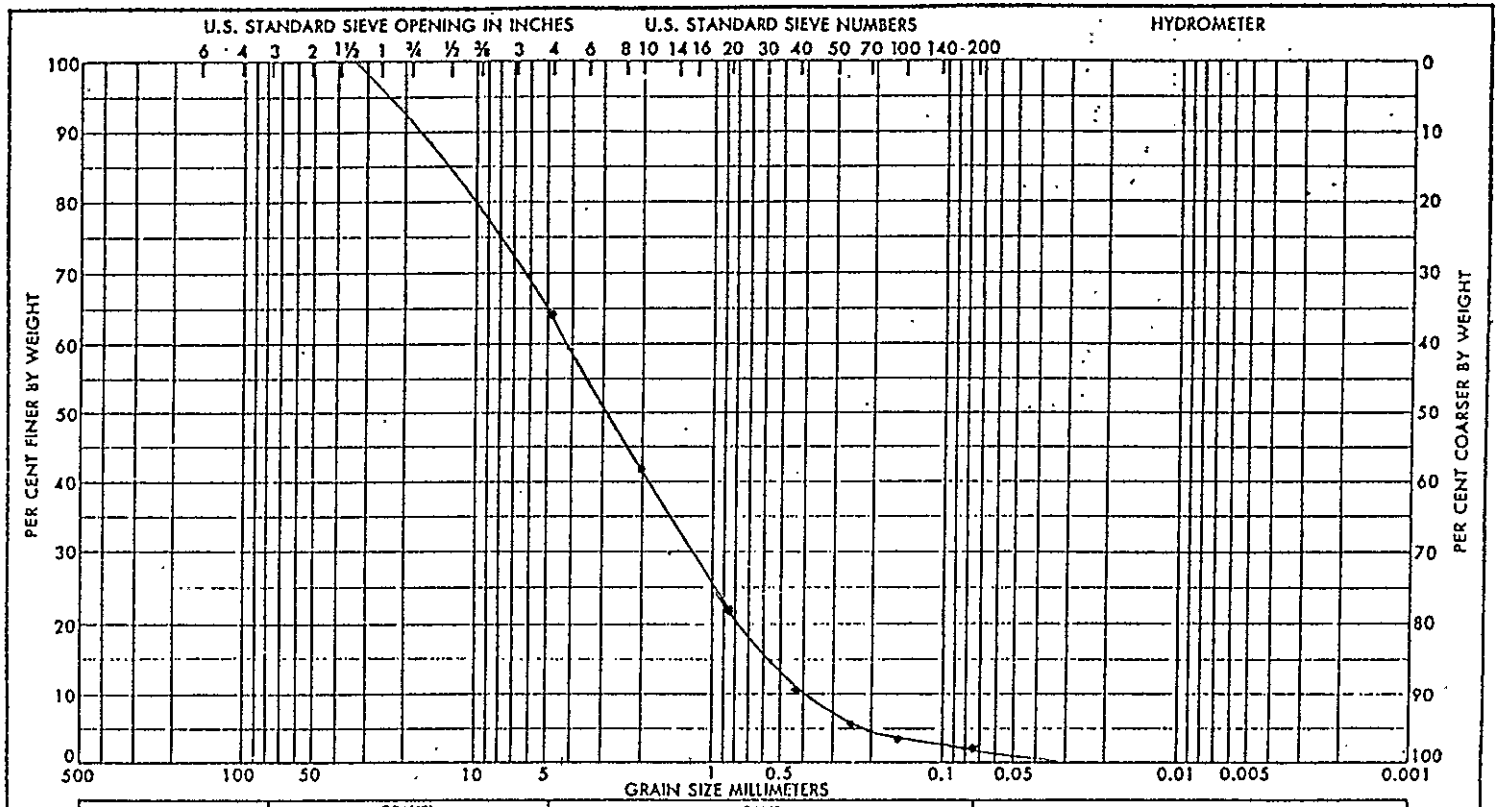

SAMPLE NO.	ELEV OR DEPTH	CLASSIFICATION	NAT W%	LL	PL	PI
14		SP	5.0			

GRADATION CURVES

PROJECT CORDOVA

AREA DEBRIS

BORING NO.

DATE JUNE 25, 1990

$C_U = \frac{4.0}{0.4} = 10.0$

$C_C = \frac{0.9^2}{4.0 \times 0.4} = 0.51$

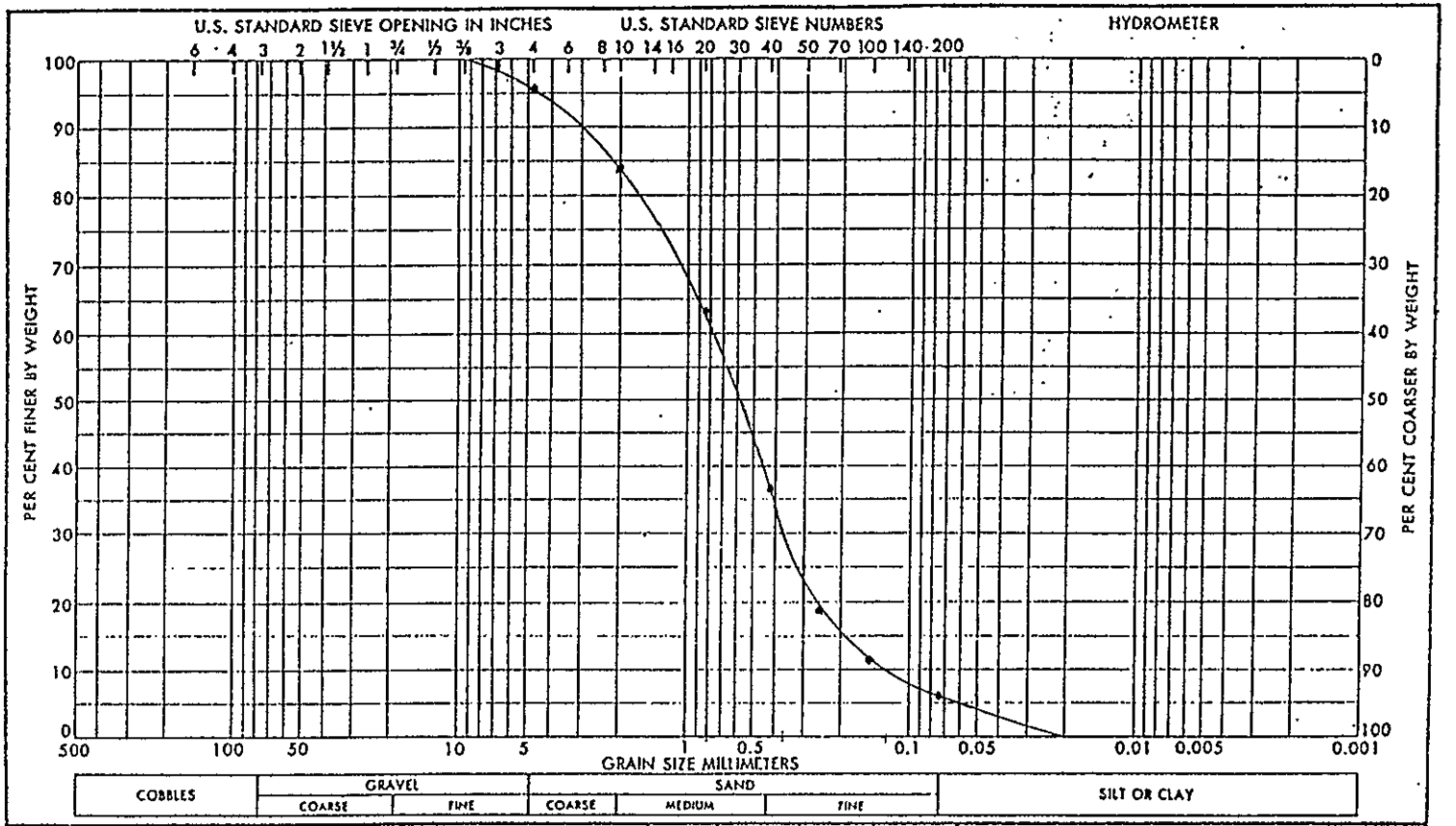

SAMPLE NO.	ELEV OR DEPTH	CLASSIFICATION	NAT W%	LL	PI	FI
15		SW-?	7.2			

GRADATION CURVES

PROJECT CORDOVA

AREA SOUTHERN SIDE OF FLOW

BORING NO.

DATE JUNE 25/90

$C_U = \frac{.8}{.14} = 5.71$

$C_c = \frac{(.36)^2}{\quad} = 1.13$

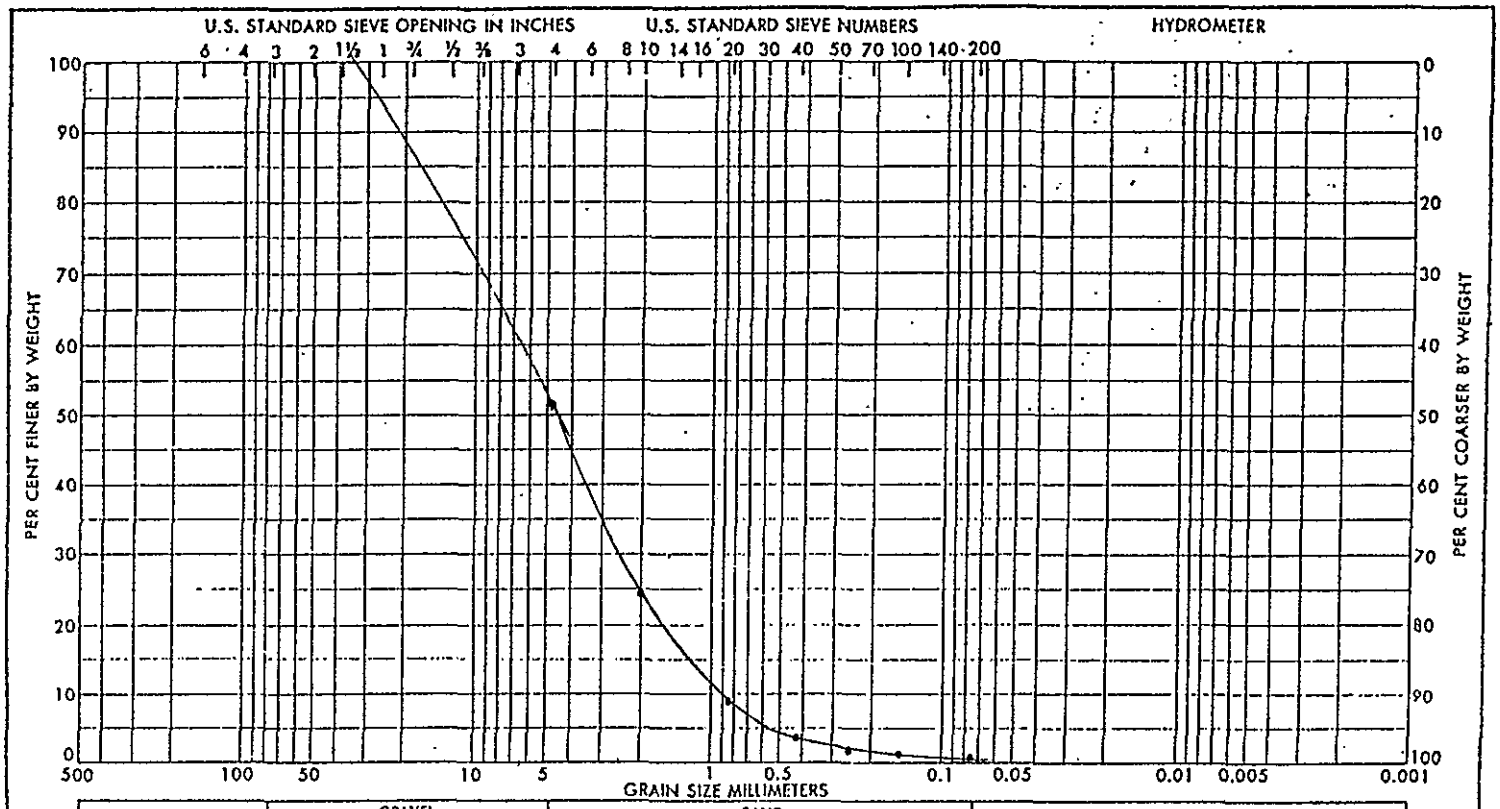

SAMPLE NO.	ELEV OR DEPTH	CLASSIFICATION	NAT W%	LL	PL	PI
16		SM	11.3			

GRADATION CURVES

PROJECT CORDOVA

AREA DISTAL END

BORING NO.

DATE JUNE 25/90

$C_U = \frac{6.5}{.9} = 7.22$

$C_C = 2.0$

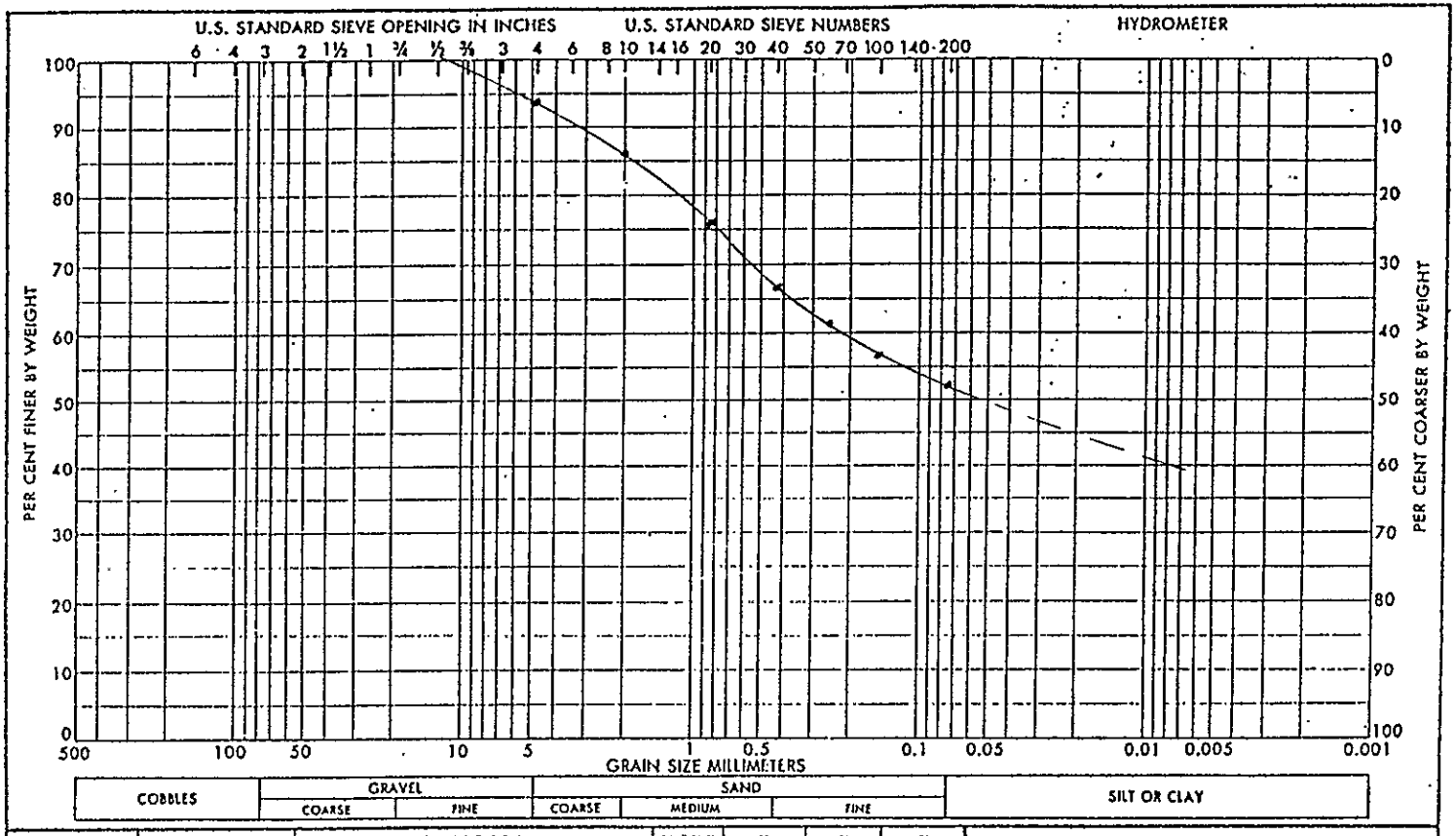

SAMPLE NO.	ELEV OR DEPTH	CLASSIFICATION	NAT W%	LL	PL	PI
17			11.5			

GRADATION CURVES

PROJECT CORDOVA DEBRIS FLOW (A)

AREA

BORING NO.

DATE JUNE 30/98

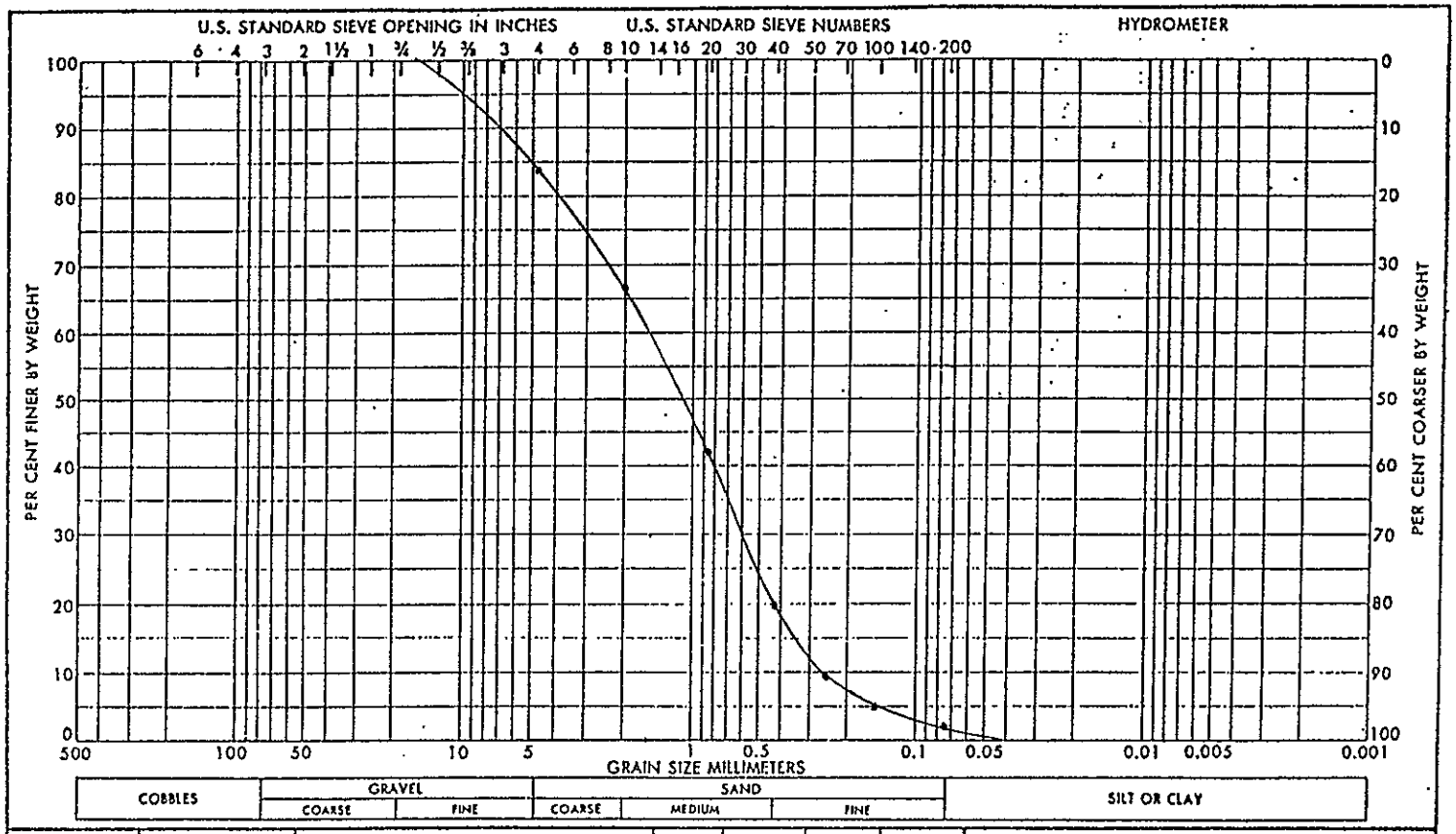

SAMPLE NO.	ELEV OR DEPTH	CLASSIFICATION	NAT W%	LL	PL	PI
18		SW	5.1			

GRADATION CURVES

PROJECT CORDOVA

AREA DEBRIS

BORING NO.

DATE JUNE 25 / 90

$C_U = \frac{1.6}{.28} = 5.71$

$C_c = \frac{0.6^2}{(1.6)(.28)} =$

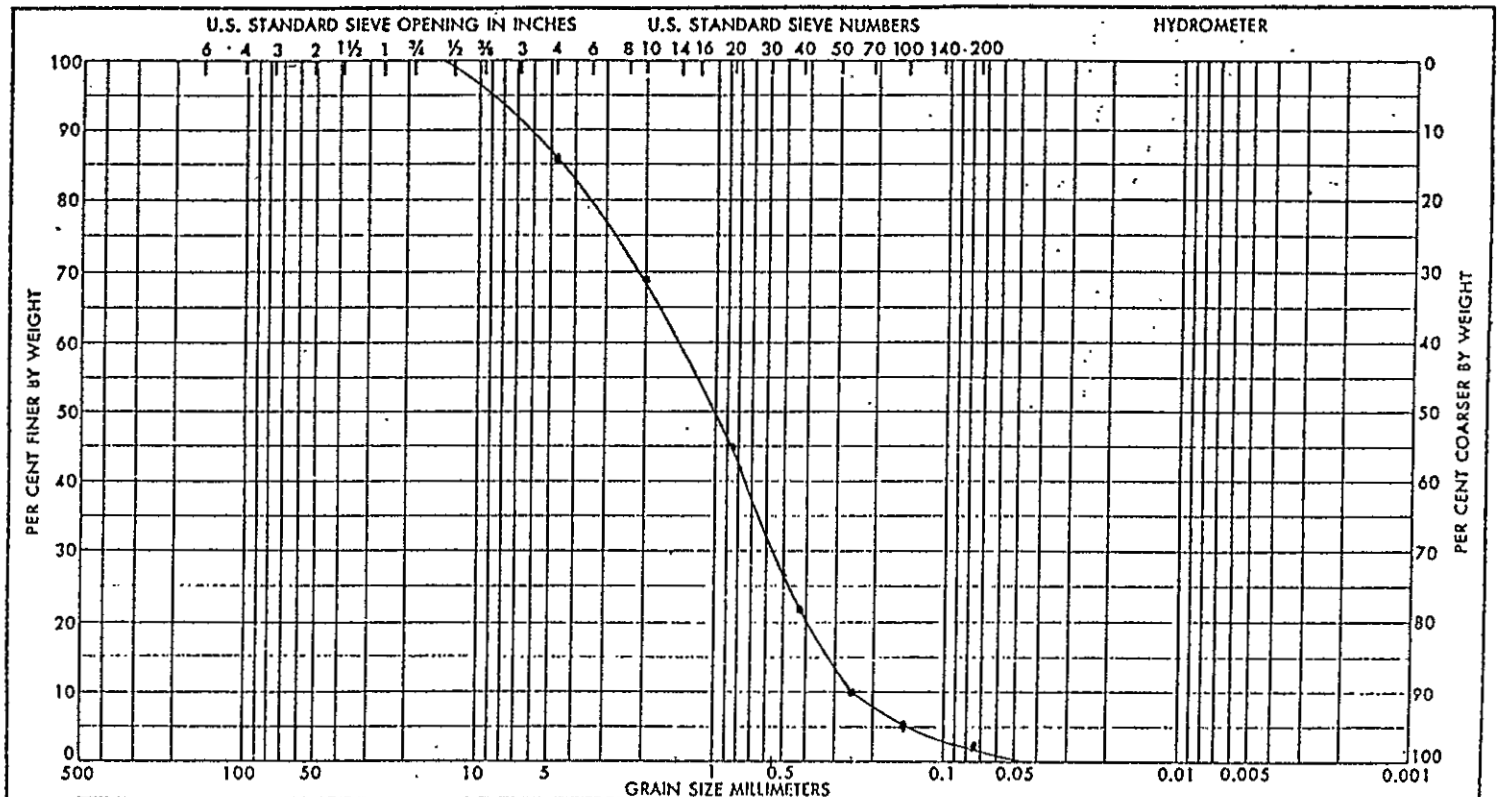

SAMPLE NO.	ELEV OR DEPTH	CLASSIFICATION	NAT W%	LL	PL	PI
19		SP	5.1			

GRADATION CURVES

PROJECT CORDOVA

AREA DEBRIS

BORING NO.

DATE JUNE 25, 1990

$C_U = \frac{1.5}{\quad} = 6.0$

$C_C = \frac{\quad}{1.5}$

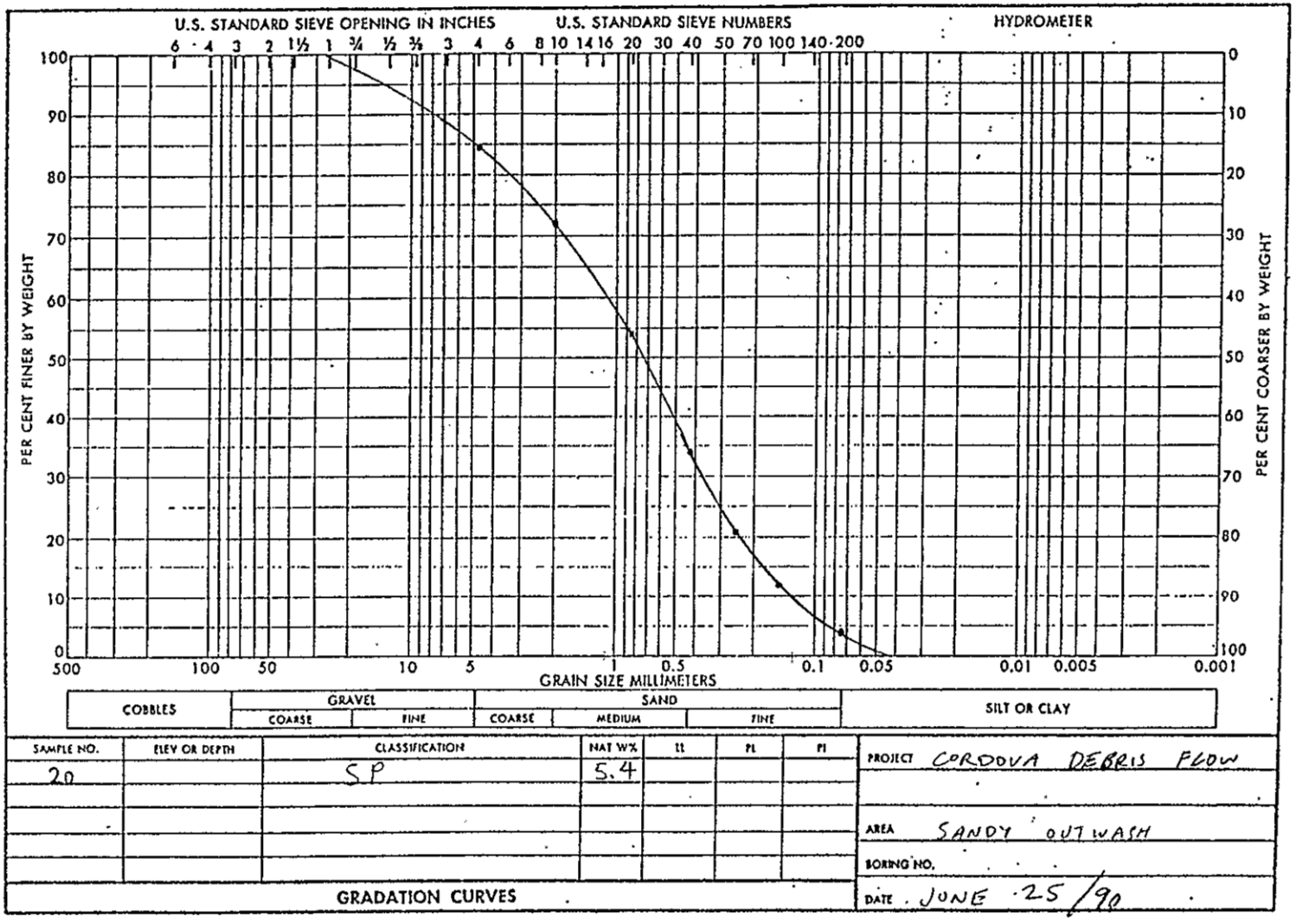

SAMPLE NO.	ELEV OR DEPTH	CLASSIFICATION	NAT W%	LL	PL	PI
20		SP	5.4			

GRADATION CURVES

PROJECT CORDOVA DEBRIS FLOW

AREA SANDY OUTWASH

BORING NO.

DATE JUNE 25/90

$C_U = \frac{1.1}{.14} = 7.86$

$C_c = \frac{(.37)^2}{(1.1)}$

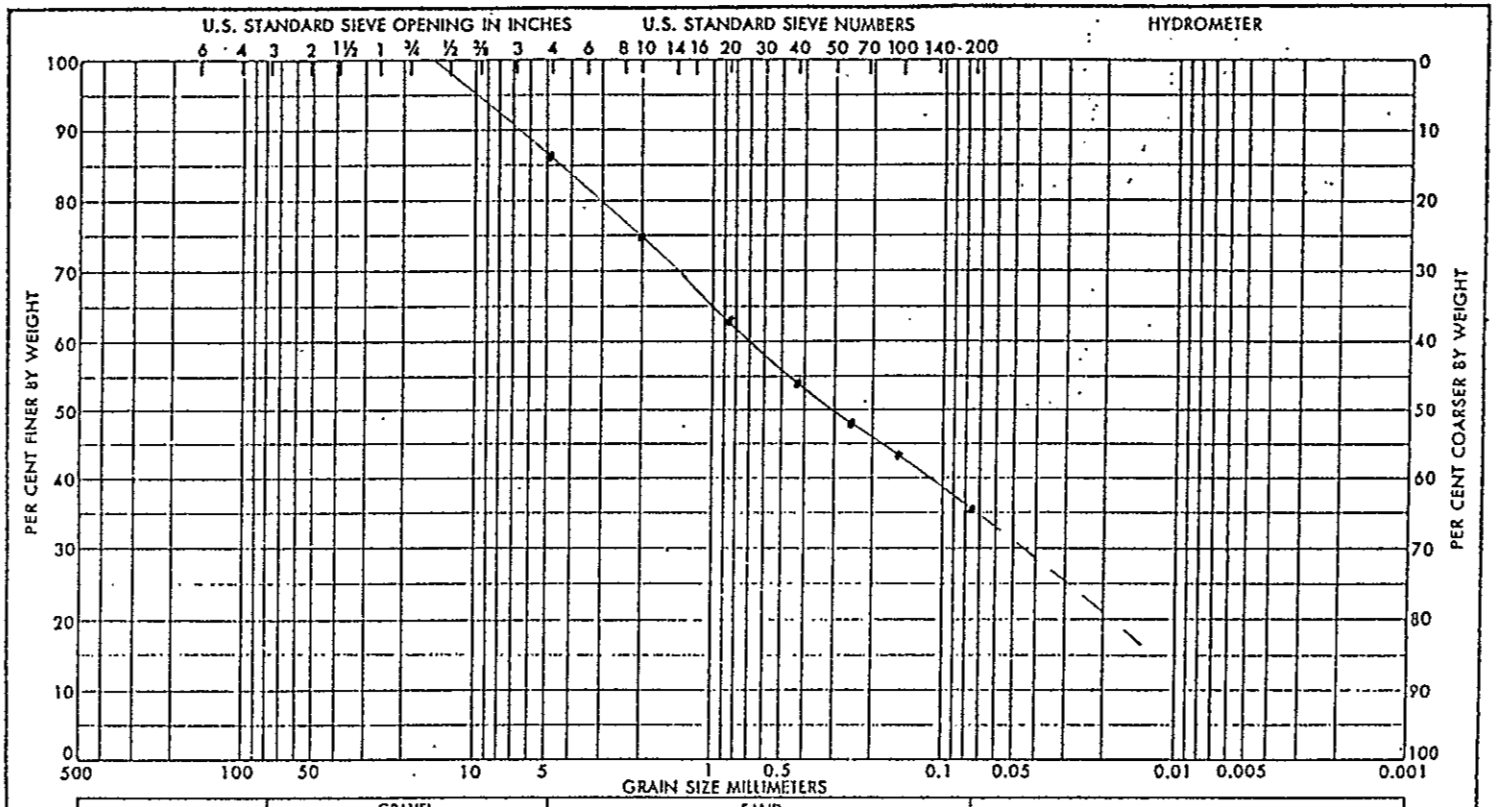

SAMPLE NO.	ELEV OR DEPTH	CLASSIFICATION	NAT W%	LL	PL	PI
21			16.2			

GRADATION CURVES

PROJECT CORDOVA DEBRIS FLOW (TOP A)

AREA

BORING NO.

DATE JUNE 29/90

$C_U = \frac{.70}{?}$

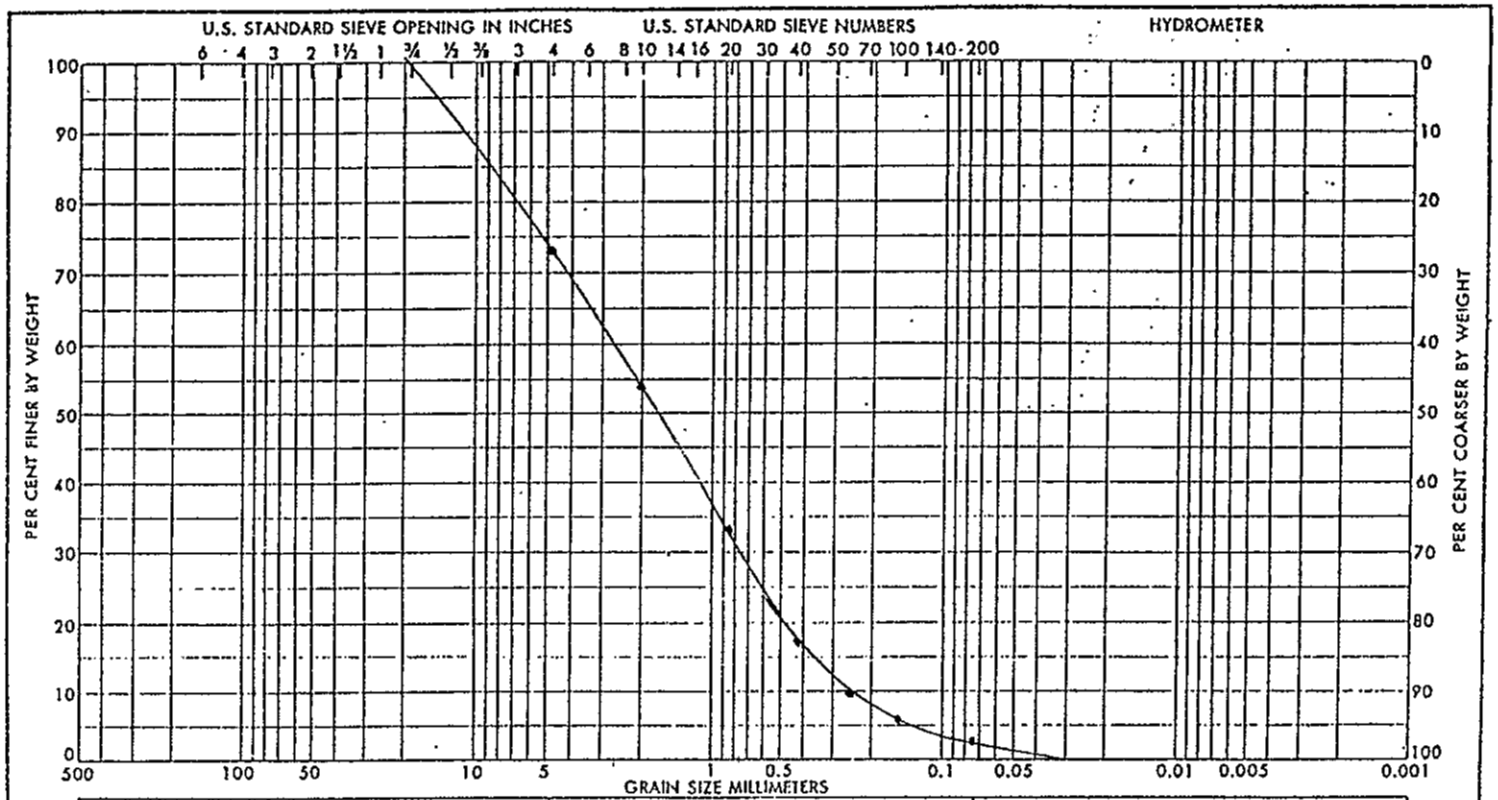

SAMPLE NO.	ELEV OR DEPTH	CLASSIFICATION	NAT W%	LL	PL	PI
22		SW	9.5			

GRADATION CURVES

PROJECT CORDOVA

AREA DEBRIS

BORING NO.

DATE JUNE 25, 1990

$C_U = \frac{2.6}{.25} = 10.4$

$C_C = \frac{(.7)^2}{2.6}$

T9

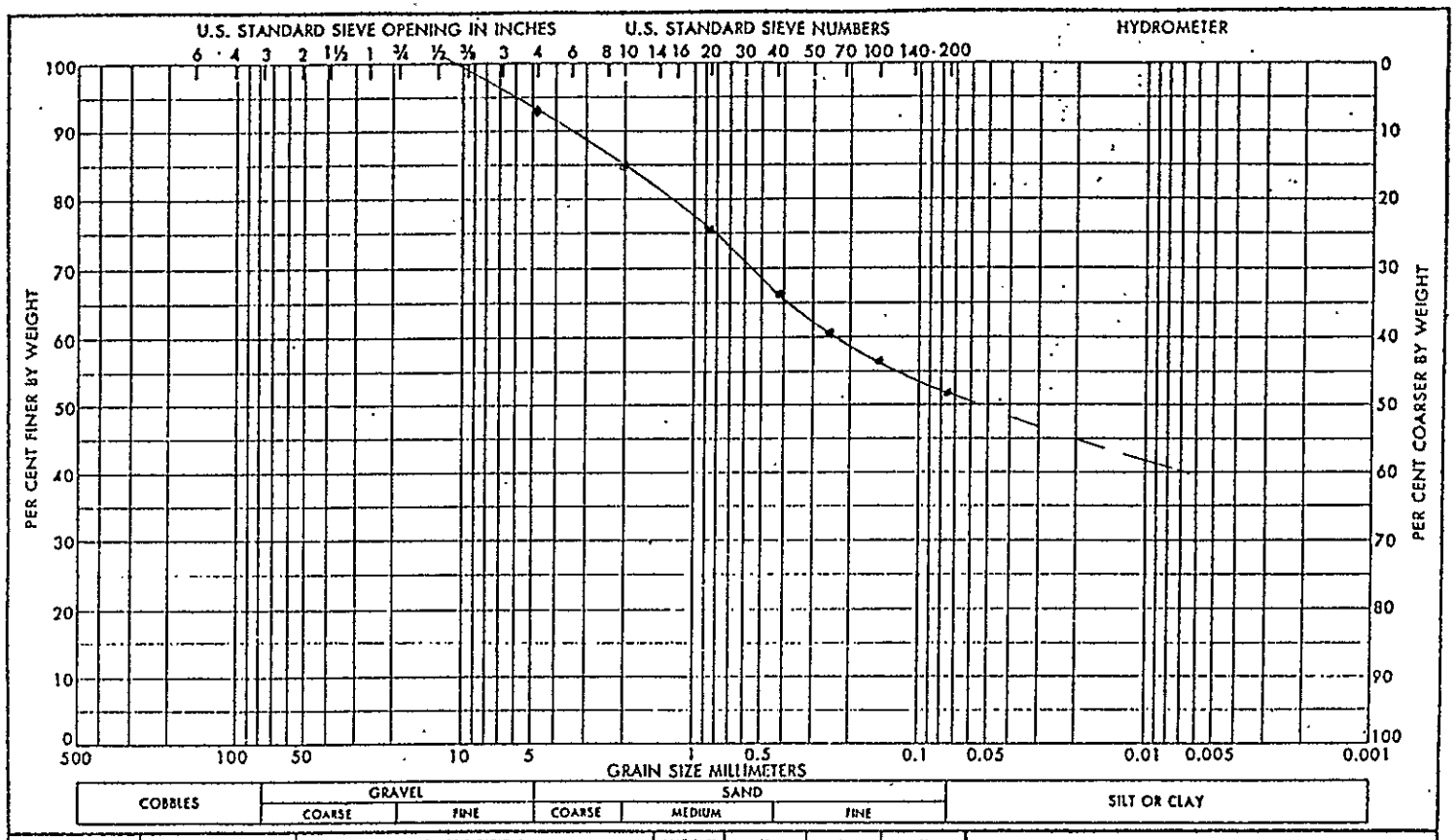

SAMPLE NO.	ELEV OR DEPTH	CLASSIFICATION	NAT W%	LL	PL	PI
23			14.1			

GRADATION CURVES

PROJECT CORDOVA DEBRIS FLOW (LOWER S/C)

AREA

BORING NO.

DATE JUNE 29/90

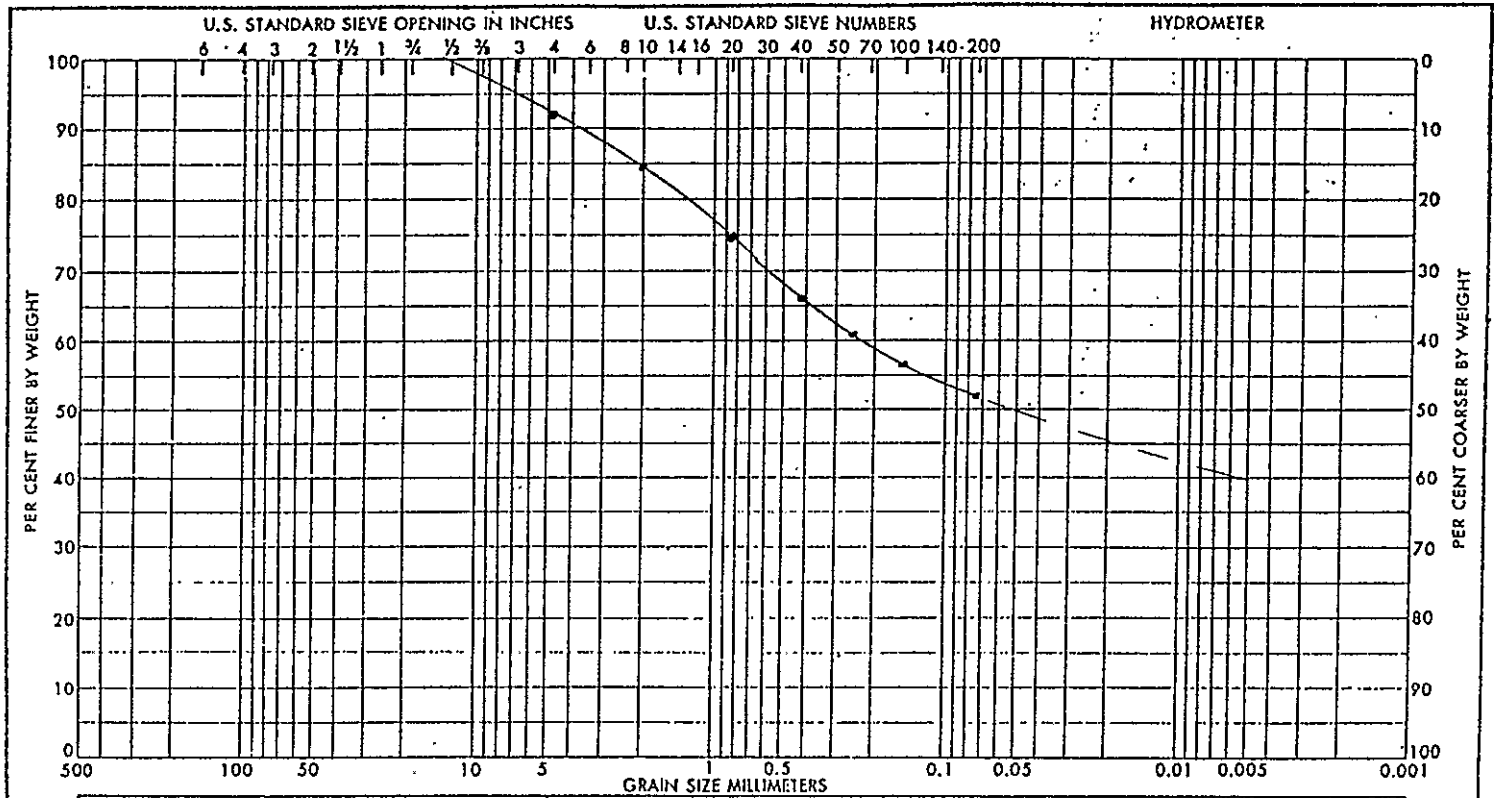

SAMPLE NO.	ELEV OR DEPTH	CLASSIFICATION	NAT W%	LL	PL	PI
24			18.1			

GRADATION CURVES

PROJECT CORDOVA DEBRIS FLOW (TOP B)
AREA
BORING NO.
DATE

Cu = ?

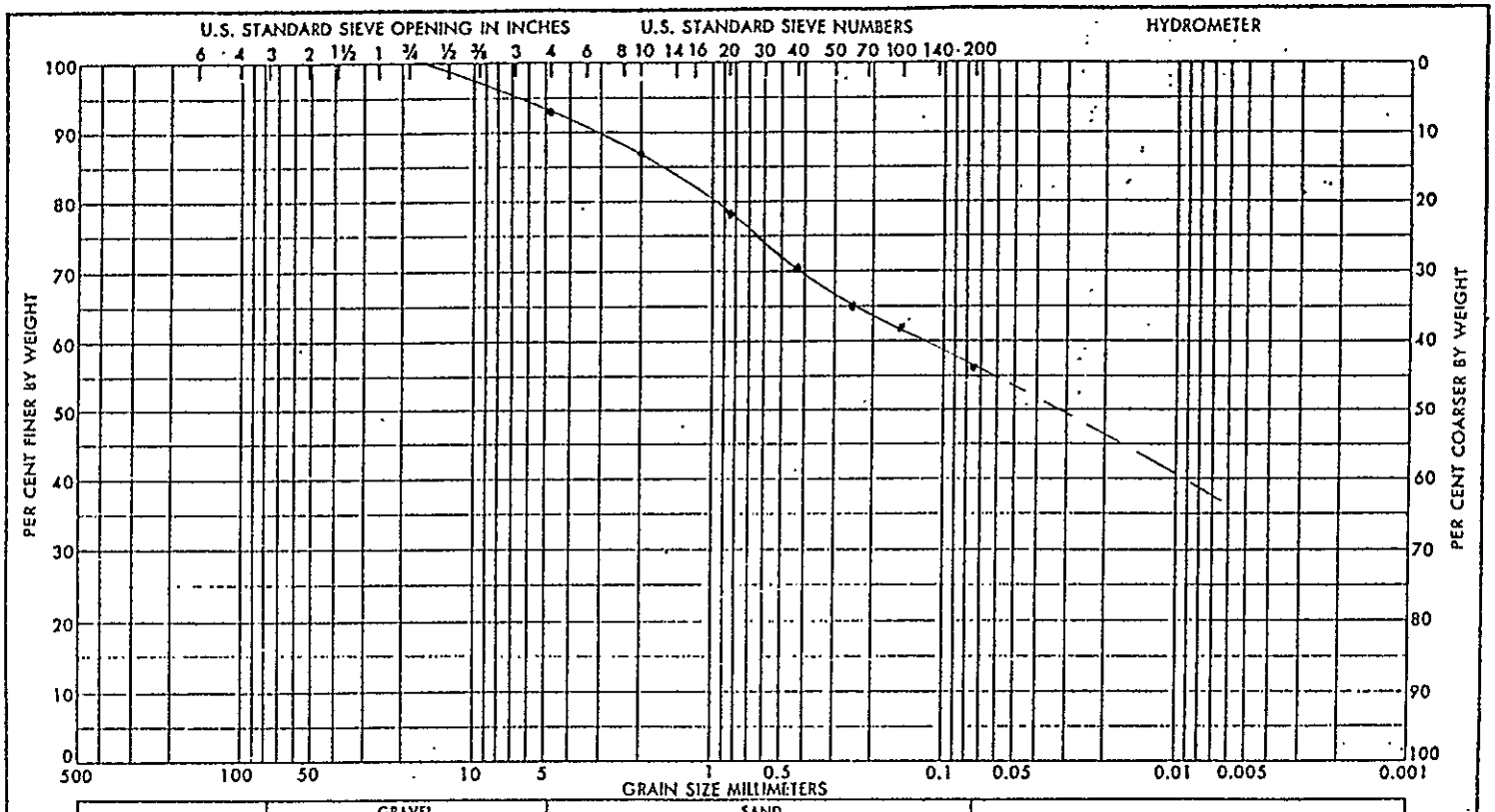

SAMPLE NO.	ELEV OR DEPTH	CLASSIFICATION	NAT W%	LL	PL	PI
25			20.9			

GRADATION CURVES

PROJECT CORDOVA DEBRIS FLOW
(BOTTOM 'A')
AREA
BORING NO.
DATE July 2/90

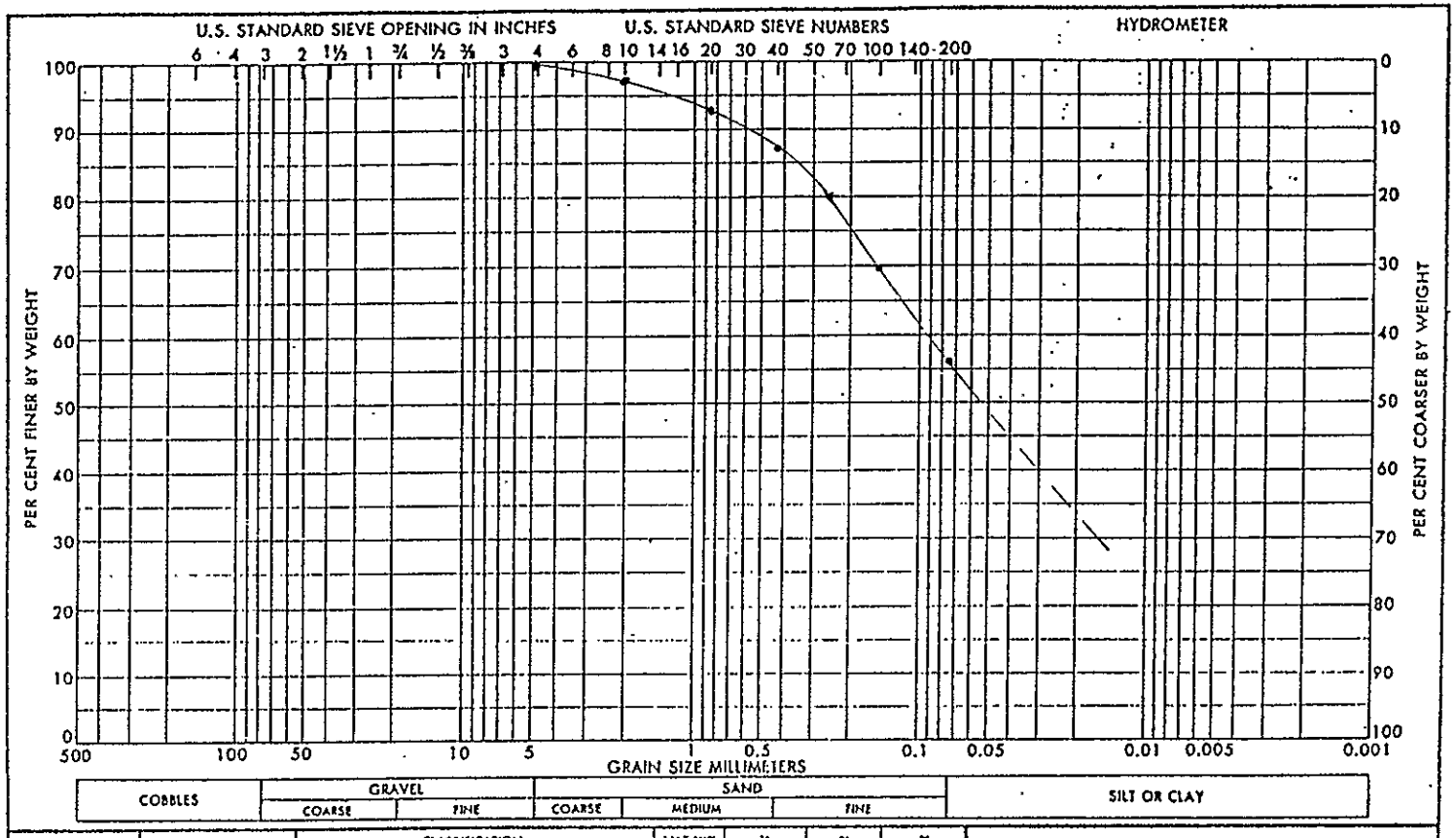

SAMPLE NO.	ELEV OR DEPTH	CLASSIFICATION	NAT W%	LL	PL	PI
26			21.6			

GRADATION CURVES

PROJECT CORDOVA DEBRIS FLOW (LOWER B)
AREA
BORING NO.
DATE JUNE 29/90

APPENDIX B

Analysis of Variance of Mean Percent Fines

MEAN PERCENT FINES

	terrace	debris	alluvial
	1.6	3.1	4.2
	3.5	3.9	0.8
	6.5	1.9	0.2
	1.7	5.8	0.2
	5.4	2.0	1.9
		1.9	0.6
		2.6	4.1
Σx	18.7	21.2	12.0
Σx^2	89.1	76.4	39.1
mean	3.7	3.0	1.7
std. dev.	2.2	1.4	1.8
n	5	7	7

variation type	sum of squares	degrees of freedom	mean square
among facies	12.9	2	6.5
within facies	49.9	16	3.1
total	62.8	18	

F = 6.5/3.1 = 2.1 for 2 and 16 degrees of freedom

F_{crit} = 3.63 for $\alpha = 0.05$
= 4.69 for $\alpha = 0.025$
= 6.23 for $\alpha = 0.01$

$F < F_{crit}$; therefore, there is no reason to believe that the mean values for all three facies were not drawn from the same population.

APPENDIX C

Least-Squares Estimation of Angle of Internal Friction for Granular Soils

Derivation of the Least Squares Model.–The angle of internal friction, ϕ, for a granular soil with no cohesive strength was calculated from direct shear test results using the least-squares method outlined in this Appendix. We assume that soil shear strength follows the traditional Mohr-Coulomb failure criterion

$$\tau = c + \sigma \tan \phi \qquad \text{Eq. B1}$$

where τ is shear strength, $c = 0$ is the cohesive strength, σ is the effective normal stress, and ϕ is the angle of internal friction. The chi-squared function (Press *et al.*, 1989, p. 502-503) is thus

$$\chi^2 = \Sigma (\tau_i - \sigma_i \tan \phi)^2 \qquad \text{Eq. B2}$$

where the summation is taken over $i = 1...N$ samples. The best-fit line will minimize the sum of the squared deviations, so differentiating Eq. B2 with respect to $\tan \phi$ and setting the result equal to zero, we get the normal equation

$$0 = \Sigma (\tau_i - \sigma_i \tan \phi)\sigma_i \qquad \text{Eq. B3}$$

Solving for $\tan \phi$

$$\phi = \arctan(\Sigma \sigma_i \tau_i / \Sigma \sigma_i^2) \qquad \text{Eq. B4}$$

The linear correlation coefficient, if desired, can be calculated using the standard expression (Press *et al.*, 1989, p. 484)

$$r = [\Sigma (\sigma_i - \sigma_{mean})(\tau_i - \tau_{mean})] / \{[\Sigma (\sigma_i - \sigma_{mean})^2]^{1/2} [\Sigma (\tau_i - \tau_{mean})^2]^{1/2}\} \qquad \text{Eq. B5}$$

Application to Cordova Debris Flow Samples.– Results of direct shear tests on sample #10 (see Appendix A) are:

i	σ_i	sat. peak τ_i	sat. residual τ_i	dry peak τ_i	dry residual τ_i
1	51 kPa	42 kPa	40 kPa	53 kPa	36 kPa
2	101 kPa	73 kPa	67 kPa	84 kPa	52 kPa

For saturated-peak shear strength:

$\Sigma \sigma_i \tau_i = 9548$
$\Sigma \sigma_i^2 = 12893$
$\tan \phi = 0.7406$
$\phi = 36°$.

For saturated residual shear strength:

$\Sigma\sigma_i\tau_i = 8837$
$\Sigma\sigma_i^2 = 12893$
$\tan\phi = 0.6854$
$\phi = 34°.$

For dry peak shear strength:

$\Sigma\sigma_i\tau_i = 11226$
$\Sigma\sigma_i^2 = 12893$
$\tan\phi = 0.8707$
$\phi = 41°.$

For dry residual shear strength:

$\Sigma\sigma_i\tau_i = 7112$
$\Sigma\sigma_i^2 = 12893$
$\tan\phi = 0.5516$
$\phi = 29°.$

If only two data points per line are used, $r = 0$ because it is always possible to draw a straight line of the form $y = b + mx$ exactly through the two points. However, by requiring that $b = 0$, we are guaranteeing that this will not happen and forcing the correlation to be weaker than necessary.

References

Press, W.H., Flannery, B.P., Teukolsky, S.A., and Vetterling, W.T., 1989, Numerical Recipes (FORTRAN edition): Cambridge, University Press, 702 p.

APPENDIX D

Clay Mineralogy Results

New Mexico Bureau of Mines & Mineral Resources
Socorro, NM 87801

A DIVISION OF
NEW MEXICO INSTITUTE OF MINING & TECHNOLOGY

Information: 505/835-5420
Publications: 505/835-5410

August 26, 1990

Dr. William Haneberg
New Mexico Bureau of Mines and Mineral Resources
Campus Station
Socorro, New Mexico 87801

Dear Bill:

The clay mineral information for the samples you gave the clay lab are on attached sheets. It is obtained from glass slides of the oriented <2μ fraction of each sample. The analysis consist of determining the peak heights of the various clay mineral reflections and evaluating them against one another. Three different x-ray traces are made: (1) without treatment, (2) after solvation in an ethylene glycol atmosphere at room temperature for at least 24 hours, and (3) after exposure to 350^{o}C heat for 30 minutes. In the case of the third diffractogram, the height of the 001 illite peak is determined while the slide is still above 100^{o}C.

Smectite in your samples is the calcium-rich variety typical of New Mexican soils. What is not typical of some of these smectites is their immaturity or poorly crystalline nature. I judge this quality based on the reduction in the collapsed 001 reflection when the samples are exposed to 350^{o}C heat. Your samples 2-8, 14-15, and 18-20 were particularly susceptible. I would be glad to you my results if you desire.

Sincerely,

George S. Austin
Sr. Industrial Minerals Geologist

Enc.

NEW MEXICO BUREAU OF MINES AND MINERAL RESOURCES

Mineralogy of Clay-size Fraction

LAB'S #	OWNER'S #	KAO	ILL	CHL	SME	I/S	OTHERS
GA90084	1	2	2	-	3	3	QTZ
GA90085	2	1	1	-	8	-	CAL + QTZ
GA90086	3	2	2	-	6	-	CAL + QTZ
GA90087	4	1	1	-	8	-	CAL + QTZ
GA90088	5	1	1	-	7	1	CAL + QTZ
GA90089	6	1	1	-	8	-	CAL + QTZ
GA90090	7	1	1	-	8	-	CAL + (QTZ)
GA90091	8	1	TR	-	9	-	CAL + (QTZ)
GA90092	10	1	2	-	6	1	CAL + QTZ
GA90093	11	2	3	-	4	1	CAL + QTZ
GA90094	12	2	3	-	4	2	QTZ + CAL
GA90095	13	2	2	-	5	1	QTZ + CAL
GA90096	14	1	1	-	8	-	CAL + (QTZ)
GA90097	15	2	1	-	6	1	CAL + QTZ
GA90098	16	2	2	-	6	TR	CAL + QTZ
GA90099	17	2	2	-	4	2	QTZ

LAB'S #	OWNER'S #	KAO	ILL	CHL	SME	I/S	OTHERS
GA90100	18	TR	TR	-	10	-	CAL + (QTZ)
GA90101	19	1	1	-	8	-	CAL + QTZ
GA90102	20	3	3	-	4	-	QTZ + CAL
GA90103	21	3	3	-	1	3	QTZ + FELD
GA90104	22	2	TR	-	7	1	CAL + QTZ
GA90105	23	2	2	-	4	2	QTZ
GA90106	24	2	1	-	5	2	QTZ + FELD?
GA90107	25	3	3	-	2	2	QTZ + FELD
GA90108	26	3	2	-	2	3	QTZ

NOTE: KAO = kaolinite, ILL = illite, CHL = chlorite, SME = smectite, and I/S = mixed-layer illite and smectite. Clay minerals reported as parts in ten; TR = trace. CAL = calcite, QTZ = quartz, FELD = feldspar, and K-SPAR = potassium felspar. "____" = much; "( )" = little; "?" = possible.

Date_____ By_____

APPENDIX E

Janbu Stability Analysis Results

JANBU SLOPE STABILITY ANALYSIS

Cordova Slope 1 (Dry)

soil wet unit weight: 16677.00 N/m^3
water unit weight: 9800.00 N/m^3
angle of internal friction: 29.00 degrees
iteration tolerance: 0.00100
FS, no interslice forces: 2.306
FS, interslice forces: 2.481 after 24 iterations
relative error: 7.03 %

AVERAGE SLICE VALUES

slice	midpoint (meters)	FS
1	70.10	0.90
2	64.81	1.76
3	59.61	1.58
4	57.75	1.56
5	53.03	1.05
6	48.15	1.07
7	45.30	1.11
8	39.00	2.04
9	33.60	2.19
10	28.95	3.45
11	20.62	10.22
12	7.95	87.83

INTERSLICE VALUES

interface	distance (meters)	ground (meters)	phreatic (meters)	failure (meters)	normal force (Newtons)	shear force (Newtons)
1	71.30	18.80	18.80	18.80	0	0
2	68.90	18.60	14.90	14.90	41865	-32831
3	60.72	18.20	12.50	12.50	94695	-54505
4	58.50	16.60	11.80	11.80	108498	-128699
5	57.00	16.50	11.30	11.30	124160	-127315
6	49.05	16.10	7.20	7.20	334614	-353342
7	47.25	14.50	6.30	6.30	382096	-442453
8	43.35	14.30	4.40	4.40	569515	-333980
9	34.66	13.80	2.20	2.20	639524	-323600
10	32.55	12.30	1.70	1.70	650908	-303711
11	25.35	11.00	0.60	0.60	563220	-96624
12	15.90	10.00	0.10	0.10	281036	13244
13	0.00	0.00	0.00	0.00	0	0

JANBU SLOPE STABILITY ANALYSIS

Cordova Slope 1 (Wet)

soil wet unit weight: 16677.00 N/m^3
water unit weight: 9800.00 N/m^3
angle of internal friction: 29.00 degrees
iteration tolerance: 0.00100
FS, no interslice forces: 0.941
FS, interslice forces: 1.022 after 9 iterations
relative error: 7.95 %

AVERAGE SLICE VALUES

slice	midpoint (meters)	FS
1	70.10	0.18
2	64.81	0.66
3	59.61	0.53
4	57.75	0.67
5	53.03	0.20
6	48.15	0.49
7	45.30	0.62
8	39.00	0.88
9	33.60	0.93
10	28.95	1.75
11	21.15	4.17
12	8.48	38.21

INTERSLICE VALUES

interface	distance (meters)	ground (meters)	phreatic (meters)	failure (meters)	normal force (Newtons)	shear force (Newtons)
1	71.30	18.80	18.80	18.80	0	0
2	68.90	18.60	18.60	14.90	46338	-40246
3	60.72	18.20	18.20	12.50	109317	-75417
4	58.50	16.60	16.60	11.80	153036	-177944
5	57.00	16.50	16.50	11.30	167795	-174358
6	49.05	16.10	16.10	7.20	450794	-429132
7	47.25	14.50	14.50	6.30	529316	-579934
8	43.35	14.30	14.30	4.40	677158	-387376
9	34.66	13.80	13.80	2.20	733951	-344493
10	32.55	12.30	12.30	1.70	742099	-335234
11	25.35	11.00	11.00	0.60	581642	-111854
12	16.95	10.00	10.00	0.10	298325	10223
13	0.00	0.00	0.00	0.00	0	0

JANBU SLOPE STABILITY ANALYSIS
Cordova Slope 2 (Dry)

soil wet unit weight: 16677.00 N/m^3
water unit weight: 9800.00 N/m^3
angle of internal friction: 29.00 degrees
iteration tolerance: 0.00100
FS, no interslice forces: 2.508
FS, interslice forces: 2.671 after 4 iterations
relative error: 6.09 %

AVERAGE SLICE VALUES

slice	midpoint (meters)	FS
1	53.78	1.10
2	48.15	1.07
3	45.30	1.11
4	39.00	2.04
5	33.60	2.19
6	28.95	3.45
7	20.62	10.22
8	7.95	87.83

INTERSLICE VALUES

interface	distance (meters)	ground (meters)	phreatic (meters)	failure (meters)	normal force (Newtons)	shear force (Newtons)
1	58.50	16.60	11.80	11.80	0	0
2	49.05	16.10	7.20	7.20	231715	-269998
3	47.25	14.50	6.30	6.30	283974	-347655
4	43.35	14.30	4.40	4.40	469502	-288428
5	34.66	13.80	2.20	2.20	561999	-292753
6	32.55	12.30	1.70	1.70	579472	-272619
7	25.35	11.00	0.60	0.60	515124	-88373
8	15.90	10.00	0.10	0.10	260750	12288
9	0.00	0.00	0.00	0.00	0	0

JANBU SLOPE STABILITY ANALYSIS

Cordova Slope 2 (Wet)

soil wet unit weight: 16677.00 N/m^3
water unit weight: 9800.00 N/m^3
angle of internal friction: 27.00 degrees
iteration tolerance: 0.00100
FS, no interslice forces: 0.958
FS, interslice forces: 1.029 after 3 iterations
relative error: 6.88 %

AVERAGE SLICE VALUES

slice	midpoint (meters)	FS
1	53.78	0.17
2	48.15	0.14
3	45.30	0.53
4	39.00	0.80
5	33.60	0.87
6	28.95	1.59
7	20.62	4.23
8	7.95	32.86

INTERSLICE VALUES

interface	distance (meters)	ground (meters)	phreatic (meters)	failure (meters)	normal force (Newtons)	shear force (Newtons)
1	58.50	16.60	16.60	11.80	0	0
2	49.05	16.10	16.10	7.20	309716	-321541
3	47.25	14.50	14.50	6.30	385234	-445519
4	43.35	14.30	14.30	4.40	551952	-331418
5	34.66	13.80	13.80	2.20	642157	-311530
6	32.55	12.30	12.30	1.70	656160	-299741
7	25.35	11.00	11.00	0.60	533269	-91486
8	15.90	10.00	10.00	0.10	253051	11925
9	0.00	0.00	0.00	0.00	0	0

JANBU SLOPE STABILITY ANALYSIS

Cordova Slope 3 (Dry)

soil wet unit weight: 16677.00 N/m^3
water unit weight: 9800.00 N/m^3
angle of internal friction: 26.00 degrees
iteration tolerance: 0.00100
FS, no interslice forces: 1.884
FS, interslice forces: 2.440 after 10 iterations
relative error: 22.80 %

AVERAGE SLICE VALUES

slice	midpoint (meters)	FS
1	40.96	0.75
2	33.60	1.98
3	28.95	3.06
4	20.62	9.02
5	7.95	77.31

INTERSLICE VALUES

interface	distance (meters)	ground (meters)	phreatic (meters)	failure (meters)	normal force (Newtons)	shear force (Newtons)
1	47.25	14.50	14.50	14.50	0	0
2	34.66	13.80	2.20	2.20	523069	-442978
3	32.55	12.30	1.70	1.70	548564	-258954
4	25.35	11.00	0.60	0.60	493011	-84579
5	15.90	10.00	0.10	0.10	250970	11827
6	0.00	0.00	0.00	0.00	0	0

JANBU SLOPE STABILITY ANALYSIS

Cordova Slope 3 (Wet)

soil wet unit weight: 16677.00 N/m^3
water unit weight: 9800.00 N/m^3
angle of internal friction: 26.00 degrees
iteration tolerance: 0.00100
FS, no interslice forces: 0.777
FS, interslice forces: 1.039 after 7 iterations
relative error: 25.26 %

AVERAGE SLICE VALUES

slice	midpoint (meters)	FS
1	40.96	0.12
2	33.60	1.25
3	28.95	1.51
4	20.62	4.03
5	7.95	31.49

INTERSLICE VALUES

interface	distance (meters)	ground (meters)	phreatic (meters)	failure (meters)	normal force (Newtons)	shear force (Newtons)
1	47.25	14.50	14.50	14.50	0	0
2	34.66	13.80	13.80	2.20	627923	-492966
3	32.55	12.30	12.30	1.70	598310	-275265
4	25.35	11.00	11.00	0.60	498393	-85502
5	15.90	10.00	10.00	0.10	239934	11307
6	0.00	0.00	0.00	0.00	0	0

JANBU SLOPE STABILITY ANALYSIS

Cordova Slope 4 (Dry)

soil wet unit weight: 16677.00 N/m^3
water unit weight: 9800.00 N/m^3
angle of internal friction: 29.00 degrees
iteration tolerance: 0.00100
FS, no interslice forces: 5.633
FS, interslice forces: 6.369 after 29 iterations
relative error: 11.55 %

AVERAGE SLICE VALUES

slice	midpoint (meters)	FS
1	23.44	1.00
2	18.18	1.72
3	12.98	4.11
4	11.15	1.54
5	8.25	27.98
6	4.12	2.16
7	1.12	3.00

INTERSLICE VALUES

interface	distance (meters)	ground (meters)	phreatic (meters)	failure (meters)	normal force (Newtons)	shear force (Newtons)
1	24.69	3.75	3.75	3.75	0	0
2	22.20	3.75	0.00	0.00	44707	-42651
3	14.16	3.60	-2.40	-2.40	174315	-100987
4	11.79	2.34	-2.70	-2.70	182452	-137664
5	10.50	2.34	-3.15	-3.15	238081	-40682
6	6.00	2.34	-3.06	-3.06	184437	47954
7	2.25	2.34	-1.65	-1.65	43322	34706
8	0.00	0.00	0.00	0.00	0	0

JANBU SLOPE STABILITY ANALYSIS

Cordova Slope 4 (Wet)

soil wet unit weight: 16677.00 N/m^3
water unit weight: 9800.00 N/m^3
angle of internal friction: 29.00 degrees
iteration tolerance: 0.00100
FS, no interslice forces: 2.323
FS, interslice forces: 2.676 after 19 iterations
relative error: 13.20 %

AVERAGE SLICE VALUES

slice	midpoint (meters)	FS
1	23.44	0.13
2	18.18	0.61
3	12.98	1.09
4	11.15	1.08
5	8.25	14.41
6	4.12	0.85
7	1.12	0.85

INTERSLICE VALUES

interface	distance (meters)	ground (meters)	phreatic (meters)	failure (meters)	normal force (Newtons)	shear force (Newtons)
1	24.69	3.75	3.75	3.75	0	0
2	22.20	3.75	3.75	0.00	46713	-45416
3	14.16	3.60	3.60	-2.40	184482	-101783
4	11.79	2.34	2.34	-2.70	197729	-143236
5	10.50	2.34	2.34	-3.15	242645	-40777
6	6.00	2.34	2.34	-3.06	179355	46632
7	2.25	2.34	2.34	-1.65	41065	32897
8	0.00	0.00	0.00	0.00	0	0